

„Da Kriege in den Köpfen der Menschen beginnen,
muss in den Köpfen der Menschen Vorsorge für den
Frieden getroffen werden.“ (UNESCO-Charta)

Acknowledgements

Looking back at whose contribution was crucial for all this, I would like to first of all acknowledge Amparo Acker-Palmer who gave me the opportunity to work as “her” first PhD student in her research group. I want to thank her for enabling me to contribute to the development of a small start-up lab into a well-running and established group of young scientists. I greatly appreciate her scientific advice, guidance, interest and support, which have been available for me at all time. I am also grateful to Amparo for encouragement and timely discussions. In addition, I would like to thank her for teaching me the way to professionally approach scientific questions, analyze them and, in the end, keep focused on what is really important.

I am moreover very much grateful to Rüdiger Klein for providing space and equipment, in particular in the very beginning, which has been a very helpful initial support for our young and growing lab. Furthermore, I would like to thank him for all the scientific discussions and suggestions, which he has given me, not only as a member of my PhD committee.

I wish to thank George Wilkinson and Inmaculada Segura for critically reading my manuscript and finally polishing it into what it is now.

Special thanks are dedicated to Barry Dickson and Thomas Lemberger as members of my PhD committee for very constructive discussions and suggestions.

I thank Inmaculada Segura, Elsa Martínez, Stefan Jordan, Tim Laumann and Jeffrey Wagner for technical help, Richard Premont and Kai Erdmann for providing reagents, Inmaculada Segura and Manuel Zimmer for sharing results and my collaborators at Cellzome for helping me with the proteomic analysis.

I acknowledge all animal care takers, technicians and Helma Tyrlas for their professional and reliable support.

I am very grateful to all the past and present members of the Acker-Palmer, Klein and Tavosanis lab for providing a great working atmosphere and the right mix of professional science and fun. Especially I thank Katrin Deininger, Svetla Dimitrova, Luca Dolce, Joaquin Egea, Ingvar Ferby, Jenny Köhler, Taija Mäkinen, Archana Mishra, Rodrigo Sanchez and Manuel Zimmer.

Vielen, vielen Dank auch an meine Eltern und meine Freundin, die mir über die ganze Zeit all die Unterstützung haben zukommen lassen.

Molecular dissection of ephrinB reverse signaling

Dissertation

Der Fakultät für Biologie der
Ludwig-Maximilians-Universität München

Eingereicht am 23. Februar 2006 von
Stefan Weinges
aus Mannheim

1. Gutachter:	PD Dr. Rüdiger Klein
2. Gutachter:	PD Dr. Mark Hübener
Tag der mündlichen Prüfung:	30. Mai 2006

The work presented in this thesis was performed in the laboratory of Signal transduction, headed by Dr. Amparo Acker-Palmer, at the Max Planck Institute of Neurobiology, Martinsried, Germany.

Erklärung

Ich versichere, dass ich die Dissertation “Molecular dissection of ephrinB reverse signaling” selbstständig, ohne unerlaubte Hilfe angefertigt, und mich dabei keiner anderen als der von mir ausdrücklich bezeichneten Hilfen und Quellen bedient habe.

Die Dissertation wurde in der jetzigen oder ähnlichen Form bei keiner anderen Hochschule eingereicht und hat noch keinen sonstigen Prüfungszwecken gedient.

(Ort, Datum)

(Stefan Weinges)

The work presented in this thesis has been submitted on January 26, 2006 for publication in Nature Neuroscience.

Grb4 and GIT1 transduce ephrinB reverse signals modulating spine morphogenesis and synapse formation.

Stefan Weinges, Inmaculada Segura, Amparo Acker-Palmer

1. Table of Contents

1. TABLE OF CONTENTS	1
2. ABBREVIATIONS	5
3. SUMMARY	9
4. INTRODUCTION	11
4.1 Actin cytoskeleton and dendritic spine formation	11
4.1.1 Spine formation	12
4.1.1.1 Filopodia as spine precursors.....	14
4.1.1.2 Spine formation from the dendritic shaft.....	14
4.1.1.3 Spine formation without synaptic contact	16
4.1.2 Spine motility.....	16
4.1.3 Spine shape and function	17
4.1.4 Spines and memory.....	17
4.1.4.1 Changes in spines after a learning experience	18
4.1.4.2 Spines and long-term depression	20
4.1.4.3 Spine persistency	20
4.1.5 Cellular processes regulated by spine signaling	21
4.1.5.1 Regulation of the actin cytoskeleton in spines by Rac	23
4.2 Eph receptors and their ephrin ligands	24
4.2.1 The Eph class of receptor tyrosine kinases: forward signaling	24
4.2.1.1 Eph-ephrin clusters	26
4.2.1.2 Activation and signaling	26
4.2.2 Ephrin ligands: reverse signaling.....	27
4.2.2.1 Signaling through transmembrane ligands	28
4.2.2.1.1 Phosphorylation-dependent signaling by ephrinB via Grb4.....	29
4.2.2.1.2 Phosphorylation-independent signaling by ephrinB.....	29
4.2.2.1.3 EphrinB ligands and Rho proteins.....	31
4.2.2.2 Signaling through GPI-anchored ligands.....	31
4.2.3 Ephs and ephrin functions in dendritic spine formation	32
4.2.4 Ephrins and Ephs in synaptic plasticity	34
5. RESULTS	38
5.1 Grb4 and GIT1 transduce ephrinB reverse signals modulating spine morphogenesis and synapse formation	38
5.1.1 EphrinB ligand signaling promotes spine maturation and is required for spine morphogenesis.....	38
5.1.2 Grb4 is enriched in post-synaptic densities and localizes to synapses in cultured hippocampal neurons	41

5.1.3	GIT1 interacts with Grb4 and forms a triple complex together with ephrinB1 in adult mice brain.....	43
5.1.4	GIT1 binds to the SH2 domain of Grb4 via its synaptic localization domain (SLD).....	46
5.1.5	Tyr392 in the SLD of GIT1 is required for Grb4 binding	49
5.1.6	EphrinB reverse signaling induces the phosphorylation of GIT1 in Tyr392 and the formation of a Grb4-GIT1 complex.....	51
5.1.7	Stimulation with EphB receptors recruits GIT1 to ephrinB patches at the synapse in hippocampal neurons.....	52
5.1.8	Disruption of ephrinB signaling via Grb4 and GIT1 affects spine morphogenesis and synapse formation	53
5.2	Proteomic analysis of PDZ-mediated ephrinB reverse signaling	57
5.2.1	Identification of GRIP1 complexes by tandem affinity purification....	57
5.2.1.1	Identification of 14-3-3 as a GRIP1 binding protein	60
5.2.1.2	14-3-3 interacts with GRIP1 in total mouse brain lysate and forms a complex with GRIP1 exclusively in raft membrane microdomains	61
5.2.1.3	EphrinB ligand, GRIP1 and 14-3-3 form a triple complex in raft membrane microdomains of mouse brain	63
5.2.1.4	Thr956 between GRIP1 PDZ6 and PDZ7 is required for 14-3-3 binding.....	64
5.2.2	Transgenic expression of GRIP1 in mice to identify protein complexes <i>in vivo</i>	66
5.2.2.1	Transgenic GRIP1-CTAP is expressed in the brain of some founders	66
5.2.2.2	GRIP1-CTAP localizes to the membrane of transgenic brain tissue ...	68
5.2.2.3	GRIP1-CTAP interacts <i>in vivo</i> with GluR2/3, a known interactor of GRIP1	69
5.2.2.4	GRIP1-CTAP is able to rescue the lethal phenotype of <i>GRIP</i> ^{-/-} mice	69
6.	DISCUSSION	71
6.1	Grb4 and GIT1 transduce ephrinB reverse signals modulating spine morphogenesis and synapse formation	71
6.1.1	Grb4 and GIT1 transduce signals downstream of ephrinB ligands	71
6.1.2	Are GIT proteins general downstream effectors of Grb4/Nck signaling?	73
6.1.3	Regulated Grb4-GIT1 interaction during phosphotyrosine-dependent ephrinB reverse signaling.....	74
6.1.4	SH3 domains contribute to Grb4 interaction with ephrinB ligand	75
6.1.5	EphrinB reverse signaling and mental retardation	76
6.2	Proteomic analysis of PDZ-mediated ephrinB reverse signaling	77
6.2.1	Identification of Grb4 and GRIP1 complexes by tandem affinity purification	77
6.2.1.1	Identification of 14-3-3 as a GRIP1 binding protein	79
6.2.1.2	GRIP1 contains three putative 14-3-3 binding sites, but only one is required	80

1. Table of Contents

6.2.1.3	What is the functional relevance of Thr956 <i>in vivo</i> ?	81
6.2.1.4	Which is the kinase required for phosphorylation of Thr956 in GRIP1?	81
6.2.1.5	GRIP1 interaction with 14-3-3 and raft microdomains	82
6.2.2	Transgenic expression of GRIP1 in mice to identify protein complexes <i>in vivo</i>	83
6.2.2.1	Transgenic GRIP1-CTAP protein is functional	84
6.3	Concluding remarks	85
7.	MATERIALS AND METHODS	86
7.1	Materials	86
7.1.1	Buffers and solutions	86
7.1.1.1	Media and antibiotics for bacterial culture	86
7.1.1.2	Media and supplements for tissue culture	86
7.1.1.3	Media and supplements for primary culture of neurons	87
7.1.1.4	Solutions for Biochemistry	87
7.1.2	Bacteria	91
7.1.3	Plasmids	91
7.1.3.1	GIT1 expression constructs	91
7.1.3.2	Grb4 expression constructs	91
7.1.3.3	GRIP1 expression constructs	92
7.1.3.4	EphrinB1 interfering peptide expression construct	92
7.1.3.5	Other expression constructs	92
7.1.4	Chemicals and commercial kits	93
7.1.5	Antibodies	94
7.1.5.1	Primary antibodies	94
7.1.5.2	Secondary antibodies	96
7.1.6	Cell lines	97
7.1.7	Other materials and equipment	98
7.2	Methods	99
7.2.1	Molecular Biology	99
7.2.1.1	Preparation of plasmid DNA	99
7.2.1.2	Enzymatic treatment of DNA	99
7.2.1.2.1	Dephosphorylation of DNA fragments	100
7.2.1.2.2	Ligating vector and insert	100
7.2.1.3	Separation of DNA on agarose gels	100
7.2.1.4	Purification of DNA	101
7.2.1.4.1	From agarose gel	101
7.2.1.4.2	From enzymatic reactions	101
7.2.1.5	Transformation of competent <i>E. coli</i> by electroporation	101
7.2.1.6	Mutagenesis	102
7.2.1.7	Extraction of genomic DNA and genotyping using PCR	102
7.2.1.7.1	DNA preparation	102
7.2.1.7.2	PCR Ubi-GRIP	102
7.2.1.7.3	PCR GRIP1-KO	103

7.2.1.8	Generation of transgenic mice	104
7.2.1.8.1	Plasmid digestion	104
7.2.1.8.2	Pronuclear injection	104
7.2.2	Cell Culture	105
7.2.2.1	Primary culture of hippocampal neurons	105
7.2.2.2	Transfection of cells	106
7.2.2.3	Stimulation of cells with Eph receptors or ephrin ligands	106
7.2.3	Biochemistry	106
7.2.3.1	Tandem affinity purification and mass spectrometry.....	106
7.2.3.2	Cell lysis, immunoprecipitation, EphB2-Fc-pulldown experiments..	107
7.2.3.3	Immunoblotting.....	108
7.2.3.4	Purification of membranes and rafts from adult mice.....	109
7.2.3.5	Postsynaptic density fractionation.....	109
7.2.3.6	Immunocytochemistry.....	110
7.2.3.6.1	Immunostaining of cells	110
7.2.3.6.2	Image analysis and quantification	111
7.2.4	Mouse work.....	111
8.	BIBLIOGRAPHY	112
9.	CURRICULUM VITAE.....	130

2. Abbreviations

α	anti
aa	amino acid(s)
Amp	ampicillin
AMPA	D-2-amino-3-hydroxy-5-methyl-4-isoxazole-propionic acid
AP	Adaptor protein
APS	Ammonium-persulfate
ARF	ADP-ribosylation factor
ATP	Adenosin-5'-triphosphate
β	beta
BBS	BES buffered saline
BES	N,N-bis[2-hydroxyethyl]-2-aminoethanesulfonic acid
Borax	sodium tetraborate
bp	base pairs
BSA	Bovine serum albumine
cAMP	Cyclic Adenosin-5'-monophosphate
CAP	Cbl associated protein
CBP	Calmodulin-binding protein
Cdc42	Cell division cycle 42
cDNA	Complementary DNA
CFP	cyan/blue fluorescent protein
CHAPS	3-[(3-Cholamidopropyl)dimethylammonio]-1-propanesulfonate
CMV	cytomegalovirus
CNS	Central nervous system
C-TAK1	CDC twenty-five associated kinase 1
CTAP	C-terminal TAP tag
C-terminus	carboxy terminus
CT	carboxy terminus
CXCR	CXC motif receptor
Cys	cysteine-rich region
Da	Dalton (g/mol)
DIG	detergent-insoluble glycolipid-enriched complexes
DIV	Days <i>in vitro</i>
DMEM	Dulbecco's modified Eagles medium
DNA	Deoxyribonucleic acid
dNTPs	deoxyribonucleoside triphosphates
Dock180	dedicator of cytokinesis 180
dsDNA	double strand DNA
DTT	1,4-Dithio-DL-threitol
E	Embryonic day
<i>E. coli</i>	Escherichia coli
ECFP	enhanced cyan/blue fluorescent protein
ECL	enhanced chemoluminescence
EDTA	Ethylenediamine-tetra acetic acid
EGF	epidermal growth factor

EGTA	Ethylen glycol-bis(aminoethylether)-tetra acetic acid
EMK	ELKL motif kinase
Eph	Erythropoietin-producing hepatocellular
ephrin	Eph family receptor interacting protein
EPSP	excitatory postsynaptic potential
EtOH	ethanol
EYFP	enhanced yellow fluorescent protein
FAK	Focal adhesion kinase
FBS	fetal bovine serum
Fc	Fragment crystallization; antibody fragment
FGF	fibroblast growth factor
Fig.	figure
FNIII	fibronectin type III
Fyn	Fgr/Yes-related Novel gene
G protein	GTP-binding protein
GAP	GTPase activating protein
GDP	guanosine diphosphate
GEF	Guanine nucleotide exchange factor
GFP	green fluorescent protein
GIT	G protein-coupled receptor kinase-interacting protein
GluR	Glutamate receptor subunit
GPI	Glycosylphosphatidylinositol
GRASP-1	GRIP-associated protein 1
Grb	growth-factor receptor bound
GRIP	glutamate receptor interacting protein
GTP	guanosine triphosphate
HBSS	Hank's balanced salt solution
HEK	human embryonic kidney
HeLa	Henrietta Lacks
Hepes	(Hydroxyethyl)-piperanzine-ethane sulfonic acid
het	heterozygous
hnRNP	heterogeneous nuclear ribonucleoprotein
Ig	Immunoglobulin
IP	Immunoprecipitation
JM	juxtramembrane domain
Kan	kanamycin monosulfate
kb	kilo bases
KD	kinase domain
KSR1	kinase suppressor of Ras1
<i>lacZ</i>	Gene encoding bgal
LB	Luria-Bertani
LC-MS/MS	liquid chromatography - tandem mass spectrometry
LTD	Long-term depression
LTP	Long-term potentiation
MARK	microtubule affinity regulating kinase
mEPSCs	miniature excitatory postsynaptic currents
MLC	myosin II regulatory light chain
MR	mental retardation

2. Abbreviations

Nck	Noncatalytic region of tyrosine kinase
NGF	nerve growth factor
NMDA	N-methyl-D-aspartate
NP-40	Nonidet P-40
N-terminus	amino terminus
N-WASP	neural Wiskott-Aldrich syndrome protein
OD	optical density
P	postnatal day
PAGE	Polyacrylamid gel electrophoresis
PAK	P21-activated kinase
PAP	Peroxidase Anti-Peroxidase
Par1	protease-activated receptor 1
PBD	PDZ binding (domain)
PBS	phosphate-buffered saline
PBST	PBS with Tween
PCR	Polymerase chain reaction
PDGF	Platelet-derived growth factor
PDZ	PSD-95/Discs large/ZO-1
PDZ-RGS	PDZ-regulator of heterotrimeric G-protein signaling
PFA	Paraformaldehyde
pH	potentium hydrogenii
PICK	Protein interacting with C kinase
PIX	p21-activated protein kinase (PAK)-interacting exchange factor
PKA	Protein kinase A
PMSF	phenylmethylsulfonyl fluoride
pre-imm	pre-immunization serum
PRK2	PKC related kinase 2
PSD	postsynaptic density
PSD-95	Postsynaptic density protein 95
PTP-BL	protein tyrosine phosphatase-basophil-like
PTPH1	protein tyrosine phosphatase H1
Rac	Ras-related C3 botulinum toxin substrate
Ras	Rat sarcoma
RGS	Regulator of G-protein signaling
Rho	Ras homologous member
RhoGAP	Ras-GTPase activating protein
RhoGEF	Ras guanine nucleotide exchange factor
RNA	Ribonucleic acid
rpm	Round per minute
RT	Room temperature
SAM	Sterile-a-motif
SDF-1	Stromal cell-derived factor 1
SDS	Sodium dodecyl sulfate
SDS-PAGE	SDS- Polyacrylamid gel electrophoresis
SFK	Src family kinase
SH	Src homology
SHD-1	Spa2 homology domain 1
SLD	synaptic localization domain

Src	Sarcoma virus transforming gene product
ssDNA	single stranded DNA
TAE	Tris-acetate EDTA
TAP	tandem affinity purification
TE	Tris-EDTA
TEMED	N,N,N',N'-Tetra-methylethylenediamine
TEV	tobacco etch virus
TfR	transferrin receptor
TIAM1	T-cell lymphoma invasion and metastasis 1
TM	transmembrane domain
TR	Texas Red
Tris	Tris[hydroxymethyl]aminomethane
TX-100	Triton X-100
U	unit(s)
UV	ultra-violet
WB	Western blot
wt	wild type
Yes	Yamaguchi sarcoma viral
YFP	yellow fluorescent protein

3. Summary

Synapses form when highly motile dendritic filopodia establish axonal contacts. When a synaptic contact is stabilized, it gives rise to the formation of a dendritic spine, which has recently been shown to involve a number of molecules that mostly regulate the actin cytoskeleton. Thus, it is not surprising that Eph receptor tyrosine kinases, as known regulators of signaling pathways involved in actin cytoskeleton remodeling, have been shown to be required for spine development and maintenance. The main characteristic of interactions of the Eph receptor with its membrane associated ephrin ligand is that they can propagate bidirectional signals. Both forward (downstream of Eph receptor) and reverse (downstream of ephrin ligand) signaling have been shown to play a role in mature synapses, where spine morphology changes are associated with synaptic plasticity. Thus, ephrinB reverse signaling might be as important for dendritic spine development as signaling pathways downstream of Eph receptors. Intrigued by this idea, we hypothesized that some of the spine morphology changes during plasticity might be regulated exclusively by ephrin reverse signaling pathways. Analyzing spine formation in cultures of dissociated hippocampal neurons, we demonstrated that stimulation of hippocampal neurons with EphB receptor bodies leads to increased spine maturation. Expression of a truncated form of ephrinB ligand, which is still able to activate EphB receptor but is unable to transduce intracellular signals, impairs spine morphology. To find new players of reverse signaling that are important in directing ephrin-mediated spine morphology, we performed a proteomic analysis of the phosphotyrosine dependent ephrin interactor Grb4 (Nck-2, Nck beta). We identified the signaling adaptor G protein-coupled receptor kinase-interacting protein (GIT)1 (Cat1) as well as the exchange factor for Rac β PIX (β -p21-activated protein kinase (PAK)-interacting exchange factor), also called RhoGEF7 or Cool-1, as novel Grb4 binding partners, which have both previously been shown to be required for spine formation. We show that Grb4 binds and recruits GIT1 to synapses downstream of activated ephrinB ligand. Interactions of Grb4 with ephrin or GIT1 are necessary for proper spine morphogenesis and synapse formation. We therefore provide evidence for an important role of ephrinB reverse signaling in spine formation and describe the ephrinB reverse signaling pathway involved in this process.

An important motif in the cytoplasmic tail of ephrinB ligand is a carboxy-terminal PDZ binding domain, which binds some multi-PDZ-domain-containing proteins. Thus, the current model for ephrinB reverse signaling implies a switch from an early and quick phosphotyrosine-dependent signaling to a more delayed and sustained PDZ domain-dependent signaling. One of these PDZ adaptors, GRIP1 (glutamate receptor interacting protein 1), is a 7 PDZ-domain containing protein that was shown to be specifically recruited into rafts through association with the cytoplasmic domain of ephrinB. In the work presented, we have used a proteomic analysis of GRIP1-binding proteins in neuroblastoma cells and *in vivo* in transgenic mice to identify protein complexes that are involved in PDZ-dependent signaling downstream of ephrinB ligands. Our results show GRIP1 binding partners with a remarkable range of cellular activities. Interaction with one binding partner, 14-3-3 proteins, was validated *in vivo* in the adult mouse brain, and more interestingly, we were able to show that this interaction occurs exclusively in rafts. Identification of a 14-3-3 binding site in GRIP1 and the formation of a triple complex of ephrinB ligand, GRIP1 and 14-3-3 in rafts strongly implicates that this new interaction has an important functional relevance in ephrinB reverse signaling.

4. Introduction

The brain serves as a center for cognitive function and neurons within the brain relay and store information about our surroundings and experiences. Modulation of neuronal circuitry allows us to process that information and respond appropriately. Proper development of neurons is therefore vital to the mental health of an individual, and perturbations in their signaling or morphology are likely to result in cognitive impairment. The development of a neuron requires a series of steps that begins with migration from its birthplace and initiation of process outgrowth, and ultimately leads to differentiation and the formation of connections that allow it to communicate with appropriate targets. Such processes require that cells communicate with each other and their environment. Information from outside of the cell is received via surface receptors that recognize specific stimuli and transduce signals into the interior of the cell in order to evoke the proper responses. Intracellular signal transduction is, however, not just a linear transmission of information. It rather involves complex networks of molecular interactions that require specific mechanisms to regulate important steps in different aspects of neuronal development including neurite outgrowth, differentiation, axon pathfinding and dendritic spine formation and maintenance.

4.1 Actin cytoskeleton and dendritic spine formation

The construction of neuronal circuits in the developing brain requires the correct assembly of trillions of synaptic connections. How, given the enormous numbers of axon and dendrites seeking contact in the growing neuropil, do the right partners manage to find one another? The challenge is met by a combination of genetically fixed routines that produce a “rough draft” of the final circuitry, followed by a process of experience-driven plasticity that refines the detailed pattern of connectivity during a critical period of juvenile learning (Berardi et al. 2004; Hensch 2004). Dendritic spines, small protrusions scattered along the dendrites of brain neurons, play a crucial part in this process (**Figure 1**). During development, immature dendrites first produce motile filopodia that search the developing neuropil for active presynaptic partners

with which to form synaptic contacts (Ziv and Smith 1996; Jontes and Smith 2000; Dunaevsky and Mason 2003; Yuste and Bonhoeffer 2004). These filopodia are later replaced by more stable mature spines, which typically comprise an expanded head joined to the dendrite shaft by a narrow neck (**Figure 2**). In this morphologically mature state, plasticity is restricted to motile ruffling of the spine head (Fischer et al. 1998; Dunaevsky et al. 1999; Roelandse et al. 2003). The motility of both filopodia and spines depends on the turnover of actin filaments in the spine cytoskeleton (Matus et al. 2000; Star et al. 2002; Portera-Cailliau et al. 2003), suggesting that the transition from filopodia to mature spines involves the down-regulation of actin dynamics.

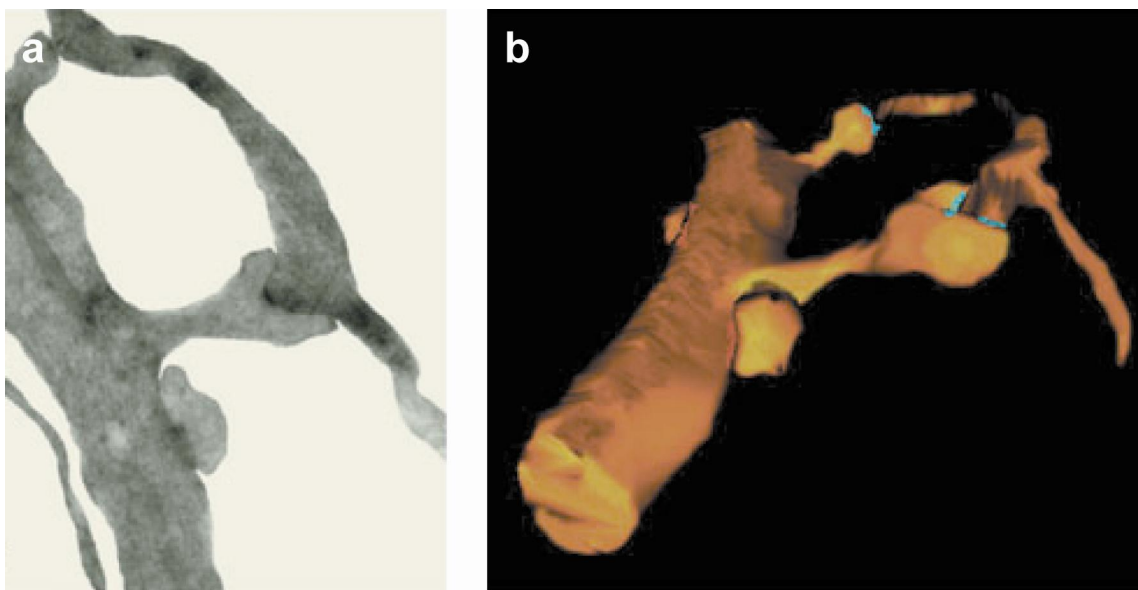


Figure 1. Three-dimensional reconstructed electron microscopy picture of a dendrite, two spines and an associated axon. (a) A single electron microscope section of a dendrite and two spines that are associated with a passing axon. The axon makes a mature synapse with one of the spines. **(b)** Reconstructed dendrite (shown at a different angle), which shows the types of connections that are formed in hippocampal cultures (modified from Luo 2000).

4.1.1 Spine formation

How do spines develop and what regulates spine formation? There are several views on the origin of dendritic spines. In most cells, dendritic spines are more prominent in older cells while dendritic filopodia are more prominent on younger dendrites (Dailey and Smith 1996). Spines can be converted from an existing shaft synapse or formed *de novo* from a filopodium, which emerges from the dendrite, forms a synapse with

4. Introduction

the presynaptic terminal and then collapses to become a short, 1-2 μm , “mature” spine (Harris and Kater 1994; Dailey and Smith 1996). The molecular mechanisms that lead to the formation of a mature, functional spine might be different for the two cases, as might the involvement of adhesion molecules and postsynaptic density protein 95 (PSD-95) (El-Husseini, 2000 #43; Abe et al. 2004). An intermediate process has been proposed, in which a filopodium searches for a presynaptic partner, makes contact and pulls the axon close to the dendritic shaft, from which it later extrudes a spine. The mechanisms for producing spines in mature neurons might differ from that in developing neurons (Dailey and Smith 1996). Therefore, the different models may not be mutually exclusive and both extrinsic and intrinsic factors could potentially regulate the formation of dendritic spines. Indeed, cell-specific differences in regulation of formation of dendritic spines have been postulated (Yuste and Bonhoeffer 2004).

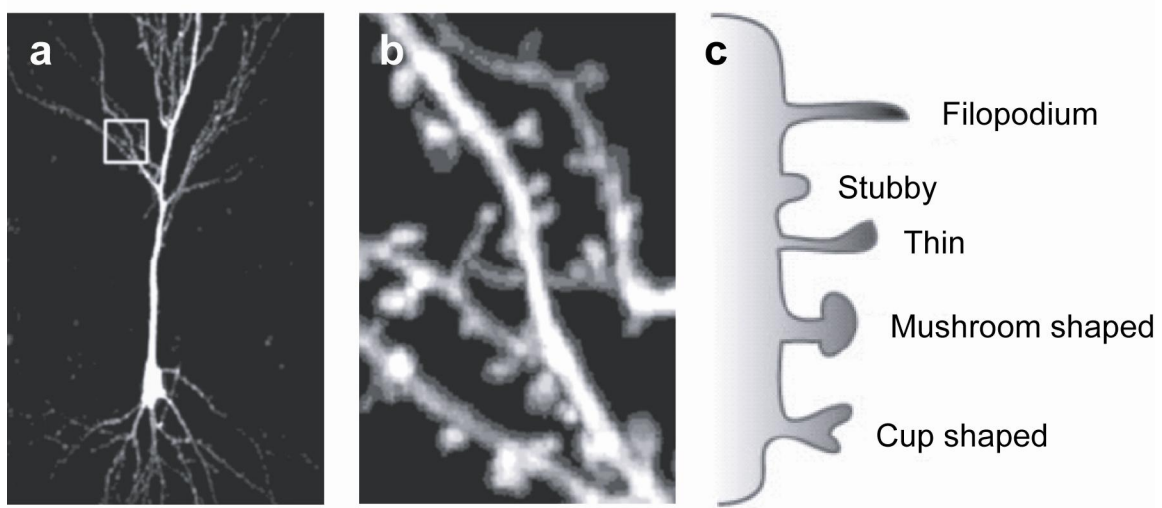


Figure 2. Morphology of dendritic spines. (a) A pyramidal neuron in hippocampal slice culture transfected with green fluorescent protein (GFP) imaged with two-photon microscopy. Dendrites are covered by small protrusions: the dendritic spines. (b) High magnification image of a hippocampal dendrite demonstrating the diversity in the morphology of dendritic spines. Most dendritic spines, however, have a narrow neck and an enlarged head. (c) A schematic representation of morphological classifications of dendritic spines (modified from Lippman and Dunaevsky 2005).

4.1.1.1 Filopodia as spine precursors

As synapses form, the number of filopodia declines and the number of stable spine-like structures increases, suggesting that filopodia are the precursors of dendritic spines. In cultures of dissociated hippocampal neurons, Ziv and Smith (1996) first succeeded in visualizing in real-time the formation of contacts between dendritic filopodia and nearby functional presynaptic terminals using two different fluorescent dyes (Ziv and Smith 1996). Based on these observations, a sequence of events was proposed in which filopodia encounter axons, engage in synaptic contact and undergo a “filopodia to spine” transformation, which involves a decrease in motility, substantial shortening and development of a mature-shaped spine containing a head and a neck (**Figure 3a**). More recently, *in vivo* data has supported the hypothesis that synapse formation triggers the transformation of filopodial structures into spines (Dailey and Smith 1996; Maletic-Savatic et al. 1999; Marrs et al. 2001; Okabe et al. 2001; Trachtenberg et al. 2002), suggesting that the function of the highly motile filopodium is to probe the space around the dendrite for an appropriate contact site on an axon. Interestingly, the release of the neurotransmitter glutamate promotes filopodial extension (Portera-Cailliau et al. 2003). Thus, it appears that this mechanism may guide filopodia to sites of presynaptic vesicle release.

4.1.1.2 Spine formation from the dendritic shaft

Spines have also been proposed to arise from synapses located on the dendritic shaft (Miller and Peters 1981), which originates from the observation that the majority of synapses in young pyramidal neurons are located on the dendritic shaft rather than on filopodia (Harris and Kater 1994). As neuronal networks mature, the number of spine synapses increases and the number of shaft synapses decreases suggesting that axonal filopodia (and not dendritic filopodia) may be involved in finding an appropriate region for synaptic contact on the dendritic shaft (**Figure 3b**). However, movement of axonal filopodia in pyramidal neurons remains to be examined, whereas electron microscopy images have indeed captured axonal filopodia in synaptic contact with the dendritic shaft (Fiala et al. 1998) and, moreover, live imaging of pyramidal neurons in

hippocampal slices have documented the emergence of mature spines from shaft synapses (Dailey and Smith 1996; Marrs et al. 2001). Therefore, it seems that spines can both emerge from the dendritic shaft and derive from filopodial precursors. A combination of these two models has also been proposed based on three-dimensional reconstruction from electron micrographs (Fiala et al. 1998) and live imaging experiments (Marrs et al. 2001) showing filopodia, which have established a synaptic contact, retract, thereby pulling the synapse towards the dendritic shaft and transforming it into a shaft synapse that later gives rise to a dendritic spine. Together, these experiments suggest that dendritic spine morphogenesis in hippocampal and cortical pyramidal neurons can occur through a combination of mechanisms. However, it is possible that a particular mechanism prevails *in vivo*.

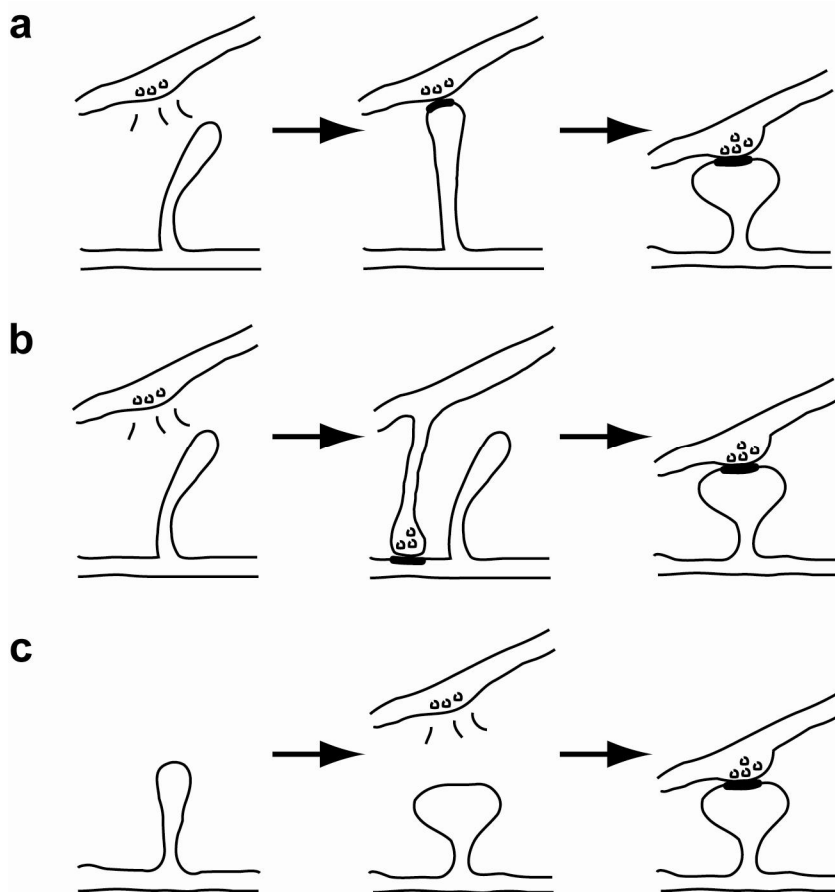


Figure 3. Three models of dendritic genesis. In model 1 (a), a dendritic filopodium captures an axonal terminal and becomes a spine. In model 2 (b), the terminal actually induces the formation of the spine. Finally, in model 3 (c), spines emerge independently of the axonal terminal (modified from Lippman and Dunaevsky 2005).

4.1.1.3 Spine formation without synaptic contact

Although in both models above, the formation of synaptic contacts induces the development of dendritic spines, it seems that the presynaptic terminal is not absolutely required for the formation of all spines (**Figure 3c**). It has been shown that spine-shaped protrusions in cerebellar Purkinje neurons form through intrinsic mechanisms in the absence of axonal contact (Sotelo et al. 1990; Takacs et al. 1997). Indeed, morphologically normal dendritic spines in Purkinje cells form before the establishment of synaptic contact with the presynaptic parallel fibers, as seen in mice with mutations causing the absence of parallel fibers.

In summary, the experimental evidence suggests that dendritic spines may form through different mechanism in different types of neurons, perhaps due to different molecular compositions (Carlin et al. 1980; Mundel et al. 1997; Rao et al. 1998; Sekerkova et al. 2003).

4.1.2 Spine motility

Live imaging of dendritic spines has revealed that dendritic protrusions are highly dynamic (Bonhoeffer and Yuste 2002). More mature dendritic spines with heads exhibit a more subtle type of motility than dendritic filopodia on young neurons, which show protrusive motility (Fischer et al. 1998). Local spine motility, or “morphing”, which might be relevant to the role of spines in memory formation, is powered by actin filament polymerization (Fischer et al. 1998; Dunaevsky et al. 1999) and might even still occur in the presence of a functional contact (Dunaevsky et al. 2001; Deng and Dunaevsky 2005). The functional significance of spine morphing is not known, but the authors of a recent study proposed that it might be involved in the diffusion of molecules through the plasma membrane into the spine (Richards et al. 2004). In this scenario, spine motility may have roles additional to the formation of initial cell-cell contacts. Such a mechanism might also be important for the fast delivery of receptors into the synapse, a process that is likely to be accelerated during the acquisition of memory. In addition, spine motility after synapse formation could serve to alter the signaling at the synapse, since alterations in spine shape have been shown to change calcium dynamics (Majewska et al. 2000). This may in turn lead to

activation of alternative pathways or potentiation of certain synapses over others and might therefore provide a mechanism for activity-dependent learning.

4.1.3 Spine shape and function

It has been reported that the size of miniature excitatory postsynaptic currents (mEPSCs) recorded at the soma after glutamate activation of single spines is positively correlated with the size of the spine head, that is, large spines produce large synaptic responses (Matsuzaki et al. 2001). It is likely that spines with larger heads accumulate more glutamate receptors and more of their interacting proteins, thereby producing larger somatic responses after synaptic activation. However, in other studies no difference or the opposite effect was seen in mEPSC properties (Murphy et al. 1998; El-Husseini et al. 2000; Pilpel and Segal 2004).

4.1.4 Spines and memory

Dendritic spines are the principal postsynaptic targets for excitatory synapses (Harris 1999) and changes in their morphology are implicated in synaptic plasticity and long-term memory (Segal and Andersen 2000). Synaptic plasticity is a term used to describe how synapses change in response to stimuli. The perforant path, an important input to the hippocampus, shows activity-dependent plasticity, which is called long-term potentiation (LTP) (Bliss and Gardner-Medwin 1973). LTP is induced by a strong presynaptic stimulus and results in an increase in synaptic efficacy that can last up to hours *in vitro* and days or weeks *in vivo*. Activity-dependent synaptic plasticity often requires N-methyl-D-aspartate (NMDA)-type glutamate receptors, which are coincidence detectors requiring both presynaptic activity (glutamate release) and postsynaptic activity (depolarization) to control Ca^{2+} entry into the postsynaptic side of excitatory synapses. Ca^{2+} influx by NMDA receptors and associated signaling pathways orchestrate synapse formation and plasticity (Helmchen 2002). If learning and memory indeed correlate with persistent changes in spine morphology, some important criteria should be met. These spine morphology changes should be temporally associated with changes in memory and, in addition, the magnitude of

changes in spines has to correlate with changes in cellular behavior. Moreover, changes in spine morphology after acquisition of a memory should be blocked or enhanced by drugs that block or enhance memory formation, respectively. If changes in spine cause changes in memory, it will be interesting to address whether the formation of a “memory” is directly inducible by generating changes in spines. Finally, depotentiation or long-term depression (LTD) is a weakening of a synapse that lasts from hours to days and may result from persistent weak synaptic patterned stimulation (e.g. a 1-Hz stimulus). To establish a causative connection between spines and the formation and/or maintenance of memory, LTD, which represents an *in vitro* model for erasure of memory, should therefore be associated with a reversal of the spine changes.

4.1.4.1 Changes in spines after a learning experience

At present, no evidence for the involvement of spine formation in memory meets any of the above mentioned criteria and the main question is still what type of spine changes take place after a learning experience. The heterogeneity of the observed changes in spine morphology may be due to a number of reasons, such as the use of different experimental conditions, timescales or type of spines. Because of its high resolution, the three-dimensional reconstruction of spines after learning experience using electron microscopy should be the ultimate approach for measuring changes in individual spines and dendrites. However, as this is the most labour-intensive method, it is not used extensively. In summary, there has not been a consistent picture yet of the changes in spine dimensions after memory formation and some of the changes observed are probably transient and diminish with different time courses.

One morphological change that has been reported by five independent groups in the past year, although to quite a heterogeneous extent, involves a rapid expansion of spine heads after tetanic stimulation in hippocampal slices or cultures. Matsuzaki and colleagues found a threefold increase in spine volume within 2-4 minutes after induction of LTP, which fell to a ~20-30% increase in spine volume after 20-40 minutes (Matsuzaki et al. 2004). A similar change, albeit much smaller and slower (18% increase in the spine/dendrite ratio) was reported by Otmakhov et al. after the induction of LTP by bath application of forskolin (Otmakhov et al. 2004). However,

another study, reported that these changes occurred in only ~6% of the imaged spines (Lang et al. 2004), which is unlikely to underlie the twofold increase in field EPSP that was recorded in the same tissue slices.

Recent evidence has confirmed that stimulation patterns associated with LTP increase the spine volume up to twofold and, moreover, using fluorescence resonance energy transfer (FRET) this has been shown to be associated with increases in levels of polymerized actin in spines (Okamoto et al. 2004). These effects are mediated by NMDA receptor activation, which also leads to an increase in the levels of both actin and actin binding proteins in the spine cytoskeleton (Furuyashiki et al. 2002; Ackermann and Matus 2003; Okamoto et al. 2004). Interestingly, drugs that inhibit actin dynamics selectively block LTP (Kim and Lisman 1999; Krucker et al. 2000; Chen et al. 2002) and slightly enhance LTD (Chen et al. 2002). And indeed, they also found that LTD was associated with spine shrinkage and an increase in the relative amount of G-actin in the spine head (Chen et al. 2002; Okamoto et al. 2004). Taken together, these data strongly suggest that in mature dendritic spines actin filament dynamics are closely coupled to LTP and LTD. Finally, Zhou reported a slow (20-60 minutes) and small (16-33%) increase in the diameter of the spine heads after high frequency stimulation (Zhou et al. 2004). This study also showed for the first time symmetry between changes in spines and synaptic responses, in that spine heads shrunk after the induction of LTD and were enlarged after the formation of LTP, which is consistent with the expansion of the postsynaptic density (Fifkova and Anderson 1981; Desmond and Levy 1986), and could underlie an enhanced synaptic response and an increase in the amplitude of mEPSCs (Matsuzaki et al. 2004).

Another morphological change in dendritic spines that can be seen is the formation of new spines, which was originally observed in cultured slices of the hippocampus and involved the accelerated formation of filopodia in response to local stimulation (Maletic-Savatic et al. 1999). A similar observation was made using a patterned LTP-producing stimulus in cultured hippocampal slices (Engert and Bonhoeffer 1999) and was reproduced and extended in dissociated hippocampal cultures (Goldin et al. 2001) and in hippocampal slices (Jourdain et al. 2003). Similar to the expansion of spine heads, it is not clear whether the formation of new spines (1-6 spines per 100 μm (Engert and Bonhoeffer 1999; Jourdain et al. 2003)) can explain the changes observed in the electrophysiological responses, which normally increase up to 50-100% above

control levels. An explanation for this may be that most new spines are non-functional and therefore new spines constitute a greater proportion of active spines.

4.1.4.2 Spines and long-term depression

What happens when LTP and memories are erased (or depotentiated) or when the synapse is depressed by the induction of LTD? As mentioned above, in contrast to the changes observed upon induction of LTP, there is a shift to a lower F-actin/G-actin ratio in the spine head in response to LTD perhaps leading to the observed spine shrinkage (Okamoto et al. 2004). Zhou found a 25-40% shrinkage in the diameter of spine heads, which persisted for an hour after LTD induction (Zhou et al. 2004). Moreover, more spines disappear in a period of 6 hours after the induction of LTD (2-3 spines per 100 μm of dendrite) than would be expected to disappear spontaneously (Nagerl et al. 2004).

Taken together, these studies show that dendritic spines shrink and/or disappear when LTD is induced, which is consistent with the hypothesis that LTP or LTD are two directly opposed mechanisms that after formation lead to larger and more or smaller and fewer spines, respectively.

4.1.4.3 Spine persistency

How persistent are the changes in spine morphology and number after a stimulus has occurred? Two studies demonstrated that there are changes in spine density in rat brains 9 hours but not 24 hours after training on a water maze (Eyre et al. 2003) and 6 hours but not 72 hours after passive avoidance training (O'Malley et al. 2000), which would indicate that morphological changes are transient. However, using two-photon microscopy in the intact brain, two recent studies came to the opposite conclusion regarding this issue. One study showed that in the mouse barrel cortex, about 50% of spines were transient, with a half-life of days (Trachtenberg et al. 2002). The other study showed that, in the mouse visual cortex, most spines (96%) were stable over months (Grutzendler et al. 2002), which might, though, also represent one extreme of the normal distribution of spine stability, whereas the first study represents a value

that is below the mean of spine stability. This discrepancy might on the other hand be explained by the fact that the studies use different cell types and different methodologies as well as by different activity patterns in the visual and somatosensory cortices.

Regardless of the discrepancy between the observations of different studies, the issue of spine persistency is important where memory is concerned. If spines are transient by nature, then their function cannot be related to long-time memory. Nevertheless, as mentioned above, some neurons might be more plastic than others and, for example, spine density on CA1 neurons can vary by 30% across the oestrus cycle, which does not necessarily mean that 30% of memories are lost during that time (Woolley and McEwen 1993).

4.1.5 Cellular processes regulated by spine signaling

Together with the regulation of AMPA receptors (Malinow and Malenka 2002) and local protein synthesis (Steward and Schuman 2003; Klann and Dever 2004), changes in the spine cytoskeleton have a crucial role in synaptic plasticity (Matus et al. 2000; Yuste and Bonhoeffer 2001; Carlisle and Kennedy 2005). Several mutations in human proteins that regulate the actin cytoskeleton cause mental retardation (Ramakers 2002). Several studies have shown that synaptic stimulation alters the spine cytoskeleton (Lin et al. 2005), and that altering the actin dynamics interferes with synaptic plasticity (Fukazawa et al. 2003; Rabenstein et al. 2005). Actin dynamics in the spine are influenced by Ca^{2+} flux through activated NMDA receptors (Fukazawa et al. 2003; Tolia et al. 2005) and by signaling through Eph receptors, which activate the Rho GTPase Rac1 (Henkemeyer et al. 2003; Penzes et al. 2003). Rac1 belongs to the Rho family of small GTPases, which transduces signals from extracellular stimuli to the actin cytoskeleton and to the nucleus. Recent evidence implicated Rho GTPases in the regulation of neuronal morphogenesis, including migration, polarity, axon growth and guidance, dendrite formation and plasticity, and synapse formation (Luo 2000). Rho GTPases constitute a subfamily of the Ras superfamily of small GTPases (~200 amino acids long). The best-studied Rho GTPases are RhoA (Ras homologous member A), Rac1 (Ras-related C3 botulinum toxin substrate 1) and Cdc42 (cell division cycle 42). Rho GTPases act as molecular switches and exist in two states: a

GDP-bound inactive state and a GTP-bound active state. Two classes of protein facilitate the switch between these two states. Guanine nucleotide exchange factors (GEFs) facilitate the exchange of GDP for GTP, thereby activating Rho GTPases. When bound to GTP, activated Rho GTPases can bind to various effectors and elicit different biological activities. By contrast, GTPase activating proteins (GAPs) increase the endogenous GTPase activity of Rho GTPases, thereby helping to switch them off (Luo 2000) (**Figure 4**).

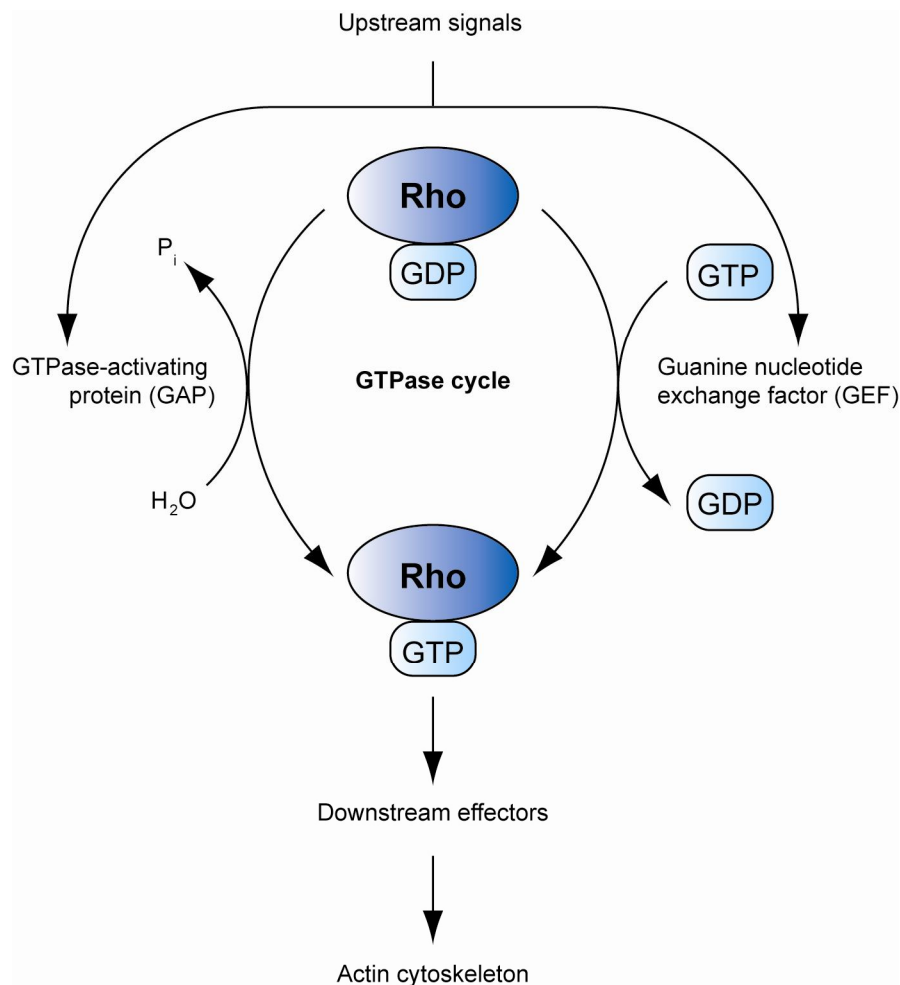


Figure 4. Rho GTPases as molecular switches. Upstream signals transduce signals to Rho GTPases through regulation of the activities of guanine nucleotide exchange factors (GEFs) or GTPase-activating proteins (GAPs), which facilitate switching on or off Rho GTPases. In their GTP-bound state, Rho GTPases bind to and activate their effectors to transduce the signal downstream.

4.1.5.1 Regulation of the actin cytoskeleton in spines by Rac

During the development of synapses, the activation of NMDA receptors and EphB receptors influences spine morphology by regulating actin remodeling (Tolias et al. 2005). In mature spines, the activation of NMDA receptors increases actin polymerization (Fukazawa et al. 2003), and activation of EphB receptors is necessary to maintain spine morphology (see below). Regulation of the cytoskeleton by NMDA receptors is mediated by TIAM1 (T-cell lymphoma invasion and metastasis 1), a Rac-specific GEF that is expressed at high levels in the developing and adult brain (Tolias et al. 2005). Knockdown of TIAM1, or expression of a dominant-negative TIAM1, in hippocampal neurons disrupts the effects of NMDA receptor activation on the spine cytoskeleton. TIAM1 is present in dendrites and spines where NMDA receptor stimulation could lead to activation of its RacGEF activity. An entirely separate mechanism for activating Rac, through EphB receptors, has also a prominent role in controlling the actin cytoskeleton, but will be discussed in greater detail in **chapter 4.2**. Other cytosolic proteins have been shown to regulate Rac activity in spines modulating spine morphology. One of these proteins, G-protein-coupled receptor kinase-interacting protein (GIT)1, has been shown to be a key regulator of spine morphology and synapse formation (Zhang, H. et al. 2003). Disrupting the synaptic localization of GIT1 by a dominant-negative mutant resulted in numerous dendritic protrusions and a significant decrease in the number of synapses and normal mushroom-shaped spines. The phenotype resulted from mislocalized GIT1 and its binding partner p21-activated protein kinase (PAK)-interacting exchange factor (PIX), an exchange factor for Rac, which is mutated in patients with nonsyndromic mental retardation. In another recent study, Zhang and colleagues were able to rescue the spine defects of GIT1 knockdown with activated PAK (p21-activated protein kinase) or myosin II regulatory light chain (MLC), which suggests that GIT1 functions through PAK and MLC (Zhang, H. et al. 2005). This points to a signaling complex consisting of GIT1, PIX, Rac and PAK that functions in regulating dendritic spine and synapse formation through modulating MLC activity. The molecule(s) that recruit this signaling complex to the synaptic membrane are currently unknown.

4.2 Eph receptors and their ephrin ligands

Eph receptors and their membrane-bound ligands, the ephrins, are unique in the receptor tyrosine kinase family because their signaling is bidirectional, through both the receptor and the ligand (Kullander and Klein 2002). The Eph/ephrin system is mainly engaged in cell-to-cell communication between adjacent cells. To date, a variety of biological functions have been demonstrated for Eph receptors and ephrins, including vascular development, tissue-border formation, cell migration, axon guidance and synaptic plasticity (Palmer and Klein 2003). Roles of Ephs and ephrins in the biology of stem cells, immune function, blood clotting and tumor formation are also beginning to be characterized (Zou et al. 1999; Conover et al. 2000; Wohlfahrt et al. 2004; Clevers and Batlle 2006). The influence of this peculiar bi-directional signaling on cell behavior is, in most cases, repellent to cellular processes such as the neuronal growth cone (Zimmer et al. 2003). However, some examples of adhesive responses mediated by Eph and ephrin have also been described (Holmberg et al. 2000). How the choice between repulsion and adhesion is regulated *in vivo* at the molecular level is so far unknown, although endocytosis of Eph and ephrin complexes have been postulated to play a role in this decision (Zimmer et al. 2003). In molecular terms, most of the signaling pathways downstream of Ephs and ephrins converge to remodel the cytoskeleton rather than having a regulatory effect on transactivation of gene expression (Murai et al. 2003; Noren and Pasquale 2004).

4.2.1 The Eph class of receptor tyrosine kinases: forward signaling

Eph receptors, which constitute the largest receptor tyrosine kinase family, are subdivided based on sequence similarity into two classes, EphA and EphB receptors. These two groups also correspond to the binding preference for the different ephrins. Promiscuous receptor-ligand interaction within each A or B class has been observed with two exceptions, ephrinA5, able to bind at high concentrations to EphB2 (Himanen et al. 2004) and EphA4, which binds to all ephrinBs (Pasquale 2005). In vertebrates there are ten EphA and six EphB receptors, EphA1 – EphA10 and EphB1 – EphB6 (Murai and Pasquale 2003; Pasquale 2004), which all share a common

4. Introduction

structure. The extracellular part of Eph receptors includes the N-terminal ephrin-binding domain, a cysteine-rich region (containing an epidermal growth factor (EGF)-like motif) and two fibronectin type-III repeats (FNIII). The intracellular part includes a juxtamembrane segment that includes two conserved tyrosine residues, a classical protein tyrosine kinase domain, a sterile- α -motif (SAM) implicated in mediating protein-protein interaction via the formation of homo and heterotypic oligomers, and a PDZ (PSD 95/Disc large/ZO-1)-binding motif. The extracellular and intracellular parts are connected by a single membrane-spanning segment (**Figure 5**). The PDZ binding motif mediates protein-protein interactions by binding to PDZ domain-containing proteins in a sequence-specific fashion.

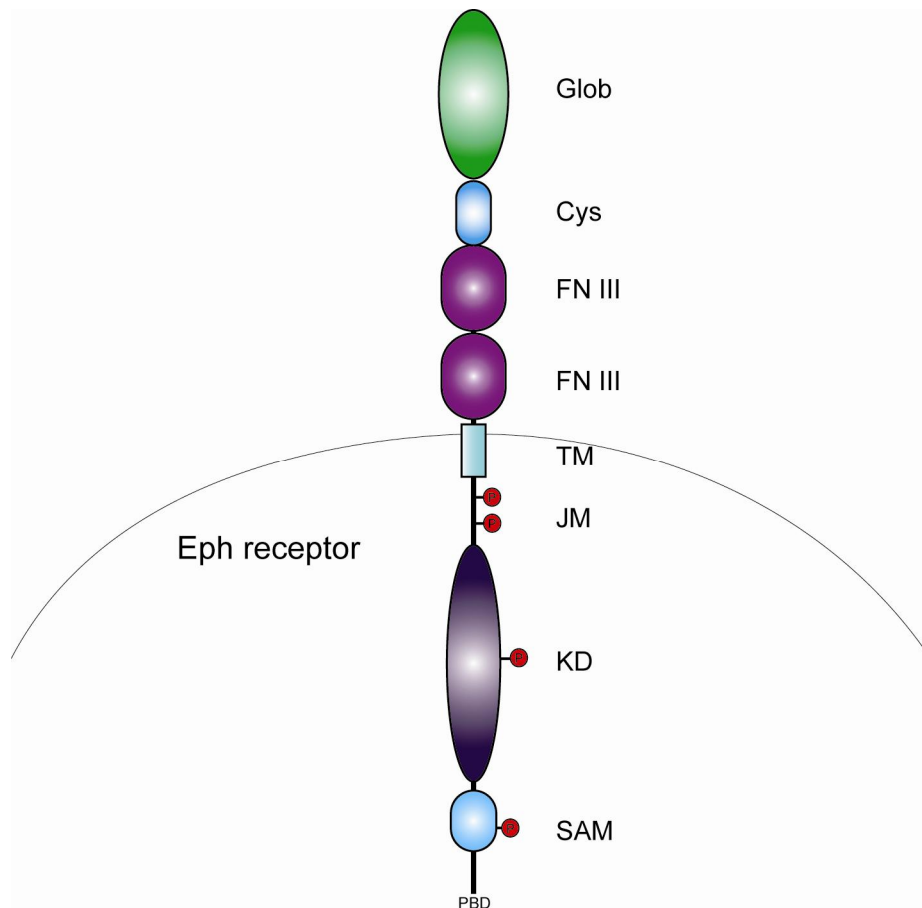


Figure 5. Eph receptors. The N-terminal globular ligand binding domain (Glob) is followed by a cysteine-rich region (Cys) and two fibronectin type III repeats (FNIII), which contain a dimerization motif. Phosphorylated tyrosine residues (P) provide docking sites for SH2 domain-containing signaling proteins. Sterile- α -motif (SAM) domains form homodimers and may regulate receptor dimerization. Signaling proteins containing PDZ domains dock to a PDZ-binding domain (PBD) in the carboxy terminus of Eph receptors. Transmembrane domain (TM), juxtamembrane region (JM), kinase domain (KD).

4.2.1.1 Eph-ephrin clusters

Another unique feature of this receptor-ligand system is that their functional signaling requires the formation of higher-order clusters (Stein et al. 1998). Upon formation of a monovalent interaction between an Eph receptor and an ephrin on juxtaposed cell surfaces with subsequent dimerization of two Eph-ephrin dimers into a tetramer, these complexes can progressively aggregate into larger clusters, the size of which might depend on the densities of Eph receptors and ephrins on the cell surface (Himanen and Nikolov 2003; Smith et al. 2004). Several weak ephrin-ephrin and receptor-receptor interactions, which include regions in the extracellular and juxtamembrane domain of ephrins, and in the ephrin-binding domain, cysteine-rich region and cytoplasmic SAM domain of Eph receptors, could promote the association of the complexes into an interconnected network (Himanen and Nikolov 2003). PDZ-domain proteins bound to Ephs and B-class ephrins might contribute to stabilize the clusters and lateral association of Eph receptors may help to expand these receptor signaling clusters beyond the region of cell-cell contact (Wimmer-Kleikamp et al. 2004).

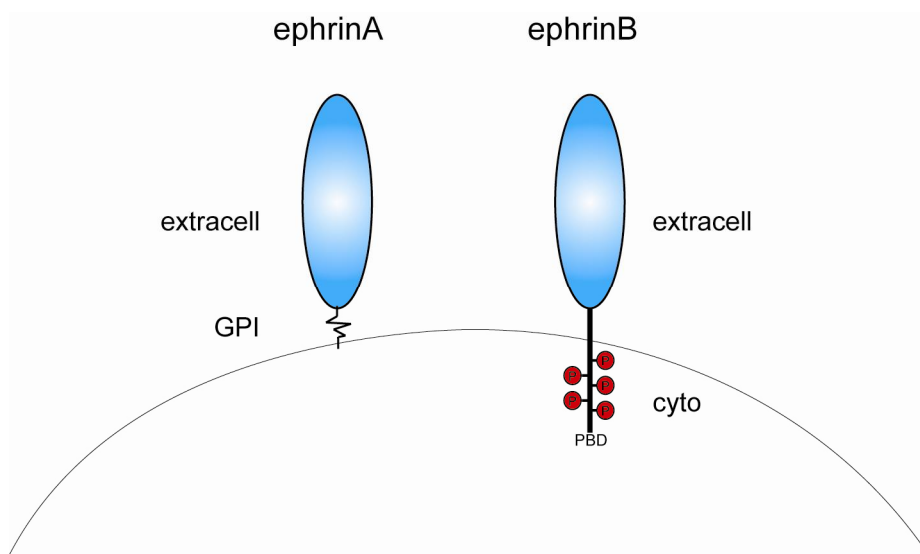
4.2.1.2 Activation and signaling

Ligand engagement of the receptor dimer induces *trans*-activation of the receptor and subsequent autophosphorylation of several juxtamembrane tyrosine residues in the partner receptor (transphosphorylation), which is required for full activation of the protein tyrosine kinase domain of the receptor (Binns et al. 2000; Zisch et al. 2000; Kullander et al. 2001). The kinase domain of one receptor from each class (EphA10 and EphB6) lacks residues that are essential for catalytic activity. Upon activation by ephrins, Eph receptors become heavily phosphorylated on tyrosine residues through Src-family kinases (SFKs) that are often associated with the receptor (Kalo and Pasquale 1999; Knoll and Drescher 2004). Upon phosphorylation of juxtamembrane tyrosine residues, the juxtamembrane domain is then released from the interaction with the kinase domain allowing the kinase domain to convert into its active state. The functional relevance of this activation in large signaling clusters has been recently revealed and shown to be important for a number of axon guidance decisions (Egea et

al. 2005). This phosphorylation via SFKs or transphosphorylation enables phosphotyrosine-binding proteins containing Src-homology-2 (SH2) domains to bind to the phosphorylated juxtamembrane domain (Kalo and Pasquale 1999; Kullander and Klein 2002; Murai et al. 2003; Prevost et al. 2003; Brantley-Sieders et al. 2004). Those adaptor proteins are a growing class of proteins that often lack intrinsic enzymatic activity and which, however, play important roles in the formation of protein complexes to connect signaling molecules to upstream and downstream signaling events. Although Eph receptors and ephrins are often co-expressed in the same cells and have been localized to lipid rafts (Wu et al. 1997; Bruckner et al. 1999; Huai and Drescher 2001; Gauthier and Robbins 2003), it is not known whether they mix and are free to interact laterally or if they are segregated in different subdomains of the plasma membrane. Interestingly, targeting of EphA receptor into ephrin-A-enriched membrane domains has been shown to also lead to *cis*-interactions, which consequently attenuates *trans*-activated signaling (Marquardt et al. 2005).

4.2.2 Ephrin ligands: reverse signaling

The ligands are also divided into two subclasses: the A-subclass (ephrinA1-ephrinA5), which are tethered to the cell membrane by a glycosylphosphatidylinositol (GPI) anchor, and the B-subclass (ephrinB1-ephrinB3), which have a transmembrane domain that is followed by a short cytoplasmic region (**Figure 6**). The ligands do not have intrinsic enzymatic activity.



4.2.2.1 Signaling through transmembrane ligands

The cytoplasmic domain of ephrinB ligands contains five conserved tyrosine residues. Three of these tyrosines (residues 312, 317 and 332) have been identified as the main *in vivo* tyrosine phosphorylation sites of activated avian ephrinB1 from neuronal tissue (Kalo and Pasquale 1999). These residues become phosphorylated following stimulation with clustered soluble ectodomain of Eph receptors (Palmer et al. 2002), with the fibroblast growth factor (FGF), presumably by the co-expressed FGF receptor (Chong et al. 2000), and by stimulation of the endogenous PDGF (platelet derived growth factor) receptor (Bruckner et al. 1997). Phosphorylation of ephrinB cytoplasmic domain is positively regulated by SFKs, which are rapidly recruited to ephrinB-containing membrane clusters by EphB2 receptor stimulation (Palmer et al. 2002) (**Figure 7a**). However, phosphorylation of ephrinB ligands is a transient event and, with delayed kinetics, the PDZ-domain containing protein-tyrosine phosphatase PTP-BL (protein tyrosine phosphatase-basophil-like) is recruited to these ephrinB membrane clusters through interaction with the PBD in ephrinB. PTPBL can thereby act as a negative regulator of ephrinB phosphorylation and Src activity. Thus, this mechanism may induce a switch from phosphotyrosine-dependent signaling to PDZ-domain-dependent-signaling (Palmer et al. 2002).

Figure 6. Ephrin ligands. The two ephrin classes differ in their type of membrane attachment, that is, GPI-anchored (ephrinA) versus transmembrane region (ephrinB). EphrinA ligands: N-terminal ephrin domain (extracell), glycosylphosphatidylinositol (GPI) anchor. EphrinB ligands: N-terminal ephrin domain (extracell), cytoplasmic domain (Cyto), PDZ-binding motif (PBD), tyrosine phosphorylation sites (P).

4.2.2.1.1 Phosphorylation-dependent signaling by ephrinB via Grb4

The SH2-SH3 domain adaptor protein Grb4 (growth-factor-receptor-bound protein 4) has been identified as an interactor and downstream effector of ephrinB1 (Cowan and Henkemeyer 2001). Grb4, but not its related adaptor protein Nck (noncatalytic region of tyrosine kinase adaptor protein 1), binds to the phosphorylated cytoplasmic tail of ephrinB1 upon EphB2 engagement of ephrinB1 and induces loss of polymerized F-actin structures, disassembly of focal adhesions and detachment of the cells from the substratum. This effect was accompanied by focal adhesion kinase (FAK) phosphorylation and redistribution of the focal adhesion protein paxillin from the plasma membrane, indicating regulated disassembly of focal adhesion sites. Moreover, EphB2-induced stimulation of ephrinB1 leads to recruitment of Grb4 and its SH3-binding partner c-Cbl-associated protein (CAP), from focal adhesions to localized regions of ephrinB1 activation (**Figure 7b**).

4.2.2.1.2 Phosphorylation-independent signaling by ephrinB

The cytoplasmic region of ephrinB ligands also contains a PDZ-binding motif (YKV) at its carboxyl terminus, which serves as docking site for both adaptor proteins that consist of only PDZ domains, such as GRIP1, GRIP2 as well as syntenin, and proteins containing PDZ domains and other protein domains, as for example protein kinase C-interacting protein (PICK)1 and the tyrosine phosphatase PTP-BL (**Figure 7**). In most cases (except for PTP-BL), the functional relevance of these interactions in ephrinB1 localization and clustering or reverse signaling events is not known. Another link that connects ephrin signaling in a phosphorylation-independent fashion to a functional read-out occurs through PDZ-RGS3, a cytoplasmic protein containing one PDZ and one “regulator of G-protein signaling” (RGS) domain, which binds constitutively to ephrinB ligands (Lu, Q. et al. 2001). RGS domains have a GAP activity for the α subunit of heterotrimeric G-proteins, thereby serving as negative regulators of G-protein signaling. EphrinB reverse signaling via PDZ-RGS interferes with the signaling of the chemokine stromal derived factor (SDF)-1 via its G-protein coupled receptor CXCR4. SDF-1 is an attractant for migrating cerebellar granule cells. The

inhibitory action of ephrinB reverse signaling was implicated in the correct layering of these cells during cerebellar development (Lu, Q. et al. 2001).

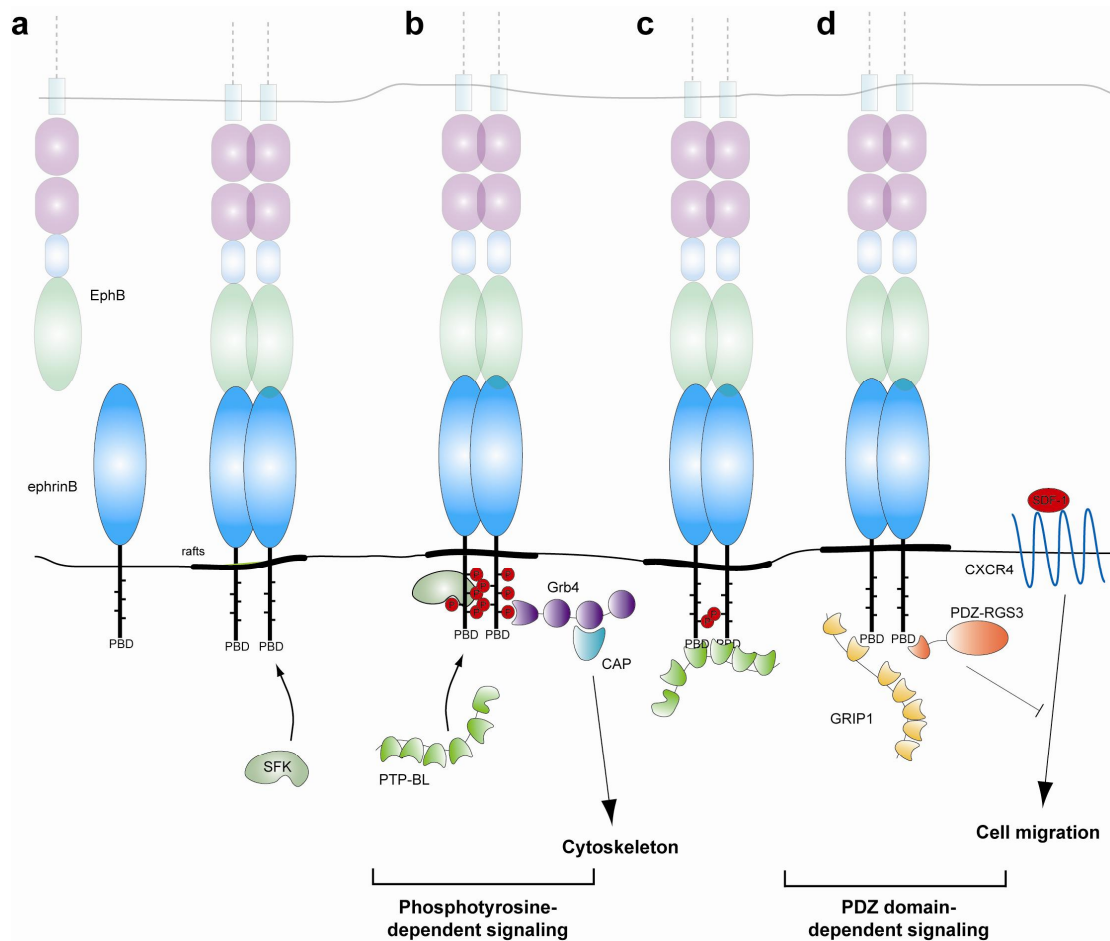


Figure 7. EphrinB-mediated reverse signaling as described in the text. (a) Following activation of the ligand, ephrinB and Src family kinases (SFKs) are recruited to the same compartments and tyrosine phosphorylation of the ephrinB cytoplasmic tail via the activity of the SFK takes place. (b) Tyrosine phosphorylated residues act as docking sites for SH2-containing molecules, such as Grb4, which transduce a phosphotyrosine-dependent signal to the interior of the cell inducing a rearrangement of the cytoskeleton. (c) PTP-BL dephosphorylates ephrinB ligands and inactivates Src and thereby switches phosphotyrosine-dependent signaling off. (d) A variety of PDZ-domain containing proteins can now interact with the extreme carboxy-termini of ephrinB molecules. The chemokine SDF-1 binds to its G-protein-coupled receptor CXCR4 and activates signaling pathways through heterotrimeric G proteins. PDZ-RGS3, a GTPase-activating protein for heterotrimeric G proteins, binds constitutively to the PDZ-binding motif of ephrinB and reverses SDF-1-induced signaling by inactivating the α subunit of the heterotrimeric complex and therefore inhibiting chemotaxis.

4.2.2.1.3 EphrinB ligands and Rho proteins

The Rho family of small GTPases has a central role in control of the dynamic reorganization of the actin cytoskeleton required for cell migration and adhesion (Hall and Nobes 2000). Although increasing evidence indicates that Eph receptors signal to the actin cytoskeleton via the Rho family of GTPases, little is known about the effects of ephrin reverse signaling on Rho family proteins. Some information comes from recent data showing that Dishevelled mediates RhoA and Rho kinase activation downstream of ephrinB1 (Tanaka et al. 2003). This demonstrates an important role for Dishevelled in both forward and reverse signaling downstream of EphB-ephrinB complexes. Another link between B-ephrins and RhoA may be src, which is required for ephrinB phosphorylation upon activation by EphB receptors (Palmer et al. 2002) and also phosphorylates p190RhoGAP (Brouns et al. 2001). However, the relevance of RhoA activation downstream of ephrins needs to be verified. Recently, there has been evidence that ephrin reverse signals activate Rac through the interaction of the Rac1-specific guanine nucleotide-exchanging factor TIAM1 with ephrinB1 and thereby mediate neurite outgrowth in cortical neurons (Tanaka et al. 2003).

4.2.2.2 Signaling through GPI-anchored ligands

Genetic studies indicated that the role of the single *Caenorhabditis elegans* Eph receptor (VAB-1) in cellular organization is, in part, kinase independent. This is in line with evidence from receptor-engaged *C. elegans* ephrinA, which mediates cell adhesion by activating the SFK member Fyn. Fyn kinase has been shown to co-localize with the activated ephrinA ligand in lipid-raft microdomains (Davy et al. 1999; Wang et al. 1999). Interestingly, available data consistently indicate that, in contrast to Eph receptors, ephrinA ligand activation, leads to enhanced integrin-dependent adhesion (Davy et al. 1999; Davy and Robbins 2000; Huai and Drescher 2001). Whereas the mechanisms for ephrinB signaling are beginning to be elucidated, as mentioned above, mechanisms for ephrinA reverse signaling, for which there is convincing biochemical and genetic evidence (Davy and Robbins 2000; Huai and Drescher 2001; Knoll et al. 2001; Holmberg et al. 2005), are largely unknown.

4.2.3 Ephs and ephrin functions in dendritic spine formation

Using mainly cultured neurons, several reports have implicated EphB receptor forward signaling as a positive signal in spine formation. Postsynaptic EphB2, but not EphA receptor, has been shown to phosphorylate the cell-surface heparan-sulfate proteoglycan syndecan-2 on cytoplasmic tyrosine residues and to associate with syndecan-2 in a phosphorylation-dependent manner (Ethell et al. 2001). The same group had demonstrated before that syndecan-2 is able to promote spine maturation in cultured hippocampal neurons, presumably by recruiting a protein complex via its C-terminus (Ethell and Yamaguchi 1999) (**Figure 8**). Inhibition of EphB2 signaling by overexpression of a kinase-inactive EphB2 mutant blocked endogenous syndecan-2 clustering and spine formation. However, ultrastructural examination of synapse morphology has not revealed major changes in *EphB2*-null mutants, suggesting functional redundancy with other co-expressed Eph receptors (Grunwald et al. 2001; Henderson et al. 2001). Using EphB receptor triple knock-out mice, Henkemeyer and co-workers have now demonstrated a highly redundant requirement for three EphB receptors (EphB1, EphB2 and EphB3) in dendritic spine morphogenesis in the hippocampus (Henkemeyer et al. 2003). *In vivo*, few spines were still formed in triple mutants, whereas mutant cultured neurons completely lacked spines. The residual spines observed *in vivo* indicate the involvement of glial cells, which are more frequently present *in vivo* and might stabilize spines by enwrapping the synapses. Moreover, ephrinB2-mediated activation of the EphBs *in vitro* transformed thin immature spines into mature forms with spacious spine heads (Henkemeyer et al. 2003). Downstream of EphB forward signaling, Moeller and colleagues very recently showed that shortening of dendritic filopodia involves the assembly of a complex, which includes focal adhesion kinase (FAK), Src, Grb2 (growth factor receptor-bound protein 2), and paxillin. Furthermore, EphB2 activation leads to the activations of FAK, Src, and paxillin, potentially initiating a number of downstream signaling pathways that are likely to contribute to the assembly of actin filaments in dendritic spines (Moeller et al. 2006). Rho-family GTPases have also been implicated in spine morphogenesis induced by Eph receptors (Irie and Yamaguchi 2002; Penzes et al. 2003). Treatment of hippocampal neurons with soluble ephrinB1-Fc induced rapid formation of spine-like protrusions, which was blocked by overexpressing a kinase-

inactive EphB2 mutant. EphB2 tyrosine kinase phosphorylated the endogenous RhoGEF kalirin in neurons, which was redistributed to larger and more synaptic clusters upon ephrinB1 stimulation. By using additional dominantly interfering tools, a pathway was outlined from Rho-GEF kalirin to filamentous actin formation and gene expression mediated by Rac1 and PAK, a key target of Rac1 (Penzes et al. 2003). EphB2 also physically associates with RhoGEF intersectin and activates its GEF activity in cooperation with neural Wiskott-Aldrich syndrome protein (N-WASP), which in turn upon stimulation with ephrinB2-Fc activates the Rho-family GTPase Cdc42 and spine morphogenesis (Irie and Yamaguchi 2002). EphrinB-mediated activation of EphB receptors also induces tyrosine phosphorylation and recruitment to dendritic spines of another Rac1 exchange factor: TIAM1 (Tanaka et al. 2004; Tolia et al. 2005). Blocking TIAM1 function with dominant-negative mutants or by RNA interference causes a marked reduction in dendritic spine numbers, suggesting a role for TIAM1 in dendritic spine development.

While axonal-dendritic spine formation may be regulated by ephrinB-EphB interactions, glial-dendritic control of spine formation may involve ephrinA-EphA4 signaling. EphA receptors have recently been shown to regulate dendritic spine morphology in hippocampal slices obtained from adult mice (Murai et al. 2003). Comparison of wild-type with *EphA4*^{-/-} slices revealed that spines lacking EphA4 were irregular in shape and significantly shorter than normal. Murai and co-workers also found highest expression of ephrinA3 on astrocytic processes near synaptic terminals suggesting that neuroglia interactions involving ephrinA3 and EphA4 forward signaling stabilize spine morphology and possibly synapses in the intact hippocampus.

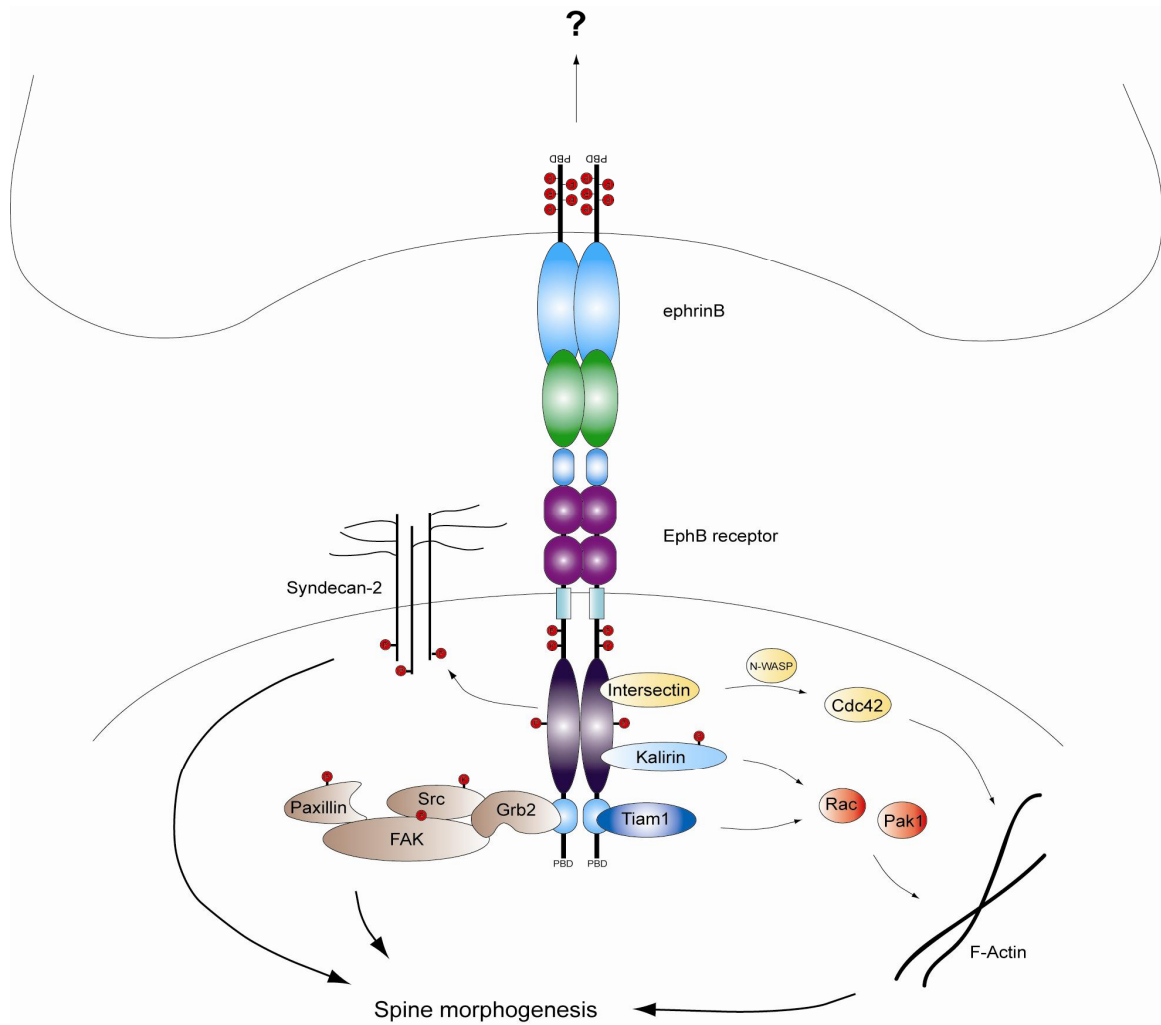


Figure 8. Eph signaling pathways leading to spine formation. The proteoglycan syndecan-2 mediates synaptic spine formation. Eph receptors activate syndecan-2 by phosphorylation. The RhoGEFs Kalirin-7 and TIAM1 have also been implicated in EphB-mediated formation of dendritic spines through recruitment and activation of the Rho GTPase Rac1 and PAK. The RhoGEF intersectin connects Eph signaling to Cdc42 inducing F-actin formation, a prerequisite of spine formation. Activation of EphB receptors results also in the association of FAK, Grb2, and Src with EphB2. Following assembly of this protein complex, Src is activated and phosphorylates FAK and paxillin, which results in RhoA activation and dendritic filopodia shortening.

4.2.4 Ephrins and Ephs in synaptic plasticity

Recent research has shown that Eph receptors and ephrins are important in the adult nervous system, for example during the processes of synapse formation and synaptic plasticity, which is dependent on neuronal activity. While control of spine formation by Eph/ephrin appears to involve redundant contributions from several family members, the signaling events leading to activity-dependent synaptic plasticity require

the presence of the EphB2 receptor, which is thought to act postsynaptically by modulating glutamate receptors (Grunwald et al. 2001; Henderson et al. 2001; Contractor et al. 2002) and which was shown to associate with and to induce clustering of NMDA receptors (**Figure 9**). This in turn may suggest that ephrinB ligands in synaptic membranes induce the maturation of glutamatergic synapses by promoting NMDA receptor aggregation (Dalva et al. 2000). A model in which ephrin-Eph signaling influences activity-dependent processes (Ca^{2+} influx) by modulating gene expression during development of synaptic connections comes from data obtained from very young cultured neurons, which showed enhanced NMDAR-mediated Ca^{2+} influx and potentiated cAMP-response element binding protein (CREB)-phosphorylation and -dependent transcriptional events upon stimulation with ephrinB1 (Grunwald et al. 2001; Takasu et al. 2002). This might mechanistically occur by the recruitment and activation of SFKs, which phosphorylate certain subunits of the NMDAR (Grunwald et al. 2001; Takasu et al. 2002). Activation of SFKs is required for EphB2-mediated enhancement of Ca^{2+} influx, at least in a transfected cell system (Takasu et al. 2002). These *in vitro* observations are consistent with findings from EphB2-deficient mice (Grunwald et al. 2001; Henderson et al. 2001) showing a reduction or even loss of hippocampal long-term potentiation and long-term depression correlated with a redistribution of a significant fraction of NMDA receptors. Interestingly, targeted expression of a kinase-deficient EphB2 receptor isoform rescued the defects in EphB2-deficient mice, suggesting that ephrinB ligand reverse signaling may be the active signaling partner at the synapse (Grunwald et al. 2001; Henderson et al. 2001).

Recent evidence indicates that in certain synapses, the Eph/ephrin system is used in an inverted manner: At the mossy fiber–CA3 synapse, ephrinB3 is specifically expressed by presynaptic dentate gyrus cells while the EphB2 receptor is expressed by both presynaptic dentate gyrus and postsynaptic CA3 neurons. In contrast, in the CA1 region of the hippocampus, ephrinBs are predominantly localized in postsynaptic neurons, whereas EphBs and EphA4 are expressed both pre- and postsynaptically (Grunwald et al. 2004) (**Figure 9**). Interestingly, conditional mutants of *ephrinB2*- and *ephrinB3*-null mutants display drastically reduced LTP. Moreover, EphA4 forward-signaling is not required since the deficit is rescued by an EphA4 receptor with the intracellular domain completely deleted. Therefore, EphA4 does not act as a receptor in the traditional sense, but rather as a ligand for postsynaptic and possibly

presynaptic ephrinBs, which are competent for reverse signaling. This supports a model in which the Eph/ephrin signaling system is used for activity-dependent plasticity in a converse fashion at different hippocampal synapses via an as-yet unknown pathway and, therefore, some of the spine morphology changes during plasticity might be regulated exclusively by ephrin reverse signaling pathways. Thus, ephrinB reverse signaling might be as important for dendritic spine development as the signaling pathways downstream of the Eph receptors. However, the ability of ephrins to initiate intracellular signals at synapses as well as the pathways involved in such signaling processes remain unknown.

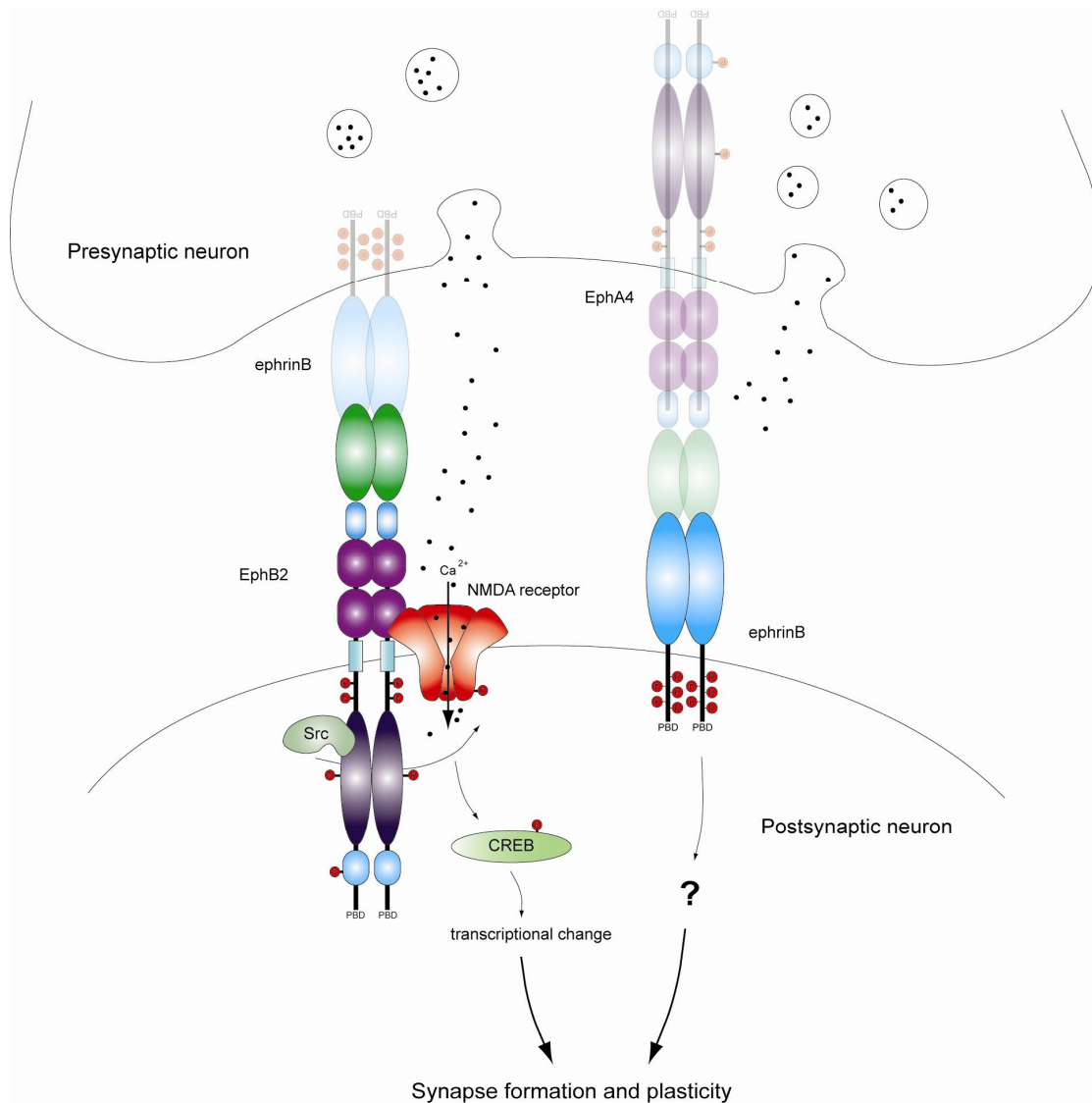


Figure 9. Eph and ephrin signaling pathways in synaptic plasticity. EphB2 enhances NMDA-dependent calcium fluxes through the cytoplasmic tyrosine kinase Src, which phosphorylates the NMDA receptor and potentiates phosphorylation of CREB. CREB-dependent transcriptional events, influenced by activity-independent EphB signaling, may affect synapse formation, maturation, and plasticity. In postsynaptic CA1 neurons, ephrinB reverse signaling is required for long-term plasticity. This raises the intriguing possibility that the bi-directional Eph/ephrin signaling system is used for activity-dependent plasticity in converse ways at different synapses. The signaling partners required for reverse signaling in the postsynaptic CA1 neurons remain unknown.

5. Results

5.1 **Grb4 and GIT1 transduce ephrinB reverse signals modulating spine morphogenesis and synapse formation**

Dendritic spines are small protrusions emerging from the dendrites that receive excitatory input. The process of spine morphogenesis occurs both in the developing brain and during synaptic plasticity. Molecules regulating cytoskeletal rearrangements have been involved in spine formation and maintenance. Work to be presented here will show that reverse signaling by the transmembrane ligands for Eph receptors, ephrinB ligands, is required for correct spine morphogenesis. The molecular mechanism underlying this function of ephrins involves the SH2/SH3 adaptor protein Grb4 and the signaling adaptor GIT1. Grb4 binds via its SH2 domain to Tyr392 in the synaptic localization domain (SLD) of GIT1. Phosphorylation of Tyr392 and the recruitment of GIT1 to synapses are regulated by ephrinB activation. Disruption of this pathway impairs spine morphogenesis and synapse formation. In the studies presented, an important role for ephrinB reverse signaling in spine formation has been shown and the required ephrinB reverse signaling pathway has been mapped.

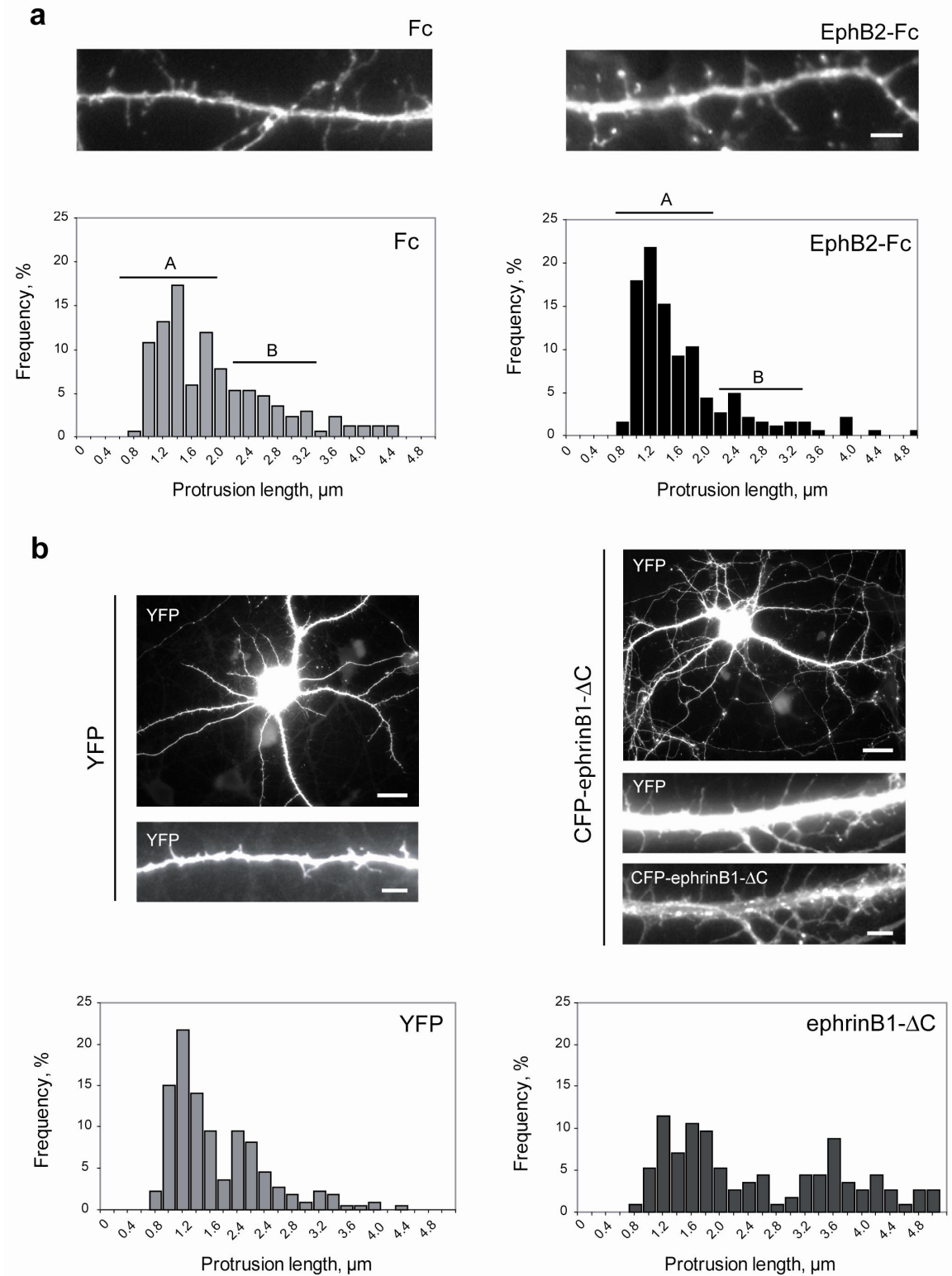
5.1.1 **EphrinB ligand signaling promotes spine maturation and is required for spine morphogenesis**

It has been previously shown that hippocampal neurons from triple EphB-deficient mice failed to make dendritic spines (Henkemeyer et al. 2003). EphrinB ligands are highly enriched in preparations of the postsynaptic density and they interact with postsynaptic proteins (Grunwald et al. 2004). In order to investigate if activation of ephrinB ligands at synapses promotes spine formation, we stimulated 12 DIV rat hippocampal neurons with a soluble pre-clustered form of EphB2 receptor ectodomain fused to the Fc portion of human IgG (EphB2-Fc). We transfected the neurons with Yellow Fluorescent Protein (YFP) at 7 DIV in order to visualize protrusions after stimulation. Activation of ephrinB ligands by EphB receptor induced

5. Results

spine maturation reflected by the shortening of the spines and the appearance of mushroom-like heads (**Figure 10a**). The average length of spines was reduced from $1.92 \pm 0.19 \mu\text{m}$ in the Fc controls to $1.66 \pm 0.02 \mu\text{m}$ in EphB2-Fc stimulated neurons. To interfere with ephrinB reverse signaling we transfected rat hippocampal neurons with a truncated form of ephrinB1 (ephrinB1- ΔC), which lacks the cytoplasmic domain and therefore is deficient in reverse signaling. EphrinB1- ΔC is expressed at the membrane and is able to bind to EphB receptors expressed in neighboring cells (Zimmer et al. 2003) therefore acting as a dominant negative molecule that will interfere with the binding of endogenous ephrinB ligands to EphB receptors. The morphology of the spines in neurons transfected with a control vector or Cyan Fluorescent Protein (CFP)-ephrinB1- ΔC was visualized by co-transfection at 7 DIV with YFP. Overexpression of the truncated ephrinB ligand induced a significant increase in immature filopodia-like protrusions without heads (**Figure 10b**). The average length of protrusions was increased from $1.91 \pm 0.29 \mu\text{m}$ in the YFP transfected controls to $2.55 \pm 0.03 \mu\text{m}$ in CFP-ephrinB1- ΔC transfected neurons. These results suggest that ephrinB reverse signaling promotes spine maturation and is necessary for correct spine development.

Figure 10. EphrinB ligand signaling and spine maturation. (a) Activation of ephrinB ligands promotes spine maturation. Rat hippocampal neurons at 7 DIV were transfected with YFP and stimulated at 12 DIV for 8 h with clustered EphB2-Fc or control Fc, fixed and analyzed for the morphology of dendritic protrusions. The length of dendritic protrusions ($n>500$) was quantified (bottom panels). Group A represents spines and group B represents dendritic filopodia based on the length. Bar, $2 \mu\text{m}$. (b) Expression of truncated ephrinB ligands impairs spine formation. Rat hippocampal neurons were transfected at 7 DIV with YFP (left panels) or co-transfected with YFP and CFP-ephrinB1- ΔC (right panels), fixed at 11 DIV and analyzed for the morphology of dendritic protrusions. The length of dendritic protrusions ($n>500$) was quantified (bottom panels). Bars: (top) $20 \mu\text{m}$; (bottom) $2 \mu\text{m}$.



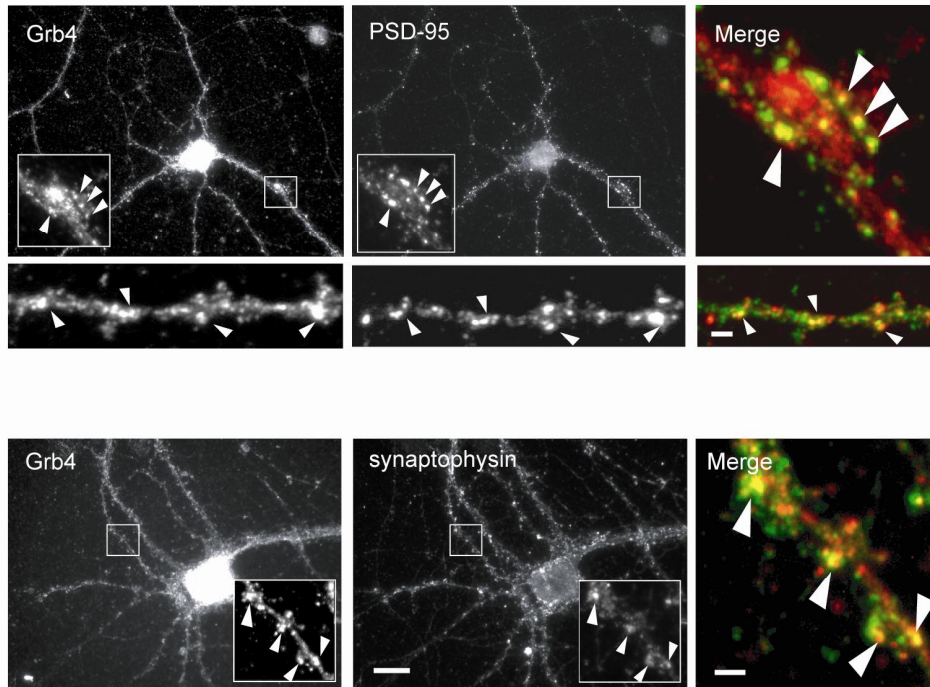
5.1.2 Grb4 is enriched in post-synaptic densities and localizes to synapses in cultured hippocampal neurons

We next attempted to elucidate the signaling events downstream of ephrinB ligands involved in spine formation. The SH2/SH3 adaptor Grb4 acts as a transducer from the phosphorylated ephrinB1 cytosolic domain to signaling pathways controlling the cytoskeleton (Cowan and Henkemeyer 2001). To investigate the involvement of Grb4 in synapse formation, and to map the signaling pathway downstream of ephrinB ligands in such a process, we examined first the subcellular distribution of Grb4 in hippocampal neurons. We immunostained low density cultures using a specific anti-Grb4 antibody (**Figure 11a**). In mature hippocampal neurons Grb4 showed characteristic synapse localization, accumulating in puncta along the neuronal processes. Double staining with the postsynaptic density protein PSD-95 confirmed the postsynaptic localization of Grb4. Presynaptic localization of Grb4 was also confirmed by double immunostaining with the presynaptic marker synaptophysin.

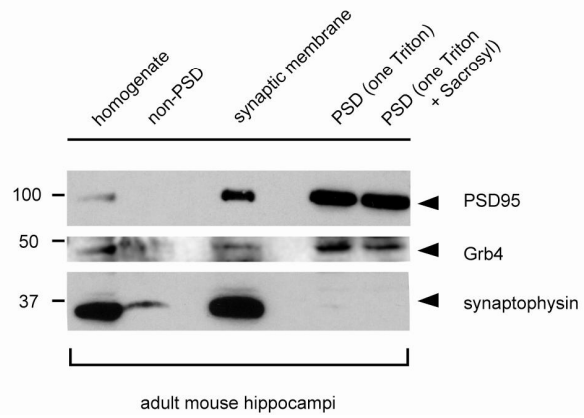
To obtain biochemical evidence that Grb4 localizes to the PSD, PSD fractions were prepared from adult mouse hippocampus using standardized sucrose gradients and triton/sarcosyl extraction (Cho et al. 1992). To assess the quality of our PSD preparations, PSD-95 and synaptophysin were used as post- and presynaptic markers respectively. Western blot analysis of the PSD preparations showed Grb4 strongly enriched in the postsynaptic density (**Figure 11b**). These findings indicate that Grb4 is positioned in the right place to mediate ephrinB reverse signaling necessary for synapse formation.

Figure 11. Grb4 localizes to synapses. (a) Grb4 colocalizes with both pre- and postsynaptic markers. Hippocampal neurons at 3 weeks in culture were immunostained for endogenous Grb4 (left column), PSD-95 (upper and middle panels in middle column) and synaptophysin (lower panel middle column). Enlargements of the area in boxes are shown at the bottom of the pictures as well as a merge of the two signals in the right column. Bars: 20 μm ; (enlargements) 2 μm . (b) Grb4 is enriched in the postsynaptic density (PSD). Different PSD subfractions, non-PSD fraction and total brain homogenate were analyzed by Western Blotting for the presence of the indicated proteins.

a



b



5.1.3 GIT1 interacts with Grb4 and forms a triple complex together with ephrinB1 in adult mice brain

To further dissect the pathway directing spine morphology downstream of ephrinB ligands, a proteomic analysis of Grb4 binding proteins from a neuroblastoma cell line was performed using the TAP-LC-MS/MS methodology (see Methods). Tandem affinity purification (TAP) has emerged as a versatile method to efficiently purify protein complexes from cells in culture (reviewed in Bauer and Kuster 2003). GIT1 (Cat1) and 2 (Cat2) as well as the p21-activated protein kinase (PAK)-interacting exchange factors α PIX (RhoGEF6, Cool-2) and β PIX (RhoGEF7, Cool-1) were all identified as putative Grb4-interacting proteins in our screen (Table 1).

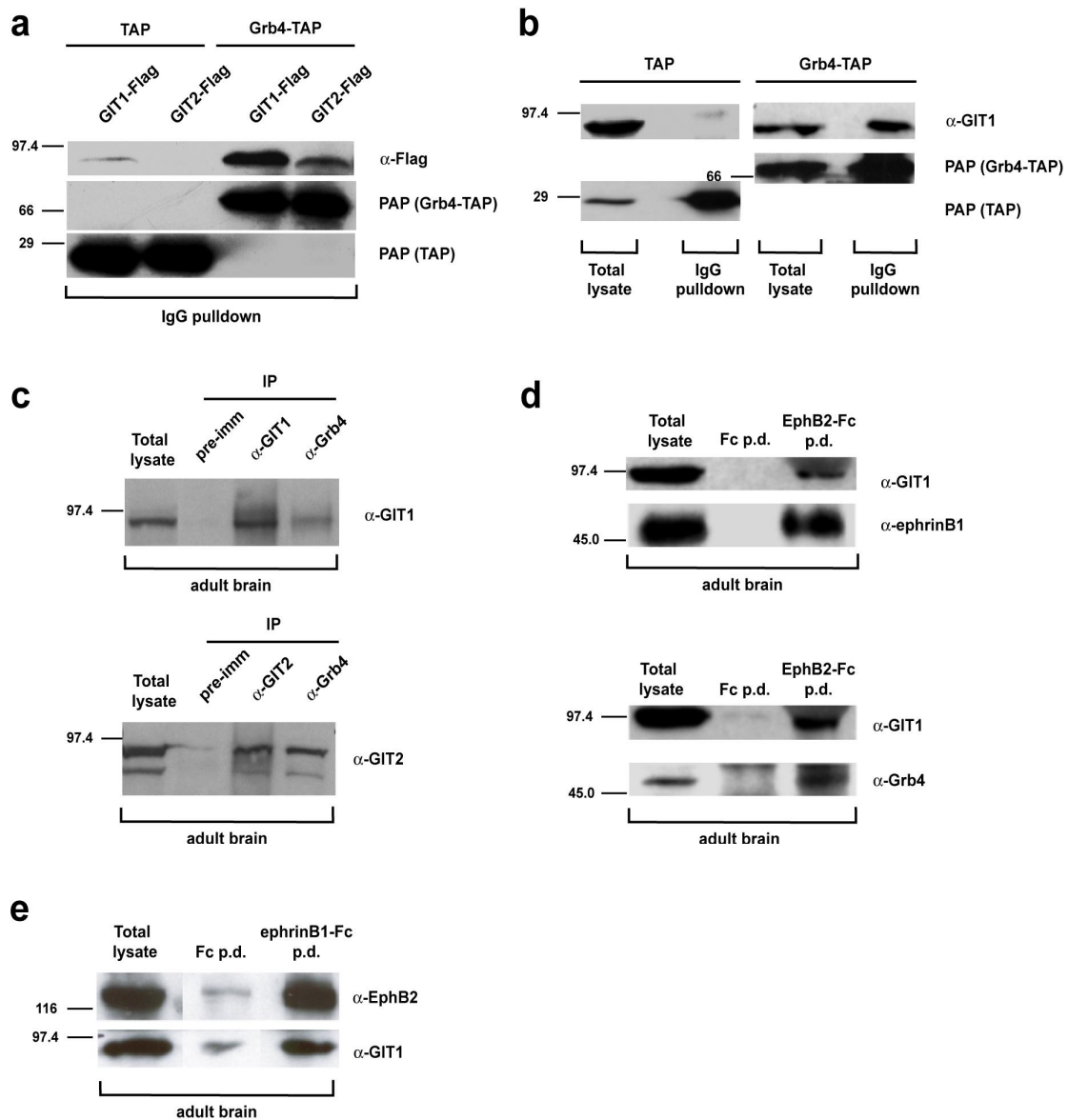
Protein name
Arf GTPase-activating protein GIT1, Cat1
Arf GTPase-activating protein GIT2, Cat2
FKSG30
Heat shock cognate protein 54
hnRNP A2/B1
inositol polyphosphate 5-phosphatase OCRL-1
prolactin-inducible protein precursor
Rho-GEF 6, Cool-2, α PIX
Rho-GEF 7, Cool-1, β PIX
similar to tubulin α -chain isotype m- α -6-mouse
similar to tubulin, beta 5
TPMSK3 (fragment)
tropomyosin 1 (ALPHA)
tropomyosin isoform
tubulin α -2 chain
voltage-gated sodium channel α -subunit

Table 1. Shortlist of Grb4 interactors identified by tandem affinity purification from SK-N-BE2 cell stably expressing Grb4-CTAP.

To validate the tandem affinity purification results, we tested the ability of Grb4 to associate with the novel interactor GIT1 in a biochemical IgG pull-down assay in HeLa cells. We transfected HeLa cells with Grb4-TAP, or TAP as a negative control, together with GIT1- or GIT2-Flag and incubated the cell lysates with rabbit IgG agarose beads, which pull down via the Protein A portion of the TAP affinity tag. Western blotting analysis of the IgG precipitates showed that GIT1- and GIT2-Flag were co-precipitated with Grb4-TAP and not detected in the co-precipitations with the control TAP (**Figure 12a**). These results were further confirmed by experiments showing endogenous GIT1 co-precipitating with Grb4-TAP in transfected HeLa cells (**Figure 12b**). We next asked whether Grb4 and GIT1 form a complex *in vivo* in the mouse brain. To address this question we performed co-immunoprecipitation experiments from adult mouse brain extracts using specific antibodies against these proteins. Immunoprecipitation with anti-Grb4 antibodies precipitated GIT1 and GIT2, but did not if pre-immunization serum was used (**Figure 12c**). These results indicate that Grb4 associates with GIT1 and GIT2 *in vivo*.

To investigate the involvement of the Grb4-GIT1 complex in ephrinB reverse signaling, we attempted to precipitate a triple complex from adult mouse brain formed by ephrinB, Grb4 and GIT1 using EphB2-Fc. Whole-brain lysates were mixed with soluble EphB2-Fc, which had been pre-clustered with anti-human immunoglobulin- γ (IgG) to pull down ephrinB and any associated protein. In these experiments, Grb4 and GIT1 were found to co-precipitate *in vivo* with ephrinB1 in brains of adult mice (**Figure 12d**). As a control, precipitation using unfused Fc did not co-precipitate any of these three molecules. Thus, Grb4 and GIT1 form a ternary complex with ephrinB ligand, suggesting a role of Grb4-GIT1 in ephrinB reverse signaling in adult mouse brain. To investigate whether GIT1 and Grb4 also play a role in Eph receptor forward signaling, we next tested the ability of GIT1 and Grb4 to bind to endogenous EphB receptor by using soluble ephrinB1-Fc pre-clustered with anti-human-IgG to co-precipitate potential EphB binding proteins. GIT1 was shown to bind to EphB receptor from adult mouse brain, while Grb4 was not detectable in these ephrinB1-Fc-pulldowns (**Figure 12e** and data not shown) indicating that GIT1 may be a general signaling compound downstream of the receptor and the ligand. In case of the receptor GIT1 appears not to be recruited by Grb4 but might be recruited instead by Nck, which has already been shown to interact with EphB receptors.

5. Results



5.1.4 GIT1 binds to the SH2 domain of Grb4 via its synaptic localization domain (SLD)

As mentioned before, GIT1 is targeted to synapses by a newly identified synaptic localization domain (SLD) and the molecules acting upstream and targeting GIT1 to the synapses remained to be elucidated (Zhang, H. et al. 2003). Therefore, we next attempted to map the region of GIT1 that is involved in the association with Grb4. Deletion of the SLD in GIT1 (GIT1 Δ SLD) (**Figure 13e**) led to the disruption of its interaction with Grb4 (**Figure 13a**). Therefore, the SLD domain is necessary for the binding to Grb4. Moreover, the SLD domain is sufficient to associate with Grb4, since the isolated SLD domain co-precipitated with Grb4 in HeLa transfected cells (**Figure 13b**). To discard the possibility of a non-proper folding of the deletion mutant we next tested the ability of GIT1 Δ SLD to bind endogenous β PIX. β PIX was shown to bind to GIT1 via SHD-1 (Spa-homology domain 1) (Zhao et al. 2000a), and indeed endogenous β PIX was still able to interact with GIT1 Δ SLD in HeLa cells (**Figure 14a**). The fact that β PIX has been found in our TAP/MS analysis may point to an indirect Grb4- β PIX interaction, which is likely to occur via GIT1.

Figure 12. GIT1 interacts with Grb4. (a) GIT1 and GIT2 interact with Grb4 in HeLa cells. Expression constructs of GIT1- and GIT2-Flag were co-expressed in HeLa cells with Grb4-TAP or the isolated TAP-tag as control. IgG pull-downs were analyzed by Western blotting with the indicated antibodies. Grb4-TAP and TAP were detected by a peroxidase (POD)-conjugated anti-POD antibody (PAP) antibody. (b) Endogenous GIT1 interacts with Grb4 in HeLa cells. HeLa cells were transiently transfected with Grb4-TAP or TAP as control. Total lysates and IgG pull-downs were analyzed by Western blotting with the indicated antibodies. (c) GIT1 and GIT2 associate with Grb4 in adult mouse brain. Whole brains from adult mice were lysed and immunoprecipitated with anti-GIT1, anti-GIT2, anti-Grb4 and pre-immunization serum (pre-imm). The immunoprecipitates were analyzed by Western blotting for GIT1 (upper panel) and GIT2 (lower panel). (d) GIT1 forms a triple complex with Grb4 and ephrinB1 in adult mouse brain. Whole brain lysates were incubated with EphB2-Fc to precipitate ephrinB or with Fc as a control. Precipitates were analyzed by Western blotting for GIT1 and ephrinB1 (upper panel) and GIT1 and Grb4 (lower panel). (e) GIT1 also interacts with EphB receptor in adult mouse brain. Whole brain lysates were incubated with ephrinB1-Fc to precipitate EphB or with Fc as a control. Precipitates were analyzed by Western blotting for EphB2 (upper panel) and GIT1 (lower panel). p.d.: pull down

5. Results

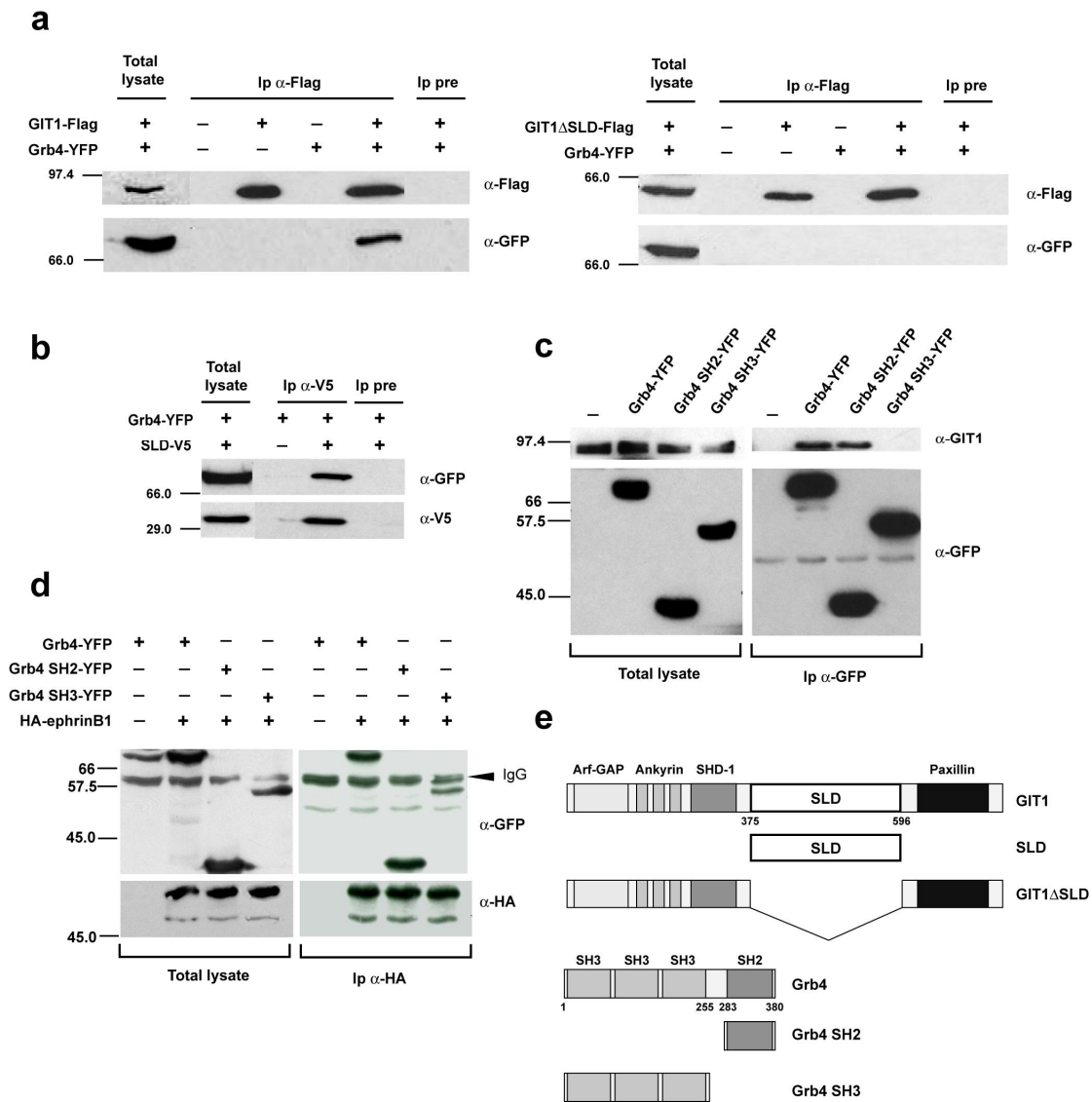


Figure 13. GIT1 binds to Grb4 through its synaptic localization domain (SLD). (a) Grb4 does not bind to SLD-deficient GIT1. Expression constructs of GIT1- (left panel) and GIT1 Δ SLD-Flag (right panel) were co-expressed in HeLa cells with Grb4-YFP. Flag-immunoprecipitates were analyzed by Western blotting with the indicated antibodies. (b) SLD in GIT1 is sufficient to bind to Grb4. HeLa cells were transiently co-transfected with SLD-V5 and Grb4-YFP. V5-immunoprecipitates were analyzed by Western blotting with the indicated antibodies. (c) Grb4 binds to GIT1 via its SH2 domain. HeLa cells were transiently transfected with full length Grb4, Grb4-SH2 and Grb4-SH3 (containing all three native SH3 domains) all fused to YFP. The GFP-immunoprecipitates were analyzed by Western blotting with anti-GFP and anti-GIT1 to detect endogenous GIT1. (d) Grb4 binds to ephrinB1 through its SH2 and SH3 domains. Expression constructs of full length Grb4-YFP, Grb4 SH2-YFP and Grb4 SH3-YFP were co-expressed in HeLa cells with HA-ephrinB1. HA-immunoprecipitates were analyzed by Western blotting with the indicated antibodies. (e) Schematic diagram of the full-length and deletion constructs of GIT1 and Grb4. The indicated domains are as follows: ADP-ribosylation factor (ARF)-GAP domain (Arf-GAP), ankyrin repeats (Ankyrin), Spa2 homology domain 1 (SHD-1), synaptic localization domain (SLD), paxillin binding site (paxillin), Src homology domain 3 (SH3) and Src homology domain 2 (SH2). pre: pre-immunization serum

Grb4 comprises three N-terminal SH3 domains and one C-terminal SH2 domain (Braverman and Quilliam 1999). To analyze the domains of Grb4 that are involved in the association with GIT1, we generated two YFP-fusion proteins, which contain either all three Grb4 SH3 domains (Grb4 SH3-YFP) or the Grb4 SH2 domain (Grb4 SH2-YFP), and tested their ability to interact with GIT1. Equal amounts of YFP-tagged Grb4, SH2 and SH3 were recovered from all transfected cells by immunoprecipitation with the anti-GFP antibody (**Figure 13c**). Endogenous GIT1, however, was only detected in the anti-GFP immunoprecipitates from HeLa cell lysates expressing either full-length Grb4-YFP or Grb4 SH2-YFP. Grb4 SH3-YFP was not able to interact with GIT1. These results were further confirmed by the converse immunoprecipitation experiments in which Grb4-YFP and Grb4 SH2-YFP were co-precipitated with GIT1-Flag (**Figure 14c**). Association of transfected YFP-fusion proteins Grb4 and SH3, but not SH2 to endogenous protein kinase C-related kinase (PRK2) (**Figure 14b**), as shown previously (Braverman and Quilliam 1999), demonstrated a proper folding of Grb4 SH3-YFP.

Grb4 SH2 domain has previously been shown to bind to phosphorylated ephrinB ligands (Cowan and Henkemeyer 2001). Since we postulate the existence of a triple complex containing ephrinB ligands, Grb4 and GIT1, and Grb4 binds to GIT1 by its SH2 domain, we next investigated the possibility that the Grb4 molecules involved in such a complex would bind to ephrinB by the SH3 domains. We co-transfected HeLa cells with YFP-tagged Grb4, Grb4 SH2 and Grb4 SH3 together with HA-ephrinB1. HA-immunoprecipitates revealed the association of ephrinB1 with both the SH2 and the SH3 domains of Grb4, suggesting that Grb4 is also able to interact with ephrinB ligands via its SH3 domains (**Figure 13d**).

5. Results

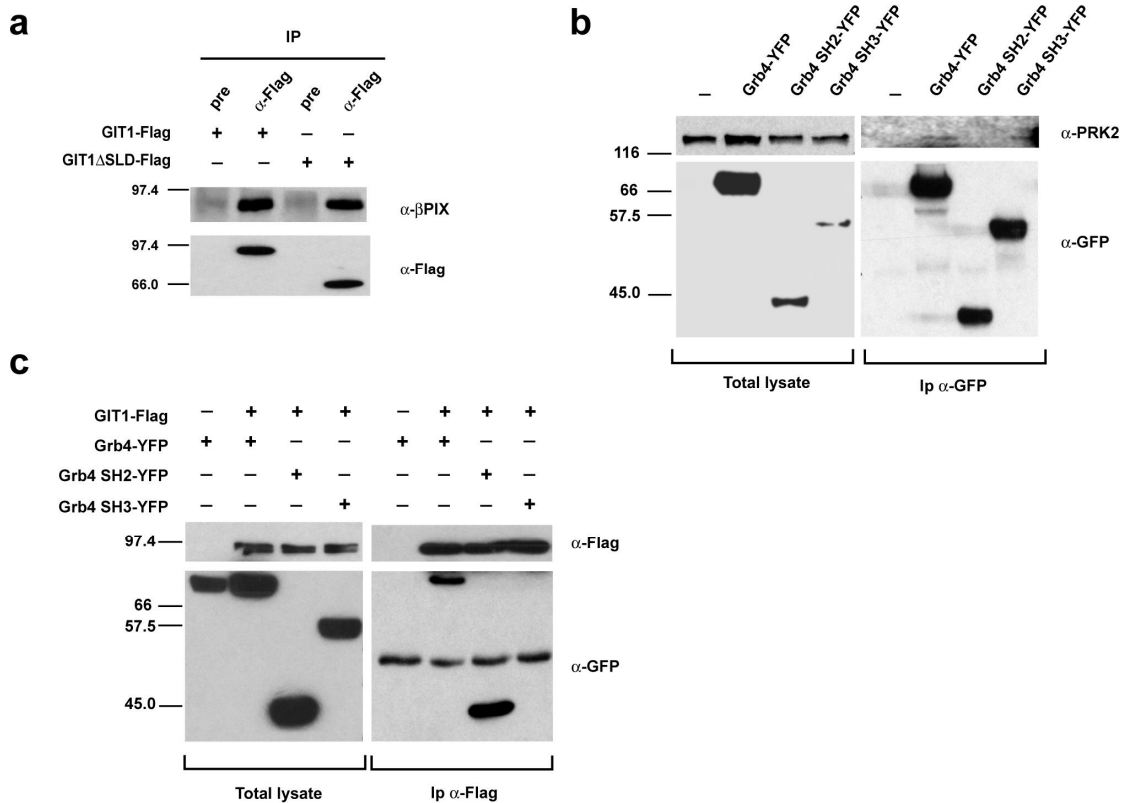
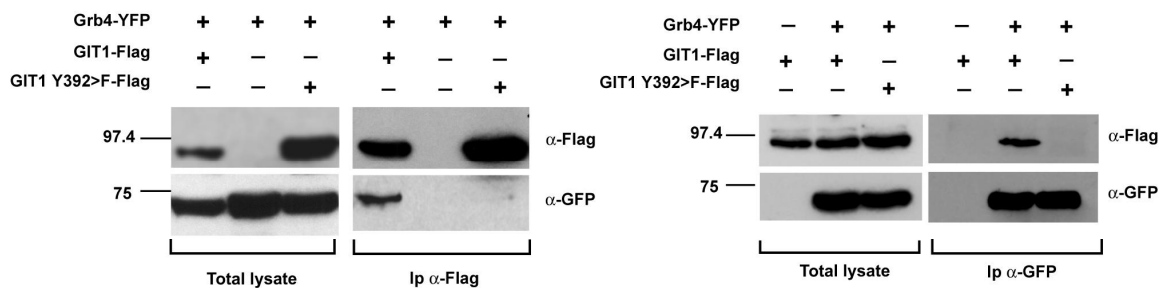
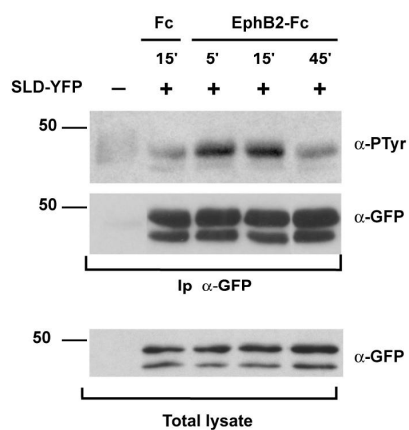
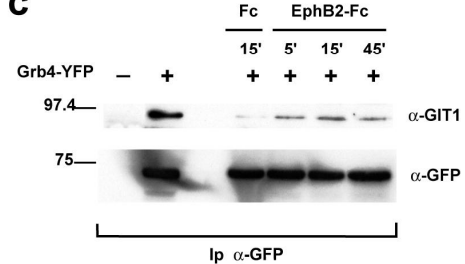
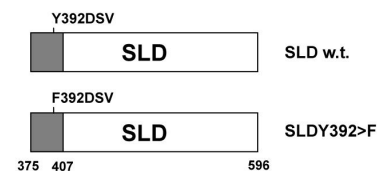


Figure 14. GIT1- and Grb4-deletion constructs are properly folded and bind to known interactors. (a) SLD-deficient GIT1 (GIT1ΔSLD) is still able to interact with βPIX. HeLa cells transiently expressing GIT1-Flag or GIT1ΔSLD-Flag were lysed, immunoprecipitated (IP) with pre-immunization serum (pre) or anti-Flag antibodies and analyzed by Western blotting with anti-Flag and anti-βPIX antibodies to detect endogenous βPIX. (b) SH2-deficient Grb4 (Grb4 SH3) still interacts with PRK2. HeLa cells were transiently transfected with full length Grb4, Grb4 SH2 or Grb4 SH3 (containing all three native SH3 domains) all fused to YFP. The GFP-immunoprecipitates were analyzed by Western blotting with anti-GFP and anti-PRK2 to detect endogenous PRK2. (c) GIT1 associates with the SH2 domain of Grb4. HeLa cells were transiently co-transfected with GIT1-Flag and full length Grb4-, Grb4 SH2- or Grb4 SH3-YFP. Flag-immunoprecipitates were analyzed by Western blotting with anti-GFP and anti-Flag antibodies.

5.1.5 Tyr392 in the SLD of GIT1 is required for Grb4 binding

The fact that the SLD domain of GIT1 binds to the SH2 domain of Grb4 suggests that tyrosine phosphorylation sites in SLD mediate such binding. Among the 5 tyrosine residues in the SLD domain, only Tyr392 in the N-terminus was predicted by NetPhos software (<http://www.cbs.dtu.dk/services/NetPhos>) to be phosphorylated with high probability. Interestingly, Tyr392 resides in a region of 32 aa in the N-terminus of the SLD and the deletion of this region has been demonstrated to significantly decrease the localization of GIT1 to synapses (Zhang, H. et al. 2003). We therefore mutated the

tyrosine 392 in GIT1 into phenylalanine (Y392>F), a non-phosphorylatable aa, to test its requirement for the interaction with Grb4. Equal amounts of Flag-tagged wild-type GIT1 and mutated GIT1Y392>F were recovered from all transfected cells by immunoprecipitation with the anti-Flag antibody (**Figure 15a**). While Grb4-YFP co-precipitated with wild-type GIT1-Flag in HeLa cells, the mutation in GIT1Y392>F-Flag led to a disruption of the interaction of Grb4-YFP with GIT1. Reverse immunoprecipitation of Grb4-YFP lead to the same results: only GIT1 wild type and not the mutant was co-precipitated with Grb4 (**Figure 15a**). Therefore, these findings suggest that phosphorylation of tyrosine 392 in the SLD domain of GIT1 is required for the interaction with Grb4. The kinase responsible for such phosphorylation is so far unknown.

a**b****c****d**

5.1.6 EphrinB reverse signaling induces the phosphorylation of GIT1 in Tyr392 and the formation of a Grb4-GIT1 complex

Since Tyr392 was required for GIT1-Grb4 binding, we next investigated whether activation of ephrinB ligands would lead to phosphorylation of the SLD domain in Tyr392. We transfected HeLa cells stably expressing ephrinB1 (HeLa-ephrinB1) with SLD-YFP and, to follow the kinetics of phosphorylation of SLD, we stimulated the cells for 5, 15 and 45 minutes with pre-clustered EphB2-Fc (**Figure 15b**). Equal amounts of SLD-YFP were recovered from all transfected cells by immunoprecipitation with the anti-GFP antibody. Immunoblotting with anti-phosphotyrosine antibody 4G10 revealed a transient, rapid increase of phosphorylated SLD-YFP after 5 minutes stimulation, which returned to baseline by 45 minutes.

Moreover, we also investigated whether the binding of GIT1 to Grb4 was regulated directly by ephrinB ligand activation. We transfected HeLa-ephrinB1 cells with Grb4-YFP and analyzed the binding of endogenous GIT1 to Grb4 after stimulation with EphB2-Fc (**Figure 15c**). After 5 minutes stimulation with pre-clustered EphB2-Fc, GFP-immunoprecipitates already showed endogenous GIT1 binding to Grb4. In agreement with the kinetics of phosphorylation of the SLD, the Grb4-GIT1 complex was transient and decreased after 45 minutes. GIT1 was practically undetectable in immunoprecipitates from Fc-stimulated cells.

Figure 15. Grb4-GIT1 binding is regulated by ephrinB reverse signaling. (a) The Y392>F mutation in GIT1 abolishes the binding of Grb4. Expression constructs of GIT1- or GIT1 Y392>F-Flag were co-expressed in HeLa cells with Grb4-YFP. Flag- (left panels) and GFP-immunoprecipitates (right panels) were analyzed by Western blotting with the indicated antibodies. (b) Tyrosine phosphorylation in SLD is induced upon ephrinB ligand activation. HeLa-ephrinB1 cells were transiently transfected with SLD-YFP and stimulated with pre-clustered EphB2-Fc or Fc for the indicated time points. Total lysate were analyzed for levels of transfected SLD-YFP (lower panel) and were immunoprecipitated with anti-GFP and analyzed by immunoblotting with α -P-Tyr (4G10) (upper panel) and anti-GFP (middle panel). (c) GIT1 is recruited to Grb4 after ephrinB ligand activation. Full length Grb4-YFP was expressed in HeLa-ephrinB1 cells. Cells were stimulated with pre-clustered EphB2-Fc or Fc for the indicated time points and GFP-immunoprecipitates were analyzed by Western blotting for endogenous GIT1 (upper panel) and for Grb4-YFP levels. (d) Schematic diagram of the SLD including Tyr392 required for binding of Grb4 and present in the NH₂-terminal 32 amino acids, which have been previously shown to contribute to efficient synaptic localization.

5.1.7 Stimulation with EphB receptors recruits GIT1 to ephrinB patches at the synapse in hippocampal neurons

We next investigated the subcellular distribution of GIT1 in hippocampal neurons and its behavior after stimulation of those neurons with EphB receptors. We stimulated dissociated hippocampal neurons (14 DIV) for 10 minutes with pre-clustered EphB2-Fc (**Figure 16i-p**) or Fc as a control (**Figure 16a-h**). Stimulation with EphB2-Fc, but not Fc, induced the formation of large clusters at the membrane visualized with anti-human Fc antibody conjugated to TexasRed (**Figure 16j, n**). Triple immunostainings with anti-human Fc, anti-GIT1 and anti-PSD-95 antibodies revealed a redistribution of endogenous GIT1 protein into clusters along the neuronal processes that overlapped with EphB/ephrinB complexes and postsynaptic marker proteins in EphB2-Fc-stimulated neurons (**Figure 16m-p**), but not in unstimulated neurons (**Figure 16e-h**). Together these data indicate that GIT1 colocalizes in a regulated fashion with activated ephrinB in postsynaptic synapses of living neurons.

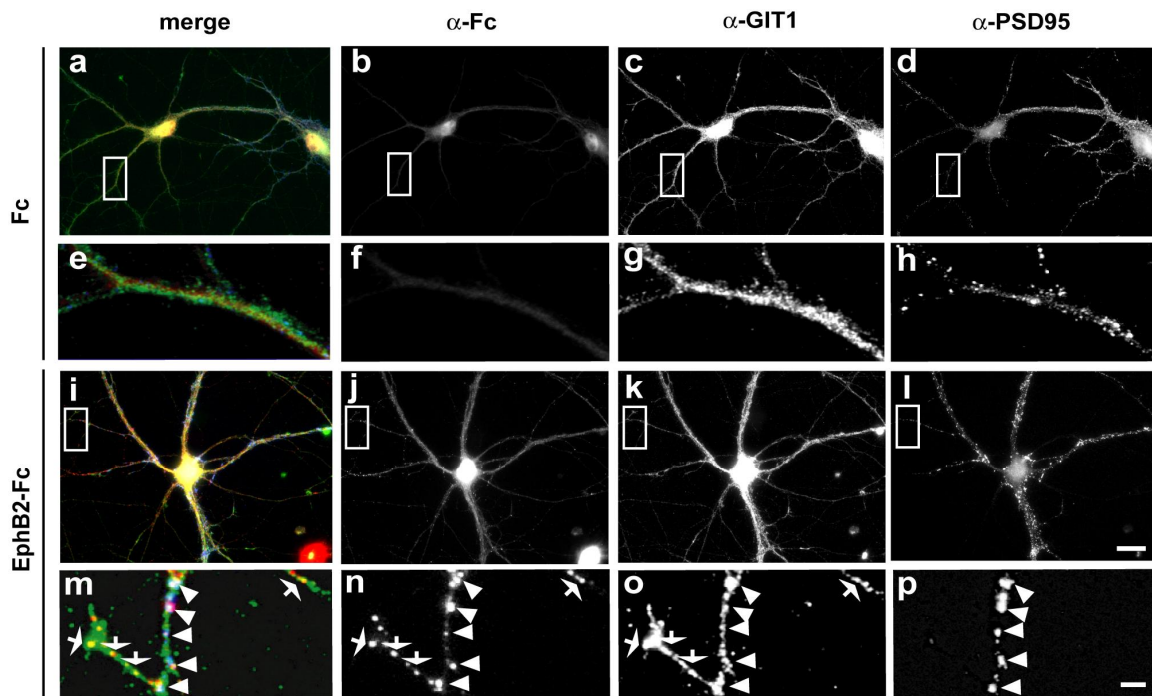


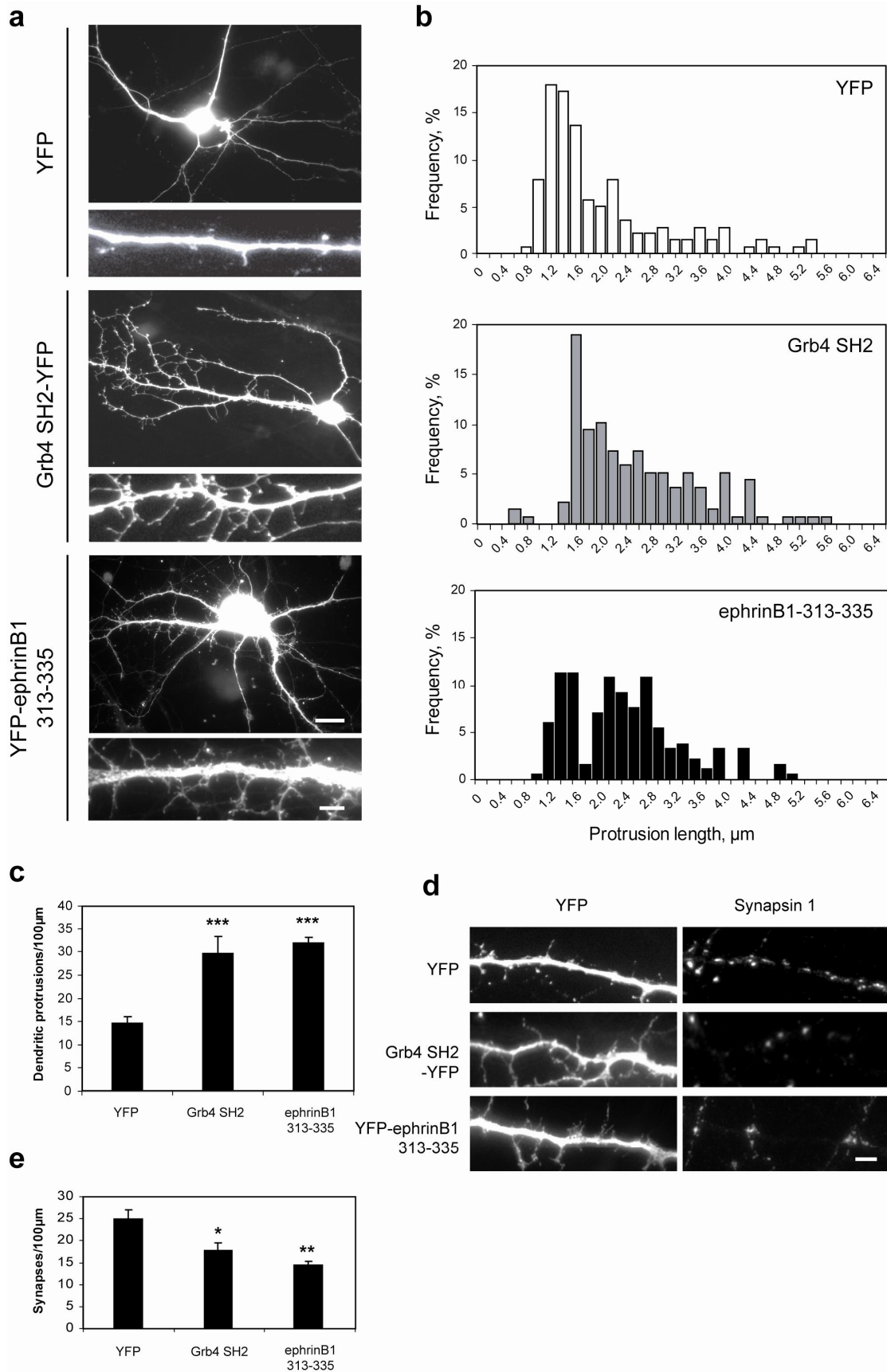
Figure 16. GIT1 is recruited to ephrin patches at the synapse. GIT1 is recruited to ephrin patches at the synapse. Primary rat hippocampal neurons isolated from E18.5 rats were cultured and were stimulated at 14 DIV with Fc (**a-h**) or EphB2-Fc (**i-p**). Receptor bodies, bound to ephrinB ligand, were visualized with an anti-human Fc antibody conjugated to TexasRed (**j, n**). Fc-stimulated neurons showed only background staining (**b, f**). Distribution of endogenous proteins detected with an anti-GIT1 polyclonal (**c, g, k, o**) and an anti-PSD-95 monoclonal antibody (**d, h, l, p**) is shown. In the merge panels (**a, e, i, m**), the three signals are shown: GIT1 (green), receptor bodies (red) and PSD-95 (blue). Bars: (top) 20 μm ; (bottom) 2 μm .

5.1.8 Disruption of ephrinB signaling via Grb4 and GIT1 affects spine morphogenesis and synapse formation

To further define the physiological significance of ephrinB/Grb4/GIT1 signaling in spine formation, we attempted to interfere with this signaling pathway by expressing two different dominant negative constructs in neurons: (1) the Grb4 SH2 domain, which interferes with the binding of endogenous GIT1 to Grb4, and (2) a small interfering ephrinB peptide containing the shortest sequence within the intracellular domain of ephrinB1 required for interaction with Grb4 (Cowan and Henkemeyer 2001), which competes away the complex Grb4-GIT1 from ephrinB ligands. As reported previously, hippocampal neurons in culture require approximately 3 weeks to fully develop mature spines under normal conditions. Before 10 DIV, the majority of

dendritic protrusions are long, filopodia-like structures (Ethell and Yamaguchi 1999). It was previously shown that the expression of the SLD domain of GIT1 induced an increase in long and thin dendritic filopodia-like protrusions, suggesting that perturbing GIT1 localization results in defects in spine morphology and synapse formation (Zhang, H. et al. 2003). Here we show that neurons expressing Grb4 SH2 domain and the ephrinB1 peptide fused to YFP, presented a high increase in the number of long, thin dendritic protrusions (**Figure 17a**). The average length of protrusions was increased from $1.86 \pm 0.04 \mu\text{m}$ in the YFP-transfected controls to $2.01 \pm 0.01 \mu\text{m}$ in the Grb4 SH2-YFP and $2.23 \pm 0.02 \mu\text{m}$ in the ephrinB1-313-335-YFP transfected neurons (**Figure 17b**). In addition, in the Grb4 SH2 domain and ephrin peptide expressing neurons, the linear density of dendritic protrusions (number of protrusions per 100 μm dendrite) increased significantly compared with neurons expressing YFP (**Figure 17c**). Thus, these data suggest that perturbing Grb4-GIT1 recruitment to ephrinB ligands at the synapse is crucial for normal spine morphogenesis. The morphological formation and maturation of spines in normal cultured hippocampal neurons directly correlates with synapse formation (Ethell and Yamaguchi 1999). We next asked if neurons, which fail to make proper mushroom-shaped spines develop correct synapses. We analyzed synapse formation by counting the number of clusters of the pre-synaptic protein synapsin1. In the Grb4 SH2- and ephrinB1 peptide-expressing neurons the linear density of synapses (number of synapses per 100- μm dendrite) decreased significantly as compared to neurons expressing YFP (**Figure 17d, e**). This is consistent with previous findings in neurons overexpressing GIT1-SLD, which also showed decreased synapsin1 staining (Zhang, H. et al. 2003). These results suggest that the proper localization of the Grb4-GIT1 complex is not only necessary for the formation of spines, but is also important for synapse formation.

Figure 17. Disruption of ephrinB signaling through Grb4 and GIT1 affects spine morphogenesis and synapse formation. (a) Rat hippocampal neurons were transfected at 7 DIV with YFP as control, Grb4 SH2-YFP or YFP-ephrinB1-313-335, fixed at 11 DIV and examined. Bars: (top) 20 μm ; (bottom) 2 μm . (b-c) Quantification of the length (b) and density (c) of dendritic protrusions ($n > 500$) analyzed for each transfection condition. Bars represent standard error of the mean. *, $P < 0.05$, **, $P < 0.005$, ***, $P < 0.0005$. (d) Effects of Grb4 SH2-YFP and YFP-ephrinB1-313-335 expression on synaptic density. Rat hippocampal neurons were transfected with the indicated constructs at 7 DIV and stained for synapsin1 (right panel) at 11 DIV. Bars, 2 μm . (e) Quantification of synaptic linear density analyzed for each transfection condition. Synapse formation was analyzed by numbers of synapsin1-positive immunoreactivities.



5.2 Proteomic analysis of PDZ-mediated ephrinB reverse signaling

To identify new components involved in PDZ domain-mediated reverse signaling downstream of ephrinB ligands, we used the tandem affinity purification (TAP) strategy. The TAP procedure is a sensitive and selective method to purify, under close-to-physiological conditions, multiprotein complexes formed *in vivo* (Rigaut et al. 1999; Gavin et al. 2002). We chose to TAP-tag the known PDZ domain-containing ephrinB interactor GRIP1 (Bruckner et al. 1999), which has recently been demonstrated to be recruited to ephrinB ligand in so-called raft membrane microdomain signaling centers. This TAP approach revealed a set of several novel GRIP1 interactors. Association with one new binding partner, 14-3-3 proteins, was further characterized and found to be restricted to raft membrane microdomains. A single Thr residue in a putative 14-3-3 binding site in GRIP1 was identified and shown to be required for the formation of the GRIP1-14-3-3 complex. Moreover, we have also applied the TAP technology *in vivo*. Transgenic mice expressing GRIP1-CTAP were generated and the tagged protein shown to form functional complexes in those mice.

5.2.1 Identification of GRIP1 complexes by tandem affinity purification

After stable integration into SK-N-BE2 cells by retrovirus-mediated gene transfer, the tagged protein was purified and TAP/MS analysis of the protein complexes formed around GRIP1 was performed. Infected clones were subjected to tandem affinity purification, a procedure consisting of two specific binding and elution steps under mild conditions, which preserve the integrity of non-transient protein-protein interactions (Rigaut et al. 1999) (**Figure 18**). The affinity-purified complexes were resolved on SDS-PAGE and Coomassie-stained (**Figure 19a**). GRIP1 interactors were identified by peptide sequencing using tandem mass spectrometry (LC-MS/MS). A database generated by large scale TAP analysis in this cell line has been assembled by collaborators at Cellzome AG (Heidelberg) containing a high number of protein-protein interactions and allowing the reliable assessment of the specificity of a given interaction (data not shown). Cellzome has also identified a set of potentially sticky

proteins, suspected to purify nonspecifically in the TAP method, which provides information about molecules, which are very likely to be false positives and should therefore be excluded from any further validation. In total, the raw data set contained 134 non-redundant protein hits. Among those 132 interactors in total, 73 (54%) were considered to be sticky (**Table 2**) due to their frequent identification as interactors of various TAP-tagged molecules. The remaining 59 interactors (**Table 2**) were to be selected for further validation by literature screening on the basis of potential relevance in ephrinB reverse signaling.

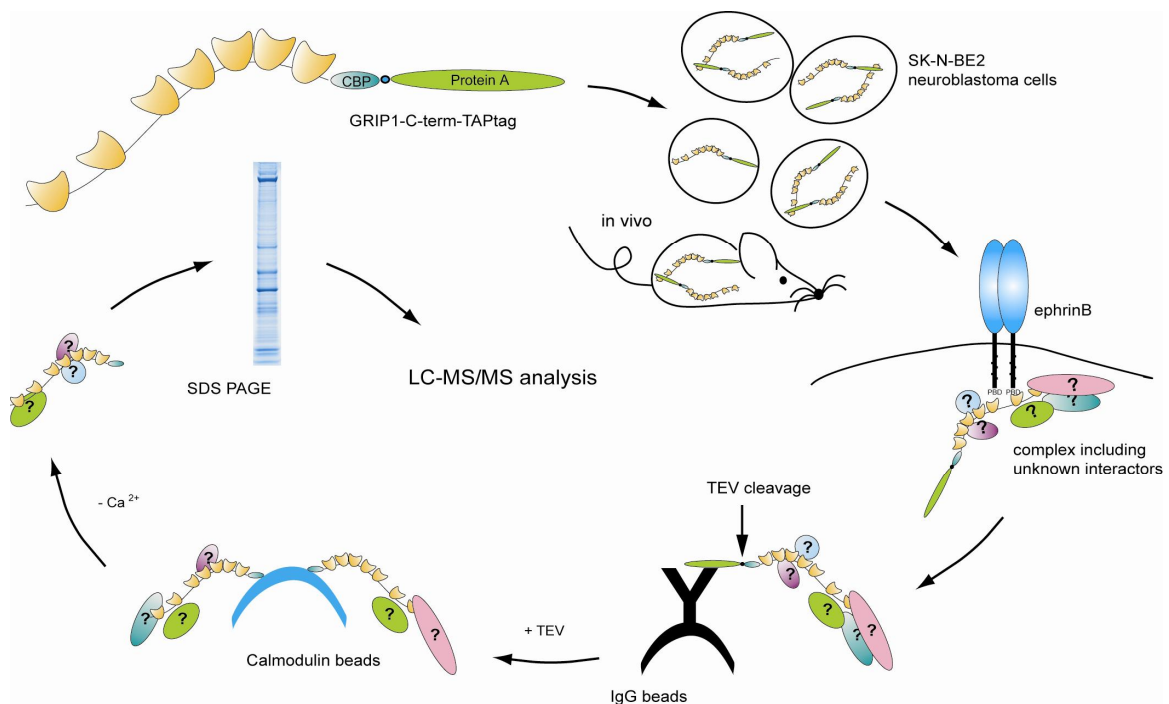


Figure 18. Overview of the Tandem Affinity Purification (TAP) strategy. The TAP tag comprises CBP (Calmodulin binding peptide) linked to a Protein A immunoglobulin (Ig)G-binding domain separated by a tobacco etch virus (TEV) protease cleavage site. The purification of tissue or cell lysate consists of four specific steps: first, high affinity binding to IgG beads; second, elution using TEV protease; third, high-affinity binding to calmodulin beads in the presence of Ca²⁺; and finally, elution using Ca²⁺-chelating agents.

5. Results

Protein name	
14-3-3 protein beta/alpha	inositol polyphosphate 5-phosphatase OCRL-1
14-3-3 protein eta	L-lactate dehydrogenase A chain
14-3-3 protein sigma	myosin heavy chain, smooth-muscle isoform
14-3-3 protein tau	myosin IC
26S proteasome non-ATPase regulatory subunit 2	myosin light chain 1, slow-twitch muscle A
ADP-ribosylation factor 4	myosin light chain alkali, smooth-muscle
ATP-dependent DNA helicase II, 70 kDa subunit	myosin, light polypeptide, non-sarcomeric
ATP-dependent DNA helicase II, 80 kDa subunit	neurabin II protein, spinophilin
cystatin A	prolactin-inducible protein precursor
DNA replication licensing factor MCM7	SCO2 protein homolog
dopamine beta-hydroxylase precursor	similar to FKSG30
dopamine beta-monoxygenase precursor	similar to heat shock 70KD protein 8
emilin precursor	similar to hnRNP A/B
endothelin-A receptor delta 3-4	similar to hnRNP A2/B1
enhancer of polycomb 1	similar to hnRNP Q2
erythrocyte tropomodulin A	similar to neu differentiation factor - human
eukaryotic translation initiation factor 3 subunit 2	similar to RIKEN cDNA 1200016G03
extracellular glycoprotein lacritin precursor	similar to synovial sarcoma, X breakpoint 4
FKSG30	similar to T-complex protein 10A - human
glial fibrillary acidic protein, astrocyte	similar to tropomyosin 1 (alpha)
growth-arrest-specific protein 1	similar to tropomyosin, fibroblast - human
GRY-RBP	similar to tubulin α -chain, m- α -6 - mouse
heat shock 27 kDa protein	ssDNA-binding protein, mitochondrial precursor
heat shock cognate protein 54	TPMSK3 (fragment)
heat shock-related 70 kDa protein 2	tropomyosin 1 (alpha)
hnRNP A2/B1	tropomyosin 1 alpha chain
histone H2A.F/Z variant, isoform 1	tropomyosin isoform
histone H2A.Z	hypothetical protein FLJ12427
hypothetical protein (fragment)	tyrosine 3-monoxygenase/tryptophan 5-monoxygenase activation protein
IKAPPAB kinase complex-associated protein	

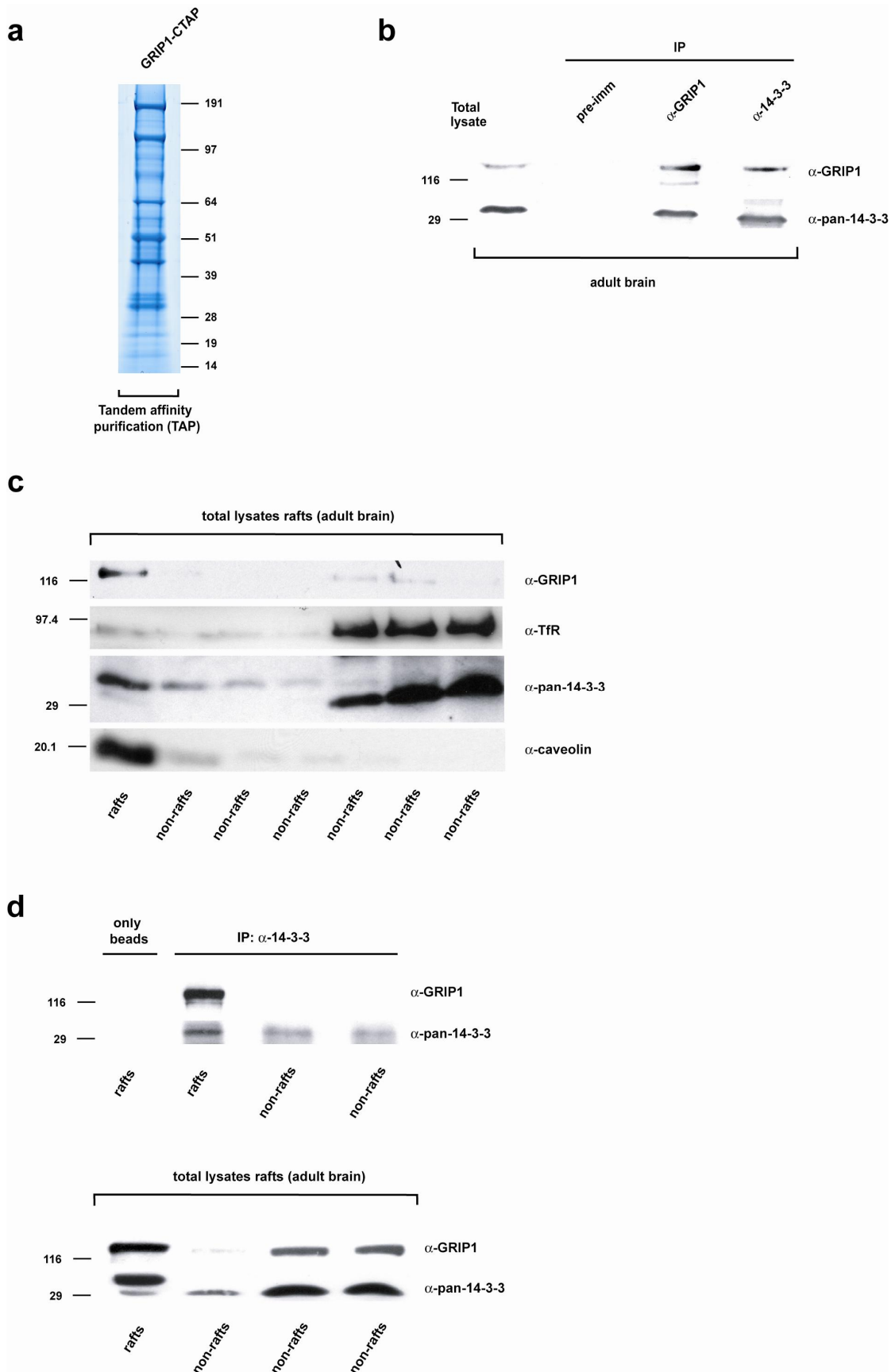
Table 2. Shortlist of GRIP1 interactors identified by tandem affinity purification from SK-N-BE2 cells stably expressing GRIP1-CTAP.

5.2.1.1 Identification of 14-3-3 as a GRIP1 binding protein

14-3-3, a key regulator of cell division, signaling and apoptosis (van Hemert et al. 2001), was identified with high confidence as a GRIP1 interactor. All 7 mammalian 14-3-3-isoforms (β , γ , ϵ , η , σ , τ and ζ) were isolated by tandem affinity purification of GRIP1-CTAP in SK-N-BE2 cells. Further data has confirmed this interaction by reciprocal protein complex purification of 14-3-3-CTAP in the same cell line (Cellzome, personal communication). 14-3-3 proteins are highly conserved small acidic proteins, which, in most cases, regulate cellular processes by binding to specific pSer and pThr motifs within target proteins (Muslin et al. 1996). Two optimal 14-3-3 phosphopeptide ligands with the consensus sequences RSXpS/TXP and RX(Y/F)XpS/TXP [where pS/T represents phosphoserine or phosphothreonine and X is any amino acid] have been defined (Yaffe et al. 1997). The roles of 14-3-3 proteins in cells have been classified on the basis of their mode of action. 14-3-3 proteins can for example induce conformational changes in target proteins as well as occlude specific sequences or structural features (reviewed in Mackintosh 2004). For all their regulatory functions 14-3-3 proteins need to associate in stable homo- and heterodimers (Chaudhri et al. 2003). The complexity of 14-3-3 actions is reflected by the increasing number of binding partners identified. Several studies have used tagged 14-3-3 proteins to purify protein complexes from cells in culture (Jin et al. 2004; Meek et al. 2004; Pozuelo Rubio et al. 2004). 14-3-3 proteins are abundant in brain tissues and, although only few binding partners in brain have been so far postulated, 14-3-3 proteins are clearly critical for brain development, memory and learning, and have been implicated as well in several neurological disorders (reviewed in Mackintosh 2004).

5.2.1.2 14-3-3 interacts with GRIP1 in total mouse brain lysate and forms a complex with GRIP1 exclusively in raft membrane microdomains

To confirm these interactions, we performed co-immunoprecipitation experiments from adult mouse brain extracts using a pan-antibody against 14-3-3. Immunoprecipitation with pan-14-3-3 antibodies co-precipitated GRIP1, but did not if pre-immunization serum was used (**Figure 19b**). Moreover, reverse co-immunoprecipitation pulling down GRIP1 with a specific antibody confirmed the interaction with 14-3-3 (**Figure 19b**) indicating that GRIP1 associates with 14-3-3 *in vivo*. In an attempt to address the functional significance of GRIP1-14-3-3 interaction, we analyzed whether these complexes occurred in raft membrane microdomains, which have been implicated in processes such as sorting in polarized cells and signal transduction. The ligand ephrinB1 has been described, upon stimulation with EphB2 receptor, to associate with GRIP1 in large raft patches that also contain a GRIP1-associated serine/threonine kinase activity (Bruckner et al. 1999). Triton X-100 (TX100)-insoluble raft membrane proteins can be identified by their ability, due to their high lipid content, to float in TX100-containing density flotation gradients as detergent-insoluble glycolipid-enriched complexes (DIGs) (Brown, D. A. and Rose 1992). This property clearly distinguishes them from insoluble complexes formed by the cytoskeleton. As shown in **Figure 19c** and **d** (bottom panel), GRIP1 and 14-3-3 are both found in the top fractions of the flotation gradient, indicating raft localization, as well as in non-raft fractions of adult mice brain. However, despite of the presence of the two proteins in rafts and non-rafts, GRIP1 can only be co-immunoprecipitated using an anti-14-3-3 antibody from the lipid-associated fraction 1 indicating localization of the GRIP1-14-3-3 complex exclusively in rafts of mouse tissue (**Figure 19d**, top panel). Since patches of raft domains are generally considered as signaling centers (Harder et al. 1998) these results show that interaction of the two molecules, may be regulated by a stimulus-dependent mechanism (e.g. Eph receptor stimulation), consistent with an important function in signal transduction .



5.2.1.3 EphrinB ligand, GRIP1 and 14-3-3 form a triple complex in raft membrane microdomains of mouse brain

We next wanted to see whether ephrinB reverse signaling might play a role in recruiting the GRIP1-14-3-3 complex to rafts. EphrinB1 interaction with GRIP2 is regulated by EphB2 receptor binding in NIH3T3 cells stably expressing ephrinB1 and GRIP2 (Manuel Zimmer, personal communication). Thus we immunoprecipitated ephrinB from raft and non-raft fractions of mouse brain using a specific antibody. Western Blot analysis revealed a triple ephrinB-GRIP1-14-3-3 complex that exclusively occurs in raft fractions (**Figure 20**). As shown in **Figure 20**, in non-rafts only ephrinB and 14-3-3 interact, albeit to a much lesser extent as compared to the raft fraction. The non-raft fractions of 14-3-3 seem to be of different isoform composition compared to the 14-3-3 fraction, which is detergent insoluble located (**Figure 19c**). These findings suggest that 14-3-3 may occur in two different pools, possibly as two different isomers: one pool of 14-3-3 interacting with GRIP1 upon its phosphorylation and subsequent recruitment to ephrinB ligand, and the other pool might be associated with the ligand with different regulatory purposes.

Figure 19. Tandem affinity purification of GRIP1-CTAP reveals new GRIP1 interactor. (a) Coomassie-stained SDS-PAGE lane showing tandem affinity-purified GRIP1-CTAP. TAP complexes were run on a NuPAGE 4-12% Bis-Tris gel with MOPS running buffer and complete gel lane was then systematically cut into slices and proteins were digested in-gel with trypsin. Protein identification was performed by LC-MS/MS. (b) 14-3-3 associates with GRIP1 in brain of adult mice. Whole brains from adult mice were lysed and immunoprecipitated with anti-14-3-3, anti-GRIP1 and pre-immunization serum. The total lysates and immunoprecipitates were analyzed by Western blotting for 14-3-3 and GRIP1. (c) A membrane preparation of an adult mouse brain homogenate was subjected to TX100 flotation followed by Optiprep flotation gradients. Seven fractions from top to bottom were collected and analyzed by Western Blotting for the presence of 14-3-3 and GRIP1 proteins. Caveolin and transferrin receptor serve as raft-associated and nonraft proteins, respectively, confirming specificity of the preparation. (d) 14-3-3 interacts with GRIP1 exclusively in rafts. Three fractions from top to bottom were collected and analyzed by Western Blotting for the presence of 14-3-3 and GRIP1 proteins (bottom panel). 14-3-3 immunoprecipitates were analyzed by Western Blotting for the presence of 14-3-3 and GRIP1 proteins (top panel).

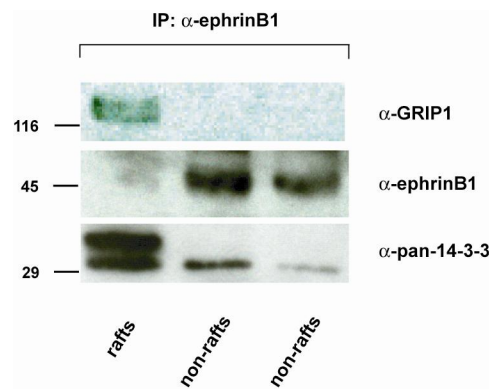


Figure 20. 14-3-3 forms a triple complex with ephrinB and GRIP1 in rafts. One DIG-enriched fraction and two nonraft fractions were immunoprecipitated (IP) with anti-ephrinB. The immunoprecipitates were analyzed by Western blotting for GRIP1, 14-3-3 and ephrinB.

5.2.1.4 Thr956 between GRIP1 PDZ6 and PDZ7 is required for 14-3-3 binding

The data obtained demonstrate that 14-3-3 interacts with GRIP1. Sequence analysis to identify motif(s) in GRIP1 contributing to 14-3-3 binding showed three putative 14-3-3 binding sites inside the linker region between PDZ6 and PDZ7 (852-857, 941-946, 953-958). These sites exactly match the optimal sequence motif of a recognition site I (Muslin et al. 1996; Yaffe et al. 1997) and either contain a serine or a threonine residue at position 0 (**Figure 21a**). To investigate the contribution of these putative recognition motifs to interaction between GRIP and 14-3-3, we mutated serine 944 and/or threonine 956 in GRIP1 into alanine, thus altering these residues predicted to be critical for the interaction with 14-3-3. Equal amounts of HA-tagged wild-type 14-3-3 was recovered from all transfected cells by immunoprecipitation with the anti-HA antibody (**Figure 21b**). While GRIP1-myc and GRIP1S944>A-myc co-precipitated with wild-type HA-14-3-3 in HeLa cells, the mutation in GRIP1T956>A-myc led to a disruption of the interaction of HA-14-3-3 with GRIP1. Mutation analysis of GRIP1 thus indicates a requirement of the most C-terminal 14-3-3 binding site, spanning aa 953-958, for the interaction with 14-3-3. The kinase responsible for such phosphorylation is currently unknown. Identification of such kinase as well as the significance of Thr956 for GRIP1 function *in vivo* will be pursued in future studies.

a**NP_114458. GRIP1 protein (rat)**

MIAVSFKRCQILRRLTKDESPTYKSASQTKPPDGALAVRRQSIPEEFKG 50
 PDZ1 STVVELMKKEGTTLGLTVSGGIDKDGKPRVSNLRQGGIAARSDQLDVGDY 100
LKAVNGINLAKFRHDEIISLLKNVGERVVLEVEYELPPVSIQGSSVMFRT 150
 PDZ2 VEVTLHKEGNTFGFVIRGGAHDDRNRKSRPVVITCVRPGGPADREGTIKPG 200
DRLLSVDGIRLLGTTHAEAMSILKQCGQEQATLLIEYDV SVMDSVATASGP 250
 PDZ3 LLVEVAKTPGASLGVALTTSVCCNKOVIVIDKIKSASTADRCGALHVGDH 300
ILSIDGTSMEYCTLAEATQFLANTDQVKLEILPHHQTRLALKGPDHVKI 350
 QRSDRQLPWPWASSQCSVHTNHHNPHHPDHCRVPALGFPPKALTPNSPP 400
 AMVSSSPTSMSAYSLSLNMGTLPRLSYSTSPRGTMRRRLKPKDFKSS 450
 LSLASSTVGLAGQVVHTETTEVVLTADPVTGFGIQLOGSVFATETLSPP 500
 PDZ4 LISYIEADSPAERCGVLOIGDRVMAINGIPTEDSTFEANOLLRRDSSITS 550
KVTLEIEFDVAESVIPSSGTFHVKLPKKHVELGITISSPSSRKPGDPLV 600
 PDZ5 ISDIKKGVAHRTGTLELGDKLLAIDNIRLDSCSMEDAVQLLQCCEDLVK 650
LKIRKDEDNSDEQEISSGAIITYVELKRYGGPLGITISGTEEPFDPIIIS 700
 PDZ6 LTKGGLAERTGAIHIGDRILAINSSSLKGPLSEAIHLLQMAGETVTLKI 750
KKQTDAPASSPKKLPISHSDDLGDGEDPSPIQRPGKLSDVYPSTVPS 800
 VDSAVDSWDGSGIDARYGSQTTFTQTSYGFNTYDWRSPKKRASLSPVPK 850
FRSQTYPDVGLSNEDWRSTASGFAGASDSADAEQENFWQALEDLETC 900
 GQSGILRELEATIMSGTMSLNHEAPTARSQGRQASFQERSNRPHYSQ 950
TTRSNTLPSDVGRKSVTLRKMKEIKEIMSPTVELHKVTLTKYKDSGMEDE 1000
 PDZ7 GFSVADGLLEKGVYVKNIRPAGPGDLGGLKPYDRLLQVNHVTRDFDCCL 1050
VVPLIAESGNKLDLVISRNPLASQKSIEQPALPSDWSEQNSAFFQQPSHG 1100
 GNLETREPTNTL 1112

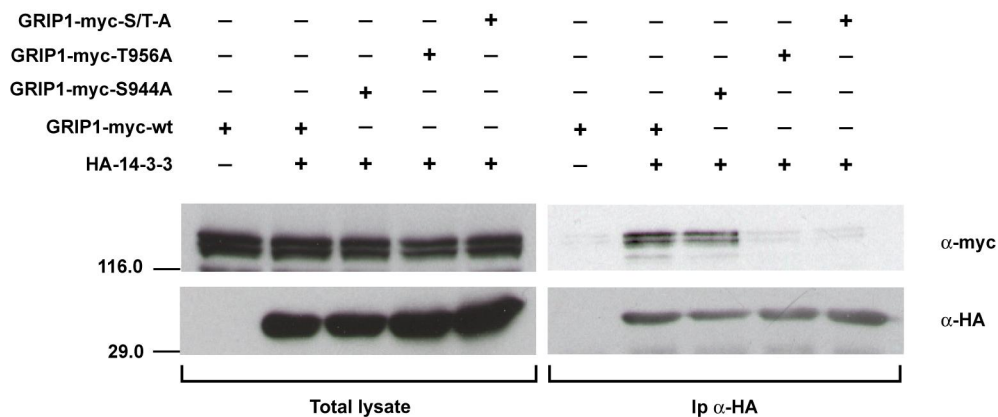
b

Figure 21. Thr956 in PDZ6 of GRIP1 is required for 14-3-3 binding. (a) Amino acid sequence of rat GRIP1. The depicted sequence contains three putative 14-3-3 binding sites in the linker region between PDZ6 and PDZ7 (indicated by red letters). Individual PDZ domains are underlined by closed horizontal bars. (b) The T956>A mutation in GRIP1 abolishes the binding of 14-3-3. Expression constructs of myc-tagged GRIP1 w.t. and GRIP1-S944>A, -T956>A or -S944+T956>A (S/T-A) were co-expressed in HeLa cells with HA-14-3-3. HA-immunoprecipitates (right panel) were analyzed by Western blotting with the indicated antibodies.

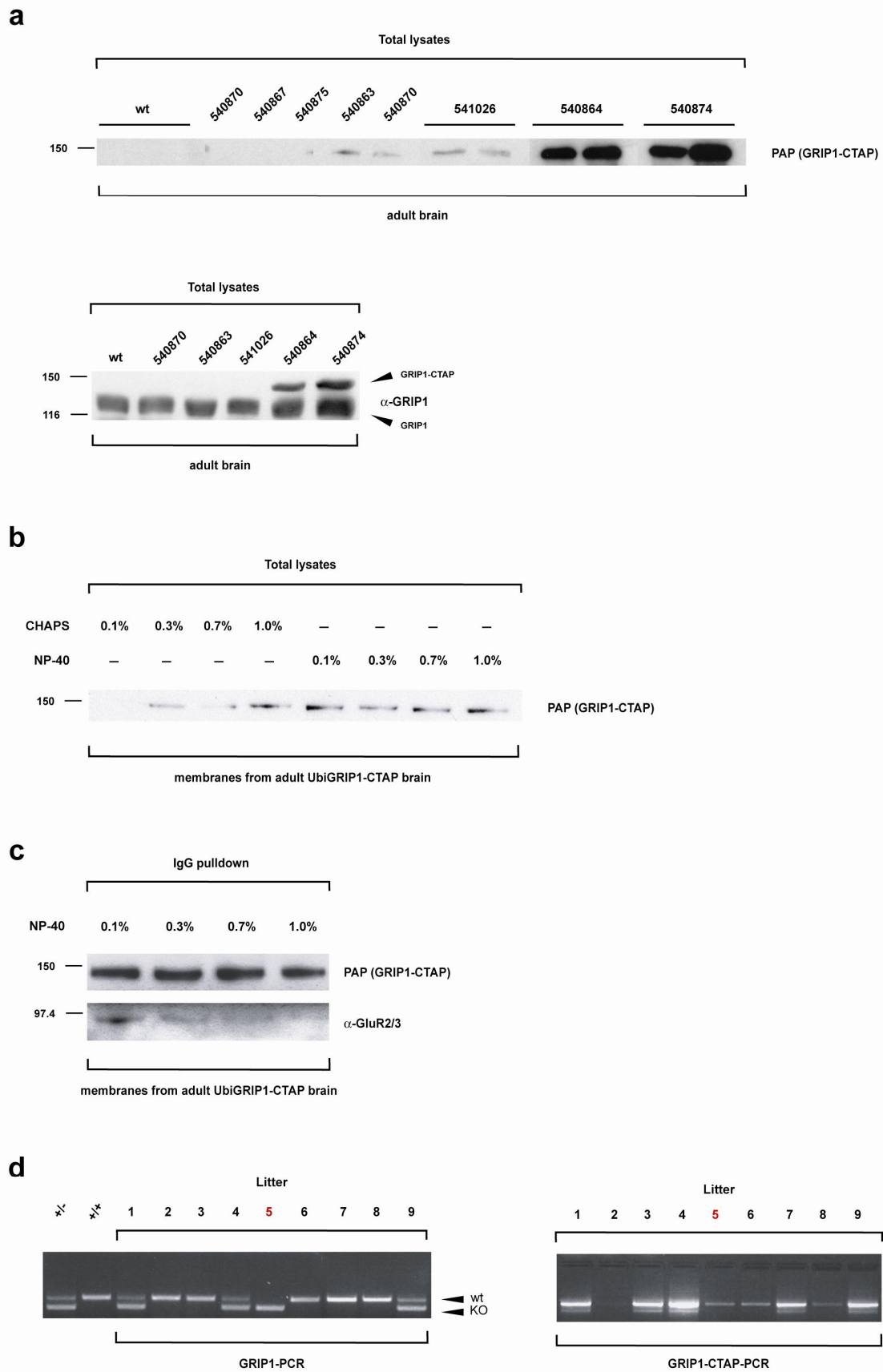
5.2.2 Transgenic expression of GRIP1 in mice to identify protein complexes *in vivo*

We also applied the TAP technology to identify *in vivo* interactors with GRIP. We generated transgenic mice expressing GRIP1-TAP under the control of the human ubiquitin C promoter (Ubi-GRIP1-CTAP). This promoter contains a 1,225-bp fragment of the human ubiquitin C promoter and directs ubiquitous expression to most mouse tissues (Schorpp et al. 1996). The TAP approach in transgenic mice has several advantages over other methods for identification of protein-protein interactions: (a) the use of an *in vivo* model; (b) the purification of a protein complex that has been established in its natural environment, and (c) the possibility of comparison of protein complexes derived from different tissues and at different developmental stages.

5.2.2.1 Transgenic GRIP1-CTAP is expressed in the brain of some founders

Eight founders of the transgenic line expressing GRIP1-CTAP driven by the ubiquitin C promoter gave offspring. UbiGRIP1-CTAP transgenic mice in a C57BL/6 genetic background were fertile and did not show any gross phenotypic abnormalities. As shown in **Figure 22a**, compared to wild-type brain only five lines showed expression in the brain, of which two lines yielded strong (founders 540864 and 540874) and three lines weak expression levels (founders 540863, 540870 and 541026). The weak expressors together with those that did not display any expression (540870, 540867 and 540875) were excluded from further analysis. The two lines displaying the strongest signal (founders 540864 and 540874) were selected and used for further experiments.

5. Results



5.2.2.2 GRIP1-CTAP localizes to the membrane of transgenic brain tissue

Stimulation of ephrinB with soluble EphB2 receptor ectodomain causes the formation of large raft patches that contain GRIP1 protein (Bruckner et al. 1999). It has furthermore been shown that GRIP1 is present in lipid raft fractions isolated from mouse (**Figure 19c, d**) and rat brains (Hering et al. 2003). In fact, two of the binding partners that associate with GRIP1, ephrinB and AMPA receptor, have been shown to be located in rafts (Dong et al. 1997; Bruckner et al. 1999). To identify complexes, which assemble around GRIP1-CTAP and are relevant in ephrinB reverse signaling *in vivo*, we will selectively purify complexes that are associated to the membrane.

To confirm that the GRIP1-CTAP transgenic mice are suitable for the purification of ephrinB-mediated GRIP1 complexes, we next asked if GRIP1-CTAP was properly expressed at the membrane in those mice. Therefore, we performed membrane fractionation assays and incubated the membrane fractions with different amounts of CHAPS or NP-40 for 1h at 4°C. GRIP1-CTAP from membrane fractions was precipitated using rabbit IgGs. IgG-pulldowns were subsequently analyzed by SDS-PAGE and immunoblotted (WB) with PAP-antibody, which specifically detected GRIP1-CTAP at approximately 150kDa (**Figure 22b**). Treatment of membrane fractions with NP-40 gave best results as compared to CHAPS. Thus, a proportion of GRIP1-CTAP is located as expected at the membrane.

Figure 22. GRIP1-CTAP forms functional complexes in transgenic mice. (a) GRIP1-CTAP is expressed at high levels in brain of some founder mice. Total brain lysates were analyzed by Western blotting with the indicated antibodies. GRIP1-CTAP was detected by a peroxidase (POD)-conjugated anti-POD antibody (PAP) or by a specific anti-GRIP1 antibody. (b) Brain homogenates from UbiGRIP1-CTAP^{+/-} mice were subjected to a flotation gradient membrane fractionation assay, treated for 1 hour with CHAPS or NP-40 at different concentrations and analyzed for the presence of GRIP1-CTAP in membranous fractions. Total lysates were analyzed by Western blotting for GRIP1-CTAP using the PAP antibody. (c) Transgenic GRIP1-CTAP interacts with the known GRIP1-interactor GluR2/3. Membranous fractions obtained from transgenic brain homogenates were treated for 1 hour with NP-40 at different concentrations and analyzed for the presence of GluR2/3 by immunoprecipitation with rabbit IgGs. IgG pulldowns were analyzed by Western blotting with the indicated antibodies. (d) GRIP1-CTAP is able to rescue the lethal phenotype of *GRIP1*^{-/-} mice. Tails from different litters were analyzed for the presence of the GRIP1-CTAP transgene and the GRIP1 KO allele.

5.2.2.3 GRIP1-CTAP interacts *in vivo* with GluR2/3, a known interactor of GRIP1

AMPA receptor GluR2/3 subunits have been shown to bind to PDZ domain containing proteins such as GRIP1 (Dong et al. 1997). This interaction occurs through their C-terminal four amino acids (-SVKI), which has been demonstrated to regulate AMPA internalization during LTD and to also be possibly involved in the expression of LTD in the hippocampus (Kim et al. 2001). To test whether transgenic expression of GRIP1-CTAP leads to formation of a properly folded protein in the mouse, we performed pulldown studies to analyze the interaction of the exogenous protein with the AMPA receptor GluR2/3 subunit as a known interactor of GRIP1. Brain lysates from heterozygous, transgenic adult mice, treated with different amounts of NP-40 for 60 minutes, were incubated with rabbit IgG agarose beads. Western blotting analysis of the IgG precipitates with specific antibodies showed that GluR2/3 was co-precipitated *in vivo* with GRIP1-CTAP (**Figure 22c**), consistent with the data obtained by Dong (1997). Moreover, GluR2/3 could be detected at highest levels when preparing the brain lysate under mild detergent conditions (0.1% NP-40) as shown in **Figure 22c**. Therefore, GRIP1-CTAP is able to interact with its known binding partner GluR2/3 in the transgenic mice indicating that it is folded properly.

5.2.2.4 GRIP1-CTAP is able to rescue the lethal phenotype of *GRIP1*^{-/-} mice

GRIP1 mutants die shortly after implantation around E12. Low, but significant, numbers of viable *GRIP1*^{-/-} embryos could be identified up to E16. Elimination of murine GRIP1 leads to development of abnormalities of the dermo-epidermal junction of *GRIP1*^{-/-} embryos, resulting in extensive skin blistering around day 12 of embryonic life (Bladt et al. 2002). Ultra-structural characterization of the blisters (or bullae) revealed cleavage of the dermo-epidermal junction below the lamina densa, an alteration reminiscent of the dystrophic form of human epidermolysis bullosa (Bladt et al. 2002) and R.L. Huganir, personal communication). In order to confirm that GRIP1-CTAP is functional *in vivo* and is able to form physiologically relevant complexes, we have performed a genetic experiment using *GRIP1*^{+/-} mice, which were

crossed with our GRIP1-CTAP transgenic mice. TAP-tagged GRIP1 transgenics when crossed to $GRIP1^{+/-}$ mutant mice (kindly provided by R.L. Huganir) give birth to $GRIP1^{-/-}; GRIP1-CTAP^{het}$ litter (**Figure 22d**). Litter #5 shows amplification of only the GRIP1 KO allele, but not the wt allele (top panel) indicating the $GRIP1^{-/-}$ genotype. The same litter carries the transgene encoding GRIP1-CTAP as detected by PCR (bottom panel). $GRIP1^{-/-}$ mice have never been observed after E16 (Bladt et al. 2002). Thus, rescuing the lethal embryonic phenotype by crossing in transgenic GRIP1-CTAP mice suggests that the GRIP1-CTAP protein is indeed functional *in vivo* and likely to be associated with most of its endogenous binding partners.

6. Discussion

6.1 Grb4 and GIT1 transduce ephrinB reverse signals modulating spine morphogenesis and synapse formation

EphrinB ligands are expressed at synapses in postsynaptic CA1 neurons and have been postulated to be the acting signaling partners for EphB receptors regulating synaptic plasticity of connections between CA3 and CA1 neurons (Grunwald et al. 2004). The molecular mechanisms of ephrinB ligand action during synaptic plasticity remain unknown. However, morphological changes associated with synaptic plasticity might be regulated by ephrinB ligand reverse signaling via the same molecular pathways as the formation of new synapses. The work presented in this thesis provides evidence for the involvement of ephrinB reverse signaling in spine morphogenesis and synapse formation and identifies molecular pathways downstream of these ligands in such processes. Activation of the ephrinB ligands in cultured hippocampal neurons leads to an increased number of mature spines with mushroom-like heads, whereas inhibition of reverse signaling by expression of the truncated ephrinB1 lacking the cytoplasmic domain renders immature spines and increased number of long and thin filopodia. Thus, ephrinB reverse signaling appears to be important for spine morphogenesis during development.

Together, our results point to a signaling complex containing Grb4 and the G-protein-coupled receptor kinase-interacting protein (GIT)1, which is involved in the regulation of spine formation by ephrinB ligands. Our work sheds light onto the molecular mechanisms that might underlie ephrinB reverse signaling function in important processes involving spine morphogenesis such as synaptic plasticity.

6.1.1 Grb4 and GIT1 transduce signals downstream of ephrinB ligands

Localized changes in the organization and dynamics of the actin cytoskeleton are thought to underlie the formation, maintenance, and plasticity of synaptic connections (Matus et al. 2000). The Rho family of small GTPases, key regulators of actin

dynamics and organization, are pivotal contributor in spinogenesis. Although Eph receptor interaction with the Rho pathway is well documented (Noren and Pasquale 2004), only little is known about how ephrin reverse signaling effects Rho family proteins and subsequent signaling to the cytoskeleton. Recent data have shown that Dishevelled mediates RhoA and Rho kinase activation downstream of ephrinB1 (Tanaka et al. 2003). Another link between ephrinBs and RhoA may be p190RhoGAP. Mice deficient in p190RhoGAP exhibit a lack of the anterior commissure (Brouns et al. 2001), a phenotype associated with a lack of ephrinB reverse signaling in *EphB2*^{-/-} mice (Henkemeyer et al. 1996). Rac, along with the other Rho family members RhoA and Cdc42, has an important role in the regulation of the actin cytoskeleton in spines (Ramakers 2002). A recent study demonstrates that a novel domain in GIT1, the synaptic localization domain (SLD), is required for spine morphogenesis and synapse formation (Zhang, H. et al. 2003) by providing a docking site for the β -p21-activated protein kinase (PAK)-interacting exchange factor (β PIX), which serves as an exchange factor for Rac. This observation has been extended now by identifying a signaling pathway downstream of Rac, including PAK and myosin II regulatory light chain (MLC) and involved in the regulation of spine morphogenesis and synapse formation (Zhang, H. et al. 2005). Therefore, GIT1 appears to organize a signaling module containing an activator and effector of Rac that localizes and regulates Rac activity in dendritic spines and synapses. A mislocalized hyperactive signaling complex leads to an overabundance of dendritic protrusions, whereas a loss-of-function mutation leads to decreased spine density (Zhang, H. et al. 2005). However, the signaling pathway or molecule that targets GIT1 and the entire signaling module to synapses and thereby induces spine formation and synaptogenesis remained so far unknown.

The findings presented here implicate the SH2/SH3-domain containing adaptor Grb4, GIT1 and β PIX as important components of the signaling apparatus downstream of ephrinB ligands. The co-expression studies in PSDs of hippocampal neurons together with previously published data (Grunwald et al. 2004) support the idea that Grb4, GIT1, β PIX and ephrinB ligands act in concert in regulating spine morphogenesis and synapse formation. As we have shown, GIT1 is targeted to membrane patches at synapses of hippocampal neurons after ephrinB activation and interacts with ephrinB1 and Grb4 in mouse brain. Moreover, we have shown that dominant negative interfering with the binding of Grb4 to ephrinB ligands (using the ephrinB1-313-335

peptide) and with GIT1 to Grb4 (using Grb4-SH2) impaired spine morphogenesis and synapse formation in dissociated rat hippocampal neurons mimicking the phenotype obtained previously when disrupting synaptic targeting of GIT1 by overexpression of the SLD domain (Zhang, H. et al. 2003). This suggests that overexpression of any of these dominant-negative molecules impairs the recruitment of endogenous Grb4-GIT1-PIX-Rac complex to ephrinB1 ligands at the synapse. The findings of the presented study therefore implicate that the molecular mechanism leading to GIT1-PIX-Rac-PAK-mediated spine formation and maintenance involves activated ephrinB ligand, its downstream interactor Grb4 and GIT1 indicating that ephrinB ligand provides the docking site for GIT1 and activated Rac to the synaptic membrane.

6.1.2 Are GIT proteins general downstream effectors of Grb4/Nck signaling?

We postulate that Grb4 serves to bridge ephrinB ligands with GIT1 at synapses. Consistent with this, we can show that the domain in GIT1 required for binding to Grb4 is indeed the SLD domain, a 221 aa stretch that has been shown to be required and sufficient for the synaptic localization of GIT1 (Zhang, H. et al. 2003). Mutant GIT1 lacking the NH₂-terminal 32 aa of the SLD has been shown to localize to synapses significantly less (Zhang, H. et al. 2003) suggesting that these 32 aa contribute to efficient synaptic localization of GIT1. Interestingly, we show that Tyr392 in GIT1, which is present in the NH₂-terminal 32 aa of GIT1 SLD, is required for GIT1 binding to the Grb4 SH2 domain. Moreover, Tyr392 is located in a sequence (YDSV) conserved among the GIT family and it resembles the consensus sequence for Nck α SH2 binding (Songyang et al. 1993).

Using the ephrinB1 ligand ectodomain, we have also been able to co-precipitate GIT proteins with EphB receptors from adult mouse brain suggesting that GIT proteins could also act downstream of the receptor. Nck α binds exclusively to the receptor (Stein et al. 1998). Thus, a Nck α -GIT complex could be transducing the signals downstream of the receptor, while the Grb4-GIT complex may be restricted to signaling events downstream of the ligand. Grb4 is involved in transducing reverse signals into ephrinB-expressing cells (Cowan and Henkemeyer 2001) most likely regulating the cytoskeleton. Half of the known SH3 domain binding partners of the Nck proteins (Grb4 and its closest relative Nck α) have direct or indirect roles in the

regulation of actin dynamics (Li et al. 2001). Among them, a number regulate the activity of the Rho family of small GTPases. These include the exchange factors for Rac, Dock180 (dedicator of cytokinesis 180) and hnRNP K (heterogeneous nuclear ribonucleoprotein K), and PAK1, which regulates both Rac and Rho. Among the Nck-SH3-effector complexes, the Nck α -PAK1-PIX-GIT1 complex is so far the best studied. Nck α relocates PAK1-PIX to the membrane proximity (Zhao et al. 2000a). The PAK1-associated PIX activates Rac (Obermeier et al. 1998) and binds to GIT1 and focal adhesion kinase (FAK) thereby promoting cell motility by regulating focal complex dynamics (Zhao et al. 2000b). Thus, as Nck has been shown to bind to GIT proteins in a number of different scenarios (Zhao et al. 2000a; Brown, M. C. et al. 2005), these proteins might very well be general downstream effectors of Grb4/Nck proteins in different biological processes.

6.1.3 Regulated Grb4-GIT1 interaction during phosphotyrosine-dependent ephrinB reverse signaling

In cells stably expressing physiological levels of ephrinB1, phosphorylation of Tyr392 and consequent interaction between endogenous GIT1 and Grb4 via its SH2 domain is not constitutive, but rather induced by EphB2 receptor engagement. The kinase required for phosphorylation of GIT1 on Tyr392 is unidentified. However, it is known that Src family kinases (SFKs) are rapidly recruited to ephrinB expression domains upon EphB receptor engagement, and this transient activation positively regulates ephrinB phosphorylation and phosphotyrosine-mediated reverse signaling (Palmer et al. 2002). The kinetics of ephrinB-mediated SLD phosphorylation correlate very well with the previously reported kinetics of Src recruitment to, and activation in ephrinB/EphB-containing membrane patches. Therefore, activation of the ephrinB ligand could recruit Src to PSDs, where ephrinB has been located (Grunwald et al. 2004), to specifically phosphorylate GIT1 at synapses. Interestingly, GIT1 has already been shown to be phosphorylated on tyrosine residues by c-Src in response to angiotensin II and epidermal growth factor in vascular endothelial cells and 293 cells (Haendeler et al. 2003), and in response to thrombin in HUVECs (van Nieuw Amerongen et al. 2004). GIT2, a family member homologous to GIT1, has been demonstrated to be phosphorylated at Tyr392 by Src and FAK (Brown, M. C. et al.

2005). GIT proteins might therefore be general substrates for SFKs downstream of different receptors.

6.1.4 SH3 domains contribute to Grb4 interaction with ephrinB ligand

Grb4 was identified as an ephrinB1 binding partner in a modified yeast two-hybrid screen, which allows for the detection of protein–protein interactions involving phosphotyrosine (Cowan and Henkemeyer 2001). The Grb4 SH2 domain was shown to associate with the cytoplasmic domain of tyrosine-phosphorylated ephrinB ligands in an Eph receptor stimulation-dependent fashion. We now identified the same domain in Grb4 to be crucial for association with phosphorylated GIT1. However, how can Grb4 be the bridging molecule in an ephrinB-Grb4-GIT1 complex and bind to ephrinB1 and to GIT1 at the same time via its SH2 domain? We have shown that Grb4 is not only able to bind to ephrinB ligands through its SH2 domain but it also binds through the SH3 domains. We postulate that Grb4 binding to ephrinB ligands is regulated by Eph receptor stimulation but is not exclusively phosphotyrosine-dependent. In agreement with this hypothesis we observe long lasting co-localization of Grb4 with ephrinB patches (Manuel Zimmer and Amparo Acker-Palmer, unpublished results), even after ephrinB ligands have undergone dephosphorylation by the phosphatase PTP-BL, which typically occurs 15 minutes after stimulation (Palmer et al. 2002). Moreover, a mutant of ephrinB1, which has all 6 tyrosines present in the intracellular domain mutated to phenylalanine, was still able to bind to Grb4 (Manuel Zimmer and Amparo Acker-Palmer, unpublished results). The assembly of the triple complex formed by ephrinB-Grb4-GIT1 might therefore occur in different scenarios: (1) the interaction of Grb4 with ephrinB might be initiated by phosphotyrosine-dependent association of the Grb4 SH2 domain with phosphorylated ephrinB ligands and later stabilized by the Grb4 SH3 domains. The stabilization would in turn release the Grb4 SH2 domain and make it available for interaction with GIT1. Consistent with this, a characteristic PXXP motif for binding SH3 domain proteins is present in ephrinB cytoplasmic tails close to the PDZ binding motif. (2) The formation of a Grb4 dimer through association of the SH3 domains may enable the interaction with ephrinB and GIT1 at the same time via the two available SH2 domains. (3) Alternatively, Grb4 may also be present in the cell in two different

populations, one that interacts with ephrinBs via the Grb4 SH3 domains and binds to GIT1 through the free Grb4 SH2 domain, and another, which does not assemble with GIT1 and interacts with ephrinBs via the Grb4 SH2 domain to exert different functions.

6.1.5 EphrinB reverse signaling and mental retardation

Pathological changes in dendritic spines are often observed in brain disorders such as nonsyndromic mental retardation (MR) (Fiala et al. 2002). As the importance of spine morphogenesis in cognitive function has become clearer, there has been accelerating interest in understanding its molecular basis. Through means of positional cloning, 13 genes associated with nonsyndromic MR have been identified to date and three of these genes encode for regulators of Rho GTPases (Allen et al. 1998; Billuart et al. 1998; Kutsche et al. 2000; Barnes and Milgram 2002; Ramakers 2002). However, the mechanisms by which these mutations lead to cognitive defects are not understood. One possibility is that decreased neuronal connectivity results from aberrant actin organization (Marin-Padilla 1972; Huttenlocher 1974; Purpura 1974; Kaufmann and Moser 2000). Indeed, some children with nonsyndromic MR show abnormalities in dendritic spine morphology in their cerebral cortex, i.e., numerous very long and thin spines and a reduction in the number of stubby and mushroom-shaped spines (Purpura 1974). In the present study, the dominant-negative molecules disrupting the interaction ephrinB-Grb4 and Grb4-GIT1 show an intriguingly similar dendritic spine phenotype in cultured neurons. These mutant constructs also cause a decrease in synaptic density. Thus, our results suggest a scenario in which aberrant Rho family signaling could lead to decreased neuronal connectivity and eventually impaired cognitive functions. Interestingly, PAK3, one of the human MR mutations linked to Rho, has been identified in the signaling module downstream of GIT1 (Zhang, H. et al. 2005) and might therefore be mislocalized upon disruption of the ephrinB-Grb4-GIT1 complex. Another gene associated with nonsyndromic MR is α PIX, a close relative of β PIX, which was as well identified as a novel Grb4 interactor in our proteomic approach.

6.2 Proteomic analysis of PDZ-mediated ephrinB reverse signaling

The cytoplasmic tail of ephrinB ligands contains a PDZ binding motif, which is important for reverse signaling. Some multi-PDZ-domain-containing proteins have been shown to bind to the carboxy-terminal (YKV) target site of ephrinB ligands. Previous work proposed the presence of a switch mechanism, which allows a shift from phosphotyrosine-dependent to PDZ-domain-dependent signaling (Palmer et al. 2002). Work presented in this thesis has been designed to dissect the nature of protein complexes that are involved in the PDZ-dependent signaling downstream of ephrinB ligands. As a target we have chosen the glutamate receptor interacting protein GRIP1, a 7 PDZ-domain containing protein that was shown to be specifically recruited into rafts through association with the cytoplasmic domain of ephrinB (Bruckner et al. 1999). The binding of GRIP1 to the cytoplasmic tail of ephrinB ligands appears to be regulated by Eph receptor binding (Manuel Zimmer, personal communication).

Besides our findings for GRIP1, I will also discuss the proteomics data mentioned in **chapter 5.1.3**, which we obtained for the phosphotyrosine-dependent ephrinB interactor Grb4. The functional and biological relevance of novel Grb4 interactions in ephrinB reverse signaling is discussed in detail in **chapter 6.1** (“Grb4 and GIT1 transduce ephrinB reverse signals modulating spine morphogenesis and synapse formation”).

6.2.1 Identification of Grb4 and GRIP1 complexes by tandem affinity purification

Using affinity purification of the two TAP-tagged ephrinB ligand-interactors Grb4 and GRIP1 from neuroblastoma cell lysates in combination with mass spectrometry, we could isolate a number of potential Grb4 (17) (**Table 1**) and GRIP1 (61) (**Table 2**) interactors. Conspicuous targets of Grb4 and GRIP1, mainly cytoskeleton-related proteins such as tubulin, actin, tropomyosin, myosin alkali light chain, but also heat shock proteins or proteins like Elongation factor 1 alpha 1 (which has been shown to bind to a number of cytoskeleton-related proteins (Gross and Kinzy 2005)), were removed from consideration by consulting a dataset of “potentially sticky proteins”

that has been provided by Cellzome, even though some of these proteins might be genuine binding partners of these proteins.

The pre-selected lists (without “potentially sticky proteins”) of Grb4- and GRIP1-interactors however did not contain any of the published interactors of the two proteins, likely because their expression levels were low or these interactions might be cell type-specific and not be present in the neuroblastoma cell line used.

Some of the newly identified binders have already been linked directly or indirectly to the regulation of the cytoskeleton, e.g. GIT1, GIT2, α PIX, β PIX or neurabin II (Brown, M. C. et al. 2005; Filipenko et al. 2005; Tsukada et al. 2005), and could therefore be potentially involved in ephrinB reverse signaling to the cytoskeleton. For other interactors, it is more difficult to determine whether they are really part of a Grb4/GRIP1 cytoskeleton remodeling complex. Some of the proteins involved in Grb4 and GRIP1 complexes, e.g. hnRNP A2/B1 or growth-arrest-specific protein 1, are likely to have additional cellular functions not related to cytoskeleton remodeling, and some of these interactors may reflect such functions. Among those remaining proteins that were co-purified are some whose known function may suggest a possible role in membrane trafficking. For example, the depletion of the GRIP1-interactor ADP-ribosylation factor 4 (ARF4) causes defects in secretory and endocytic traffic (Volpicelli-Daley et al. 2005).

So far, most systematic protein-protein interaction studies and protein networks have relied on yeast two-hybrid techniques (Drewes and Bouwmeester 2003). Compared with these approaches, affinity purification of complexes coupled to mass spectrometry-based protein identification offers the advantage of studying actual molecular assemblies made up by direct and cooperative interactions. Moreover this approach allows purification from human cells, different types of tissue (for example, from the UbiGRIP1-TAP mouse), or even subcellular compartments (e.g. membrane, PSDs) under close to physiological conditions, rather than relying on reconstituted bimolecular interactions *ex vivo* (Gavin et al. 2002). Finally, the introduction of a dual purification strategy, TAP-tagging, represents a major improvement in sample purification for mass spectrometry. Compared to single purification steps, the double purification gives a much better purity yield resulting in a better specificity of binding partners. Due to the high degree of specificity conferred by the tandem purification, stringent washes are not necessary, allowing better preservation of less stable multiprotein complexes. The number and quantity of contaminating proteins is also

low. The strength of the dual purification strategy, as compared with a single purification step with either tag alone, has also been demonstrated in the original publication of the TAP strategy (Rigaut et al. 1999).

In summary, my interaction proteomics approach has provided a list of Grb4 and GRIP1 protein complexes demonstrating an expected correlation with cytoskeleton remodeling. We have identified a number of novel interactors, some of which have previously been demonstrated to form complexes with each other. The data provided in this study should provide a point of departure for more in depth studies that will eventually lead to a more complete description of events occurring downstream of Grb4 and GRIP1, some of them in ephrinB reverse signaling.

From our list, we decided to continue characterizing in more detail two interactions: between GRIP1 and 14-3-3 and between Grb4 and GIT1. Four potential interactors of Grb4 have been identified: GIT1 (Cat1), GIT2 (Cat2), α PIX (RhoGEF6, Cool-2) and β PIX (RhoGEF7, Cool-1) (**Table 1**). Each of these has been reported previously to associate with the others (Bagrodia et al. 1999). The interaction Grb4-GIT1 was subject of the first part of my thesis. The interaction between GRIP1 and 14-3-3, which was additionally verified by reverse tandem affinity purification (Cellzome, personal communication) will be discussed below.

6.2.1.1 Identification of 14-3-3 as a GRIP1 binding protein

Signaling pathways regulate the dynamics of cell behavior by directing the assembly of multicomponent complexes (Hubbard and Cohen 1993; Pawson and Scott 1997; Pawson and Nash 2003). How can this be achieved within the crowded environment of a cell? The emerging answer is that many proteins have modular structures and contain distinct adapter domains that are specialized for binding to the most prevalent means of posttranslational modification, which is protein phosphorylation. Interestingly, many aspects of dynamic cellular behavior are regulated by reversible protein phosphorylation (Hunter 2000). Protein kinases frequently exert their biological effects by creating docking sites for adaptor domains, which selectively recognize phosphorylated motifs in their binding partners (Pawson and Nash 2003). 14-3-3 proteins for example bind to serine/threonine-phosphorylated residues in a context-specific manner, analogous to the Src homology 2 (SH2) and phosphotyrosine

binding (PTB) domains, which associate with tyrosine-phosphorylated residues. Interestingly, it has been shown that GRIP1 may be phosphorylated on serine/threonine residues by an unknown serine/threonine kinase that associates with a complex formed by ephrinB and GRIP1 (Bruckner et al. 1999). Our observations show that association between GRIP1 and 14-3-3 occurs via a conserved 14-3-3 binding site in the C-terminus of GRIP1. Furthermore, 14-3-3, GRIP1 and ephrinB1 ligand interact exclusively in rafts of mouse brain supporting their signaling function *in vivo* and indicating that the GRIP1-14-3-3 complex may have an important function in organizing a signaling complex for ephrinB reverse signal transduction.

6.2.1.2 GRIP1 contains three putative 14-3-3 binding sites, but only one is required for interaction

14-3-3 proteins were the first polypeptides shown to have phosphothreonine/serine (pSer/Thr) binding properties (Muslin et al. 1996). Structural analysis has shown that each 14-3-3 protomer folds into an α -helical structure with a conserved binding groove that accommodates pSer/Thr-binding sites (Yaffe et al. 1997; Obsil et al. 2001), typically generated by basophilic kinases such as cAMP-dependent protein kinase (PKA) and protein kinase B (PKB) (Fu et al. 2000; Yaffe 2002). Accordingly, two optimal 14-3-3 phosphopeptide ligands with the consensus sequences RSXpSXP (mode I) and RXY/FXpSXP (mode II), where X is any amino acid, have been defined with degenerated peptide libraries (Muslin et al. 1996; Yaffe et al. 1997). Although we identified three putative 14-3-3 binding sites inside the linker region between PDZ6 and PDZ7 of GRIP1, which all exactly match the optimal sequence motif of mode I, mutation analysis showed only one of them to be required for 14-3-3 binding to GRIP1. Interestingly, the identified motif (RSNTLP) encompassing threonine 956 is the only one out of all three, which is specific for GRIP1 and therefore not conserved in GRIP1-homolog GRIP2. Indeed, preliminary data indicate that 14-3-3 interaction is exclusively restricted to GRIP1 (Inmaculada Segura, personal communication). However, previous studies have shown that GRIP1 may be able to form homomultimers or heteromultimers with GRIP2, allowing the formation of very large macromolecular complexes that might also include 14-3-3, which is recruited by GRIP1 (Dong et al. 1999).

6.2.1.3 What is the functional relevance of Thr956 *in vivo*?

Setou and colleagues (Setou et al. 2002) have previously shown that GRIP1 can directly interact with kinesin and mapped the kinesin-binding domain in GRIP1 to the linker region between PDZ6 and PDZ7 (753-987, termed L2), which also contains the 14-3-3 recognition motif we identified. Kinesin heavy chain (also known as KIF5) knockout and dominant-negative experiments showed an abnormal perinuclear clustering of GRIP, and overexpression of the KIF5-binding domain of GRIP in neurons resulted in an accumulation of kinesin in dendrites. Therefore, it has been postulated that GRIP “steers” kinesin transport into dendrites, thereby sorting specific protein complexes to dendritic structures (for example, AMPA receptors) (Setou et al. 2002). Moreover, Hoogenraad and co-workers recently demonstrated a molecular mechanism in which KIF5-dependent trafficking of a GRIP1/EphB receptor complex is critical for dendrite morphogenesis (Hoogenraad et al. 2005). However, the exact site within L2 of GRIP1, which is necessary for GRIP1-KIF5 interaction, has not been mapped and thus it remains for future studies to test the role of Thr956 in GRIP1 in this interaction and whether this residue is functionally relevant *in vivo*. Interestingly, a mutant of GRIP1, in which Thr956 is replaced by Ala and therefore cannot bind to 14-3-3 any longer, disrupts the formation and growth of dendrites in hippocampal neurons (Inmaculada Segura, personal communication). These data suggest that 14-3-3 could bridge GRIP1 and KIF5 together in a phosphorylation-dependent manner to anchor these two proteins within close proximity of one another. Interestingly, KIF5B has been shown to be a target of 14-3-3 protein as well (Ichimura et al. 2002).

6.2.1.4 Which is the kinase required for phosphorylation of Thr956 in GRIP1?

GRIP1 is associated with a serine/threonine kinase activity when forming a complex with ephrinB ligands (Bruckner et al. 1999). This kinase might phosphorylate serines or threonines in GRIP1 upon ephrin activation, creating docking sites for 14-3-3 molecules. Support for this idea comes from an observation by Amparo Acker-Palmer (personal communication), which shows that only the C-terminal half that contains the identified 14-3-3 binding site, but not the N-terminal half of GRIP1, becomes

phosphorylated after Eph receptor stimulation. A potential kinase that regulates the phosphorylation state of GRIP1 in ephrinB reverse signaling, might be the protein kinase Cdc25C-associated kinase 1 (C-TAK1), which has been co-purified with GRIP1 in a TAP approach using 14-3-3-eta- and -zeta-TAP (Cellzome, personal communication). C-TAK1 is a member of the EMK/MARK/Par1 kinase family and was first cloned based on its ability to associate with and phosphorylate Cdc25C (Ogg et al. 1994; Peng et al. 1998). Subsequently, the tyrosine phosphatase PTPH1 and KSR1 were found to be phosphorylated by C-TAK1 (Zhang, S. H. et al. 1997; Muller et al. 2001). Strikingly, for all known substrates of C-TAK1 (KSR1, Cdc25C and PTPH1), the residue phosphorylated by C-TAK1 serves as a 14-3-3 binding site. However, the exact identity of the kinase and its relevance in GRIP1 phosphorylation in response to Eph/ephrin signaling will have to be further explored. So far, the presented data only indicate the requirement of Thr956 for GRIP1 binding to 14-3-3. It would be of great interest to test if Thr956 is a major phosphorylation site *in vivo* and whether phosphorylation of this residue indeed directly increases the affinity of GRIP1 to 14-3-3.

6.2.1.5 GRIP1 interaction with 14-3-3 and raft microdomains

Previous work has shown that ephrinB ligands and SFKs, positive regulators of ephrinB phosphorylation, are both located in lipid rafts, and stimulation with soluble EphB receptor leads to reorganization of ephrinB- and Src-containing rafts into larger membrane patches (Palmer et al. 2002). Additionally, GRIP1 co-localizes with ephrinB1 raft patches (Bruckner et al. 1999). These specialized membrane microdomains are proposed to serve as sites of signal integration of signaling in a wide variety of processes (e.g. signal transduction), based on the many molecules known to be involved in intracellular signaling, which are enriched in this fraction (Simons and Toomre 2000; Zajchowski and Robbins 2002).

Strikingly, the interaction of 14-3-3 with GRIP1 was found to be restricted to raft microdomains in mouse brain, indicating that both molecules associate with each other only upon an external stimulus, which then recruits the complex to these signaling centers. Furthermore, a small but significant and isoform-selective proportion of the 14-3-3 in mouse brain was raft associated, suggesting that this 14-3-

3 might acquire new or enhanced functions on association with GRIP1 in raft microdomains. Although only a small proportion of the total brain 14-3-3 localizes to rafts, the association of it with only a specific subset of membranes suggests that it is functionally important. Similarly, Martin and co-workers have found that some of the 14-3-3 in rat brain is selectively associated with some synaptic membranes raising the possibility that their presence in synapses might indicate a role in controlling phosphorylation of synaptic proteins (Martin et al. 1994). Our finding that ephrinB ligand interacts with GRIP1 and 14-3-3 in rafts support the hypothesis of ephrinB ligands signaling from highly organized signaling centers such as raft microdomains. Assembly of this signaling complex may be induced by EphB2 receptor binding to ephrinB1 (Manuel Zimmer, personal communication). Whether the interaction between GRIP1 and 14-3-3 is actually regulated by EphB receptor engagement of the ligand still needs to be investigated.

6.2.2 Transgenic expression of GRIP1 in mice to identify protein complexes *in vivo*

Because of its multi PDZ-domain structure GRIP1 is likely to interact with other cytoplasmic proteins. One of these proteins is the ras-GTP-exchange factor GRASP-1 (GRIP-associated protein 1) (Ye et al. 2000), however many others have been described as well, such as GluR2, EphB receptor, liprin-alpha, Fras1, PICK1 and NEEP21 (Dong et al. 1997; Torres et al. 1998; Wyszynski et al. 2002; Takamiya et al. 2004; Lu, W. and Ziff 2005; Steiner et al. 2005). Together the available data suggests that GRIP1 molecules could serve as scaffolds for large protein complexes involved in signaling at the plasma membrane. To identify the complete “GRIP-signaling-complex” we also applied the TAP tag technology *in vivo* by expressing TAP-tagged GRIP1 in transgenic mice using an ubiquitous promoter. This approach has several advantages over other methods for identification of protein-protein interactions: (a) the use of an *in vivo* model; (b) the purification of a protein complex that has been established in its natural environment, and (c) the comparison of GRIP1-protein complexes derived from different tissues/subcellular compartments (e.g. rafts or synaptic membranes).

6.2.2.1 Transgenic GRIP1-CTAP protein is functional

Transgenic GRIP1-CTAP mice did not show any overt abnormalities, and several founders were tested for GRIP1-CTAP protein expression. The founders expressed varying levels of GRIP1-TAP, but in general the expression was moderate, possibly not more than 2-3 fold above endogenous levels. GRIP1-CTAP purified by tandem affinity purification associates in membrane fractions with its known interaction partner GluR2/3 providing further evidence for GRIP1-CTAP assembling with functional and physiologically relevant protein complexes. In order to confirm that the TAP-tagged protein is functional *in vivo*, we performed a genetic experiment with the GRIP1-CTAP transgenic mice. TAP-tagged GRIP1 transgenics when crossed with *GRIP1*^{-/-} mutant mice (provided by R.L. Huganir) rescued the lethal phenotype of this null mutation, indicating that the GRIP1-CTAP protein is functional *in vivo* and likely to be associated with its endogenous binding partners. Therefore, these mice could also serve in the future as a tool for the verification of *in vivo* interactions with the candidates obtained in a first round of purification with the neuroblastoma cell line stably expressing GRIP1-CTAP. Moreover, since the transgene rescues the lethal phenotype of the GRIP1 KO, we could also use the transgenic mice as a genetic tool to try to identify regions in the GRIP1 protein and interactions with other proteins required for its *in vivo* function.

6.3 Concluding remarks

Our studies reveal a new function of ephrinB reverse signaling in spine morphogenesis and synapse formation, which might be related to the known functional relevance of reverse signaling in synaptic plasticity (Grunwald et al. 2004). The pathway downstream of the ligand, which we demonstrated to be required for this function, involves the SH2-SH3 adaptor Grb4 and the scaffolding protein GIT1. Interestingly, GIT1 has been very recently shown to form a signaling complex with PIX, Rac, and PAK playing an essential role in the regulation of dendritic spine and synapse formation through modulating MLC activity (Zhang, H. et al. 2005). Thus, the ephrinB signaling pathway could serve as the upstream signaling cascade leading to the regulated formation and localization of this complex.

The analysis of ephrinB1/2/3 triple mutant mice is in progress and will help to elucidate the function of the ephrinB ligands in the context of spine development in an intact hippocampus. However, the lack of ephrinB ligands in these mice may lead to a decreased activation of EphB forward signaling and, therefore, abnormal spine development might be at least to some extent caused by disruption of signaling pathways downstream of the receptor.

A number of issues remain unanswered. For instance, are effects of CA3-CA1 long-term plasticity mediated by similar signaling mechanisms as in spine formation? What role does internalization of the Eph/ephrinB complex, a process that was recently shown to regulate the cellular response to Eph/ephrin signaling (Marston et al. 2003; Zimmer et al. 2003), have at the synapse? Is the novel Grb4 interactor α PIX, mutations of which have been found in patients with nonsyndromic mental retardation, involved in ephrinB-mediated spinogenesis as well? And does the switch from phosphorylation- to PDZ-dependent ephrinB reverse signaling, as suggested by Palmer and colleagues (Palmer et al. 2002), play a role in synapse formation? This could be relevant for multi-PDZ protein GRIP1-mediated AMPA receptor targeting and organization of postsynaptic complexes, which, interestingly, seems to also require GIT1 (Wyszynski et al. 2002; Ko et al. 2003). These issues could be addressed in future studies using the tools and observations described in this thesis.

7. Materials and Methods

7.1 Materials

7.1.1 Buffers and solutions

7.1.1.1 Media and antibiotics for bacterial culture

LB (Luria-Bertani-) media	10 g Bacto-Trypton 5 g Yeast extract 5 g NaCl add H ₂ O to 1 l, adjust pH to 7.5
LB plates	supplement with 15 g/l agar
Antibiotics	diluted 1:1000
<i>Ampicillin</i>	Stock 100 mg/ml in H ₂ O
<i>Kanamycinsulfate</i>	Stock 50 mg/l in H ₂ O

7.1.1.2 Media and supplements for tissue culture

DMEM	Dulbecco's Modified Eagle medium
DMEM FBS G418	DMEM, 10% Foetal bovine serum, 0.292 mg/ml L-Glutamine, 100 U/ml Penicillin, 100 µg/ml Streptomycin, 350 µg/ml geneticin sulfate (G418).
Neurobasal, 2% B27	neurobasal medium (Invitrogen) was supplemented with B27 supplement (Invitrogen)
OptiMEM GlutaMAX, 5% Iron suppl. CS	Optimem medium (Invitrogen) was supplemented with Iron suppl. Calf Serum (Sigma)

7.1.1.3 Media and supplements for primary culture of neurons

Borate Buffer (500 ml)	1.24 g boric acid, 1.9 g Borax ad 400 ml H ₂ O (pH 8.5)
HBSS	135 mM NaCl ₂ , 20 mM Hepes, 4 mM KCl, 1 mM Na ₂ HPO ₄ , 2 mM CaCl ₂ , 1 mM MgCl ₂ , 10 mM glucose (pH 7.3)

7.1.1.4 Solutions for Biochemistry

Laemmli stacking gel	4% w/v acrylamid/bis 29:1 130 mM Tris-HCl (pH 6.8), 0.4% SDS 0.1% APS 0.1% TEMED
10% Laemmli separating gel	10% w/v acrylamid/bis 25:1 130 mM Tris-HCl (pH 8.8), 0.4% SDS 0.05% APS 0.05% TEMED
5x Laemmli electrophoresis buffer	130 mM Tris base 960 mM Glycine 17 mM SDS
10x Transfer buffer (2.5 l)	200 mM Tris base 1.5 M Glycine 34 mM SDS
Stripping buffer	5 mM sodium phosphate buffer (pH 7.25) 2 mM β-mercaptoethanol 2% SDS

6x Sample buffer for reducing conditions	42 mM SDS 300 mM Tris-HCl (pH 6.8) 600 mM DTT 52% Glycerol Bromophenol blue
Lysis buffer, 0.5-1% Triton X-100	50 mM Tris-HCl (pH 7.5) 0.15 mM NaCl 0.5-1% Triton X-100 <i>Add fresh:</i> 1 mM Na ₃ VO ₄ 10 mM NaPPi 20 mM NaF Protease inhibitor cocktail tablet (complete) (1 tablet/50 ml)
PLC lysis buffer	50 mM Hepes (pH 7.5) 150 mM NaCl 10% Glycerol 0.1% Triton X-100 1.5 mM MgCl ₂ 1 mM EGTA <i>Add fresh:</i> 1 mM Na ₃ VO ₄ 10 mM NaPPi 20 mM NaF Protease inhibitor cocktail tablet (complete) (1 tablet/50 ml)
HNTG buffer (100 ml)	20 mM Hepes (pH 7.5) 150 mM NaCl 10% Glycerol 0.1% Triton X-100 <i>Add fresh:</i> 1 mM Na ₃ VO ₄ Protease inhibitor cocktail tablet (complete)

7. Materials and Methods

	(1 tablet/50 ml)
Lysis buffer (TAP)	50 mM Tris-HCl (pH 7.5) 5% Glycerol 0.2% NP-40 1.5 mM MgCl ₂ 1 mM DTT 100 mM NaCl <i>Add fresh:</i> 50 mM NaF 1 mM Na ₃ VO ₄ 2 μM microcystine-LR Protease inhibitor cocktail tablet (complete), EDTA-free (1 tablet/50 ml)
TEV Cleavage buffer (TAP)	10 mM Tris-HCl (pH 7.5) 100 mM NaCl 0.1% NP-40 0.5 mM EDTA 1 mM DTT
CBP washing buffer (TAP)	10 mM Tris-HCl, (pH 7.5) 100 mM NaCl 0.1% NP-40 1 mM Mg(CH ₃ COOH) ₂ 1 mM Imidazole 2 mM CaCl ₂ 1 mM DTT
2x CBP dilution buffer (TAP)	10 mM Tris-HCl (pH 7.5) 100 mM NaCl 0.1% NP-40 2 mM MgAc 2 mM Imidazole 4 mM CaCl ₂ 1 mM DTT
CBP elution buffer (TAP)	10 mM Tris-HCl (pH 8.0)

	5 mM EGTA
Solution A (PSD purification)	0.32 M sucrose 20 mM HEPES (pH 7.4) <i>Add fresh:</i> 50 mM NaF 1 mM Na ₃ VO ₄ 1 mM PMSF Protease inhibitor cocktail tablet (complete) (1 tablet/50 ml)
Solution B (PSD purification)	0.32 M sucrose 20 mM HEPES (pH 7.4)
Solution C (PSD purification)	12 mM Tris (pH 8.0) 1% Triton X-100
Solution D (PSD purification)	40 mM Tris (pH 8.0)
Solution E (PSD purification)	12 mM Tris (pH 8.0) 6% sarcosyl (N-lauryl-sarcosine)
Tail lysis buffer	50 mM KCl 1.5 mM MgCl ₂ 10 mM Tris (pH 7.5/8.5) 0.45% NP-40 0.45% Tween20
TNE buffer	25 mM Tris-HCl (pH 7.5) 150 mM NaCl 0.8 mM EDTA, 250 mM sucrose <i>Add fresh:</i> 50 mM NaF 1 mM Na ₃ VO ₄ 2 μM microcystine-LR Protease inhibitor cocktail tablet (complete) (1 tablet/50 ml)

7.1.2 Bacteria

TOP10	<i>F- mcrA D(mrr-hsdRMS-mcrBC) F80 lacZ DM15 DlacX74 recA1 araD139 D(ara-leu7697) galU galK rpsL (Strr) endA1 nupG</i>
DH5 α	<i>supE44 DlacU169 (F80 lacZ DM15) hsdR17 recA1 endA1 gyrA96 thi-1 relA1</i>

7.1.3 Plasmids

7.1.3.1 GIT1 expression constructs

Expression construct encoding full-length rat GIT1-Flag was a gift from R.T. Premont and is described (Premont et al. 1998). To generate GIT1 Δ SLD-Flag, two restriction sites were inserted by mutagenesis into GIT1-Flag. Point-mutated rat GIT1-Flag was generated by site directed mutagenesis leading to exchange of Tyr392 to Phe. To generate SLD-YFP, the SLD coding region (384-596) was cloned into pEYFP-N1 (Clontech) using XhoI and XmaI restriction sites. An expression construct encoding SLD-V5 was generated using the Gateway site-specific recombination system (Invitrogen) to insert SLD into pcDNA3.2/V5-DEST (Invitrogen).

7.1.3.2 Grb4 expression constructs

To obtain Grb4-CTAP, the Grb4 coding region was subcloned from clone IRALp962J117Q2 (RZPD) into pRVCTAPGw (Cellzome) by the Gateway site-specific recombination system (Invitrogen). To generate Grb4-YFP, Grb4 SH2-YFP or Grb4 SH3-YFP, the Grb4, SH2 (283-380) or SH3 (1-255) coding region from clone IRALp962J117Q2 was cloned into pECFP-N1 (Clontech) using BamHI and XhoI restriction sites.

7.1.3.3 GRIP1 expression constructs

To obtain UbiKOZ-GRIP1-CTAP for injection into oocytes, the CTAP and GRIP1 coding regions were subcloned from pRVCTAP-GRIP1 (Cellzome) into UbiKOZ (based on pUC18, Francesca Diella) using XhoI (CTAP) and NotI (GRIP1) restriction sites. To generate GRIP1-myc, the GRIP1 coding region was subcloned from pRVCTAP-GRIP1 into pCDNA3.1Amyc/his using XbaI and KpnI restriction sites. Point-mutated GRIP1-myc was generated by site directed mutagenesis leading to exchange of Ser944, Thr956 or Ser944 and Thr956 to Ala.

7.1.3.4 EphrinB1 interfering peptide expression construct

To generate ephrinB1-313-335-EYFP, the respective ephrinB1 coding regions from HA-ephrinB1 (see below) were cloned into pEYFP-N1 (Clontech) using BamHI and HindIII restriction sites.

7.1.3.5 Other expression constructs

The expression construct of HA-ephrinB1 was provided by Manuel Zimmer and ECFP-ephrinB1- Δ C by Jenny Köhler. Expression construct encoding β PIX-Flag was a gift from Dongeun Park and is described (Lee et al. 2001). The expression constructs of EphB2-Flag is described (Dalva et al. 2000). Expression vector encoding HA-14-3-3 was generated using the Gateway site-specific recombination system (Invitrogen) to insert the PCR-amplified ORF of 14-3-3 ζ (IMAGE: 2988020; RZPD) into the HA-tagged version of the MoMLV-based vector pZome1 (Cellzome).

7.1.4 Chemicals and commercial kits

100x L-glutamine (Invitrogen)
100x penicillin / streptomycin. (Invitrogen)
30% Acrylamid/Bis 25:1 (Biorad)
β -Mercaptoethanol (Sigma)
BES (Sigma)
Biorad D _c Protein Assay (Biorad)
BSA (Sigma)
Complete, Protease inhibitor cocktail tablets (Roche)
Complete EDTA-free, Protease inhibitor cocktail tablets (Roche)
Dithiothreitol (DTT) (Sigma)
ECL Western Blot detection reagent (Amersham)
EDTA (Sigma)
EGTA (Sigma)
EphB2-Fc chimera, mouse (R&D)
Films, Kodak Biomax MS Film (Sigma)
Foetal bovine serum (FBS) (Invitrogen)
Gateway-specific recombination system (Invitrogen)
Gel/Mount (Biomed)
Geneticin sulfate (G418) (Invitrogen)
Glutathione-sepharose beads (Pharmacia)
Iron-supplemented calf serum (Sigma)
Human IgG-Fc fragment (Dianova)
Mouse-laminin, natural (Invitrogen)
Normal Donkey Serum (Dianova)
Normal Goat Serum (Dianova)
Nonidet P-40, IGEPAL CA-630 (Roche)
OptiMEM GlutaMAX (Invitrogen)
Optiprep (Nycomed Pharma)
Orange G (Sigma)
PfuUltra High-Fidelity DNA polymerase (Stratagene)
phenylmethylsulfonyl fluoride (PMSF) (Sigma)
Poly-D-lysine (Sigma)
Poly-L-lysine (Sigma)
PonceauS solution (Serva)
Precision Plus Protein Standard (Biorad)
Protein A Sepharose 4B (Amersham)
Protein G Sepharose 4B (Amersham)
Pyruvic acid (Sigma)
QuikChange (XL-) Site-directed mutagenesis kit (Stratagene)
TEMED (Biorad)
Triton X-100, analytical grade (Serva)
Trypsin/EDTA (Invitrogen)

7.1.5 Antibodies

7.1.5.1 Primary antibodies

Affinity purified anti-14-3-3 (06-511, Upstate)	Western-Blotting: 1:1000 14-3-3 staining in Fig. 19, 20 Immunoprecipitation: 4 µg/IP
Affinity purified rabbit anti-caveolin-1 (sc-894, Santa Cruz Biotechnology)	Western Blotting 1:1000 caveolin staining in Fig. 19
Rabbit serum anti-(SAM)EphB2 (Grunwald et al. 2001)	Western Blotting: 1:2000 EphB2 staining in Fig. 12
Affinity purified goat anti-ephrinB1 (AF473, R&D)	Western Blotting: 1:1000 ephrinB1 staining in Fig. 12, 20
Mouse anti-Flag (F3165, clone M2, Sigma)	Western Blotting: 1:5000 GIT1-/GIT1Y>F-Flag staining in Fig. 12, 13, 14, 15 Immunoprecipitation: 1 µg/IP
Affinity purified rabbit anti-Flag (V10303, Biomeda)	Immunoprecipitation: 2 µg/IP
Affinity purified goat anti-GIT1 (sc-9657, Santa Cruz Biotechnology)	Western Blotting: 1:500 GIT1 staining in Fig. 12, 13, 15
Rabbit anti-GIT1 (DU139, (Premont et al. 1998; Bagrodia et al. 1999)	Western Blotting: 1:2000 Immunocytochemistry: 1:1000 GIT1 staining in Fig. 16 Immunoprecipitation: 1 µl/IP
Rabbit anti-GIT2 (DU137, (Premont et al. 1998; Bagrodia et al. 1999)	Western Blotting: 1:2000 GIT2 staining in Fig. 12
Mouse anti-GFP (8371-2, clone JL-8, Clontech)	Western Blotting: 1:5000 Grb4(SH2/SH3)-GFP staining in Fig. 13, 14, 15

7. Materials and Methods

Affinity purified rabbit anti-GFP (RDI-GRNFB4abr, RDI)	Western Blotting: 1:3000 Grb4(SH2/SH3)-GFP staining in Fig. 13d Immunoprecipitation: 1 µg/IP
Affinity purified rabbit anti-Grb4 (07-100, Upstate)	Western Blotting: 1:1000 Grb4 staining in Fig. 11, 12 Immunocytochemistry: 1:200
Mouse anti-GRIP (611318, clone 32, BD Transduction Lab.)	Western Blotting: 1:5000 GRIP staining in Fig. 19, 20, 22
Affinity purified rabbit anti-GRIP1, CT (06-986, Upstate)	Immunoprecipitation: 2 µg/IP
Affinity purified mouse anti-HA (1583816, clone 12CA5, Roche)	Western Blotting: 1:1000 HA staining in Fig. 13, 21 Immunoprecipitation: 4 µg/IP
Affinity purified goat anti-human Fc (109-005-098, Dianova)	Fc-clustering: 1:10 w/w
TR-conjugated goat anti human Fc _γ (Jackson ImmunoResearch)	Immunocytochemistry: 7.5 µg/ml anti-Fc staining in Fig. 16
Mouse anti-myc (clone 9E10) agarose beads (A7470, Sigma)	Immunoprecipitation: 10 µl/IP
Mouse ascities anti-myc (clone 9E10)	Western Blotting: 1:1000 GRIP1-myc staining in Fig. 21
Rabbit serum anti-βPIX (DU248, (Premont et al. 1998; Bagrodia et al. 1999)	Western Blotting: 1:2000 anti-βPIX staining in Fig. 14
Mouse anti-PRK2 (610794, clone 22, BD Biosciences Pharmingen)	Western Blotting: 1:1000 PRK2 staining in Fig. 14
Affinity purified mouse anti-phospho- tyrosine (hybridoma clone 4G10)	Western Blotting: 1:5000 Phospho-SLD-YFP staining in Fig. 15
Mouse anti-PSD-95 (P-246, clone 7E3-IB8, Sigma)	Immunocytochemistry: 1:200 PSD-95 staining in Fig. 11
Mouse anti-synapsin 1 (106 021, clone 46.1, Synaptic Systems)	Immunocytochemistry: 1:500 synapsin 1 staining in Fig. 17
Rabbit anti-synaptophysin 1	Western Blotting: 1:1000

(101002, Synaptic Systems)	synaptophysin 1 staining in Fig. 11
Affinity purified mouse anti-human transferrin receptor (13-6800, clone H68.4, Zymed Laboratories Inc.)	Western Blotting: 1:1000 transferrin receptor staining in Fig. 19
Mouse anti-V5 (R960-25, Invitrogen)	Western Blotting: 1:5000 SLD-V5 staining in Fig. 13
Rabbit IgG Agarose (A-2909, Sigma)	Immunoprecipitation: 20 µl/IP
ephrinB1-Fc (473-EB, R&D)	Pulldown: 10 µg/pulldown
EphB2-Fc (467-B2, R&D)	Pulldown: 10 µg/pulldown

7.1.5.2 Secondary antibodies

Donkey anti-mouse-Cy3, -Cy5, -Texas Red (715-165-151, 715-175-151, 715-075-151, Jackson ImmunoResearch)	Immunocytochemistry: 3.75 µg/ml
Donkey anti-rabbit-Cy3, -Cy5 (711-165-152, 711-175-152, Jackson ImmunoResearch)	Immunocytochemistry: 3.75 µg/ml
Donkey anti-goat antibody HRP conjugate (705-035-003, Jackson ImmunoResearch)	Western Blotting: 1:3000
Goat anti-mouse antibody HRP conjugate (115-055-003, Jackson ImmunoResearch)	Western Blotting: 1:3000
Goat anti-rabbit antibody HRP conjugate (111-035-003, Jackson ImmunoResearch)	Western Blotting: 1:3000
Peroxidase Anti-Peroxidase (PAP) Soluble Complex antibody produced in rabbit (P-1291, Sigma)	Western Blotting: 1:3000 PAP staining in Fig. 12

7.1.6 Cell lines

HeLa	Human cervix carcinoma cells	DMEM, FCS
HeLa ephrinB1 (kindly provided by KS Erdmann, Ruhr University Bochum)	Human cervix carcinoma cells stably expressing ephrinB1 constructs	DMEM, FCS, G418
SK-N-BE2	Human Caucasian neuroblastoma cells	OptiMEM I GlutaMAX, Iron suppl. CS
SK-N-BE2 Grb4-CTAP (clone ZF_C2)	Human Caucasian neuroblastoma cells stably expressing Grb4-CTAP	OptiMEM I GlutaMAX, Iron suppl. CS
SK-N-BE2 GRIP1-CTAP (clone XB C-180)	Human Caucasian neuroblastoma cells stably expressing GRIP1-CTAP	OptiMEM I GlutaMAX, Iron suppl. CS

7.1.7 Other materials and equipment

Centrifuge Varifuge 3.0R (Kendro)
Centrifuge Centrifuge 5810 (Eppendorf)
Rotor GSA rotor & type 3 (Sorvall)
Table centrifuge Centrifuge 5415 D (Eppendorf)
Mini centrifuge Quickspin Minifuges, C-1200 (International Labnet)
Incubator shaker Unitron-Pro (Infors)
Thermo mixer Thermomixer comfort (Eppendorf)
Balance XT2220M-DR (Precisa)
Fine balance XT2220A-FR (Precisa)
Magnetic stirring bar 50 × 8 mm (Brand)
pH Meter Inolab, pH Level 1 (WTW)
Electrophoresis power supply EPS 601 (Amersham)
Water purification system Milli-Q Biocel A10 (Millipore)
PCR machine Peltier Thermal Cycler, PTC-225 (MJ Research)
Shaker IKA Schüttler MTS 4 IKA® (Werke)
Shaker POLYMAX 2040 (Heidolph)
Magnetic Stirrer with heating IKAMAG®Ret IKA® (Werke)
Hood HERAsafe (Kendro)
Laminar air flow hood HERAguard (Kendro)
CO ₂ incubator HERAcell® 240 (Kendro)
Spectrophotometer Ultrospec 3000 (Amersham)
Vacuum sucking system VacuSafe (Integra Biosciences)
Sequencer ABI Prism 377 DNA sequencer (Applied Biosystems)
Vortexer VF2 IKA® (Werke)
Epifluorescence microscope Zeiss Axioplan (Zeiss)
Digital camera SpotRT (Diagnostics Instruments)
Semidry blotting apparatus (Pharmacia)
Nitrocellulose membrane, 0.45µm pore size (Scleicher & Schuell)
BioRad gel system (BioRad)
Straight forceps, Biology tip Dumont #5 (11252-20, Fine Science Tools)
Vannas-Tübingen spring scissors (15003-08, Fine Science Tools)
Dissection stereomicroscope Stemi SV 11 (Zeiss)
Dissection lamp KL 1500 LCD (Leica)

7.2 Methods

7.2.1 Molecular Biology

7.2.1.1 Preparation of plasmid DNA

Plasmid DNA was purified from small-scale (5 ml, minipreparation) or from large-scale (100 ml, maxipreparation) bacterial cultures. For this, single colonies of transformed bacteria or from a bacterial glycerol stock were picked each into 2 ml LB medium containing 100 µg/ml ampicillin or kanamycin and grown over day. 100ml LB medium containing the antibiotics were then inoculated with 1ml from this 2 ml-culture and grown overnight (ON) at 37°C with vigorous shaking. The bacterial suspension was pelleted by centrifugation at 4,000 rpm for 20 min at 4°C. The pellet was resuspended in buffer P1 (QIAGEN). Mini- and maxipreparation of plasmid DNA were carried out according to the QIAGEN protocol (Qiagen Miniprep Spin kit, Qiagen HiSpeed Maxi Kit) using lysis of the cells and binding of the plasmid DNA to a special resin. After washing, elution and precipitation the plasmid DNA was redissolved in a suitable volume of H₂O for minipreparation or endotoxin-free TE buffer (QIAGEN) for maxipreparation. DNA concentration was measured in a UV spectrometer at 260 nm. The following formula was used: dsDNA: $OD \times 50 \times \text{dilution factor} = X \mu\text{g/ml}$

7.2.1.2 Enzymatic treatment of DNA

Cleavage of plasmid DNA: Approximately 1 µg of DNA was cut in 50 µl of the appropriate NEB-buffer, 1xBSA (if required) and 2 to 5 units (U) restriction enzyme (NEB) for 1 to 2 h at an appropriate temperature.

7.2.1.2.1 Dephosphorylation of DNA fragments

For dephosphorylation of DNA fragments, 1 U (1 μ l) of shrimp alkaline phosphatase (1758250, Roche) was added to a 50 μ l-restriction enzyme reaction, incubated for 60 min at 37°C and heat-inactivated at 65°C for 15 min. Subsequently, the dephosphorylated DNA fragments were purified from the reaction mix (see purification of DNA).

7.2.1.2.2 Ligating vector and insert

A 10 μ l reaction containing purified linearized and dephosphorylated vector and DNA fragments (“insert”) in equimolar ratio, 1 μ l of T4 DNA ligase (M0202L, NEB) and ligation buffer (10 \times T4 DNA ligase buffer, NEB) was incubated ON at 16°C or at RT for 1 h, followed by 30 min at 37°C for sticky end ligations. Then, 2 μ l of the ligation reaction were used to transform competent bacteria.

7.2.1.3 Separation of DNA on agarose gels

The DNA mix and approximately 1/6 of the volume of 6 \times loading buffer were loaded onto an 0.8-2% agarose gel in TAE buffer containing ethidium bromide (2218.2, Roth, use 1 μ l per 100 ml) and run for approximate 30 to 35 min at 100-200 V. After electrophoresis a photograph of the gel was taken in the transilluminator on a UV light box and printed. In a preparative gel, the DNA band was excised from the agarose gel with a clean, sharp scalpel and purified (see purification of DNA).

7.2.1.4 Purification of DNA

7.2.1.4.1 From agarose gel

Following extraction, purification of DNA fragments from agarose gels was carried out using the QIAquick Gel Extraction Kit (28704, QIAGEN) as recommended by the manufacturer. The DNA was eluted in 30 μ l H₂O.

7.2.1.4.2 From enzymatic reactions

To clean-up DNA fragments from salts, enzymes, unincorporated nucleotides, the QIAquick Nucleotide Removal Kit (28104, QIAGEN) was used according to the protocol of QIAGEN. The DNA was eluted in 30 μ l H₂O.

7.2.1.5 Transformation of competent *E. coli* by electroporation

50 μ l of electro competent bacteria were gently thawed on ice, mixed with 1-2 μ l of the ligation product. Sterile 0.2 cm (green) cuvettes were placed on ice. Gene pulser apparatus (BioRad) was set at 25 μ F and to 2.5 kV; the pulse controller to 200 W. The mixture of bacteria and DNA was transferred to a cold electroporation cuvette and knocked down to the bottom of the cuvette. The cuvette was placed in the chamber slide, pushed into the chamber and pulsed once at the above settings. 1 ml LB medium was immediately added to the cuvette. The cells were resuspended, transferred to a reaction tube and incubated at 37°C for 60 min with shaking at 225-250 rpm. The bacteria were then plated on LB agar plates containing the appropriate antibiotic for the plasmid vector and incubated at 37°C ON.

7.2.1.6 Mutagenesis

All mutagenesis (see plasmids) were performed using the QuikChange Site-Directed Mutagenesis Kit according to the protocol of Stratagene (200519). All desired mutations were verified by sequencing procedure (Ms. Thyrlas, MPI of Neurobiology).

7.2.1.7 Extraction of genomic DNA and genotyping using PCR

7.2.1.7.1 DNA preparation

DNA was prepared from mouse tail by treatment with 100 µg/ml Proteinase K in tail lysis buffer. 40 µl of tail lysis buffer including Proteinase K was added to each approximate 2 mm mouse tail, which was placed at 56°C for 2 h. Proteinase K was then heat-inactivated for 5-10 min at 95°C. Before PCR, the genomic DNA prep was diluted with 900 µl H₂O.

7.2.1.7.2 PCR Ubi-GRIP

1 µl of DNA per 50 µl PCR reaction was used for PCR amplification to check the DNA for the presence of the transgene.

PCR master mix:

5 µl 10×PCR buffer (Roche)

0.5 µl 25 mM dNTPs

0.5 µl 100 pmol/µl Sense-primer (GRIP1.9_Seq)

0.5 µl 100 pmol/µl Antisense-primer (TAPgeno2_AS)

1 µl Taq DNA polymerase (M0267L, NEB)

1 µl genomic DNA

to **50 µl** add distilled water

7. Materials and Methods

Segment	Cycles	Temperature	Time
1	1	95°C	2 min
2	35	95°C	1 min
		60°C	1 min
		72°C	1 min
3	1	72°C	10 min

The PCR product was mixed with 6×loading buffer, loaded on a 1.5% agarose gel and then electrophoresed for approximately 30 min at 200 V.

7.2.1.7.3 PCR GRIP1-KO

1 µl of DNA per 55 µl PCR reaction was used for PCR amplification to check the DNA for the presence of the KO allele.

PCR master mix:

5.5 µl 10×PCR buffer (Roche)

0.5 µl 25 mM dNTPs

0.25 µl 100 pmol/µl RHKT83

0.25 µl 100 pmol/µl RHKT63

0.25 µl 100pmol/µl RHKT55

1 µl Taq DNA polymerase (M0267L, NEB)

1 µl genomic DNA

to **55 µl** add distilled water

Segment	Cycles	Temperature	Time
1	1	95°C	2 min
2	35	95°C	1 min
		60°C	1 min
		72°C	20 sec
3	1	72°C	5 min

The PCR product was mixed with 6×loading buffer, loaded on a 1.5% agarose gel and then electrophoresed for approximately 30 min at 200 V.

7.2.1.8 Generation of transgenic mice

Vector sequences, particularly prokaryotic promoter and origin (ori) sequences impair the expression of the transgene. Therefore, single cutting restrictions sites should flank the final DNA fragment and this should be taken into consideration during design of the construct.

7.2.1.8.1 Plasmid digestion

Plasmid UbiKOZ-GRIP1-CTAP (see plasmids) was purified for pronuclear injection from large-scale bacterial cultures using the HiSpeed Plasmid Maxi Kit without EtOH (12663, QIAGEN). About 110 µg of the plasmid were digested with 70 U of the restriction enzyme XmaI (NEB) and 220 U of NdeI (NEB) overnight. Next day, another 70 U of the restriction enzyme XmaI and 220 U of NdeI were added and again incubated overnight. 500 ng of the reaction mix was loaded and run on an agarose gel to check if digestion was complete.

7.2.1.8.2 Pronuclear injection

The pronuclear injection was carried out by the transgenic mice service of the EMBL, Heidelberg (Kristine Vintersten).

7.2.2 Cell Culture

7.2.2.1 Primary culture of hippocampal neurons

Before preparation, coverslips were pre-coated with 1mg/ml Poly-D-lysine in borate buffer for at least 4 h at 37°C. Coverslips in 24-well plates were washed twice with sterile water and dried in a sterile hood. After coating overnight at 37°C with 5 µg/ml mouse laminin in PBS, coverslips were washed twice with PBS and then replaced by Neurobasal-B27 medium. Media were left to equilibrate for at least one hour in the incubator with 5% CO₂ atmosphere. Hippocampal neurons were taken from pregnant Wistar rats (MpiChbb:Thom, animal house, MPI of Neurobiology) at E18.5. Pregnant rats were deeply anesthetized using diethyl ether. After cervical dislocation, embryos were obtained and kept in ice-cold dissection medium. The preparation was then continued under an open sterile hood. Embryo heads were cut off and the skull opened to take out the brain. Embryonic brains were placed in fresh dissection medium and dissected under a stereomicroscope. Brain cortices were removed from the midbrain and brainstem and the meninges were pulled off. The striatum was cut out. The hippocampus was separated from the cortex and placed in fresh 15 ml dissection medium on ice. After removing the medium, hippocampi were incubated in 1.5 ml 0.25% Trypsin/1mM EDTA-HBSS-solution (25200-056, Invitrogen) for 20 min at 37°C. After carefully removing Trypsin/EDTA-HBSS-solution, the digestion reaction was stopped and the hippocampi were washed three times with 3 ml DMEM 10% FBS. Then the tissue was triturated approximately 20 times using a fire-polished glass pasteur pipette until the suspension was homogenous. Subsequently, the cell suspension was centrifuged for 5 min at 80 g to remove debris and the pellet resuspended in 2 ml Neurobasal-B27 medium. Cells were counted in a hemacytometer and plated on coated glass coverslips in a 24-well plate at a density of 620 cells/mm². Cells were incubated for 11-21 days *in vitro* (DIV) at 37°C in a humidified incubator with an atmosphere of 5% CO₂. After 7 or 12 DIV the hippocampal cultures were transfected using the Ca-phosphate-DNA precipitation procedure.

7.2.2.2 Transfection of cells

HeLa cells were transfected following a conventional Ca-phosphate-DNA precipitation procedure (Sambrook et al. 1989). For calcium phosphate transfection of hippocampal neurons on coverslips, all solutions were warmed up to room temperature. The CaCl₂-DNA-BBS mixture was added drop wise to 0.9 ml medium in a polystyrene-tube (Falcon) while vortexing. After collecting the remaining medium from 4 wells, 250 µl of the transfection solution was immediately added to each well. The collected medium was filter-sterilized and kept in the incubator. Cells were incubated at 37°C in a humidified incubator with an atmosphere of 5% CO₂ for the desired transfection time (1-3 h). Afterwards, the transfection medium was removed and cultures were washed with prewarmed HBSS (14025-050, Invitrogen) twice and kept for 10 min each time in a 37°C incubator (no CO₂ atmosphere). Then the “old” prewarmed culture medium was readded.

7.2.2.3 Stimulation of cells with Eph receptors or ephrin ligands

All cell types were stimulated with EphB2-Fc or Fc (Biochemistry: 1 µg/ml, Immunocytochemistry: 4 µg/ml), which had been pre-clustered for 1 h at room temperature using 1/10 (w/w) goat anti-human IgG (Jackson Immunoresearch). Before stimulation, all cell types except hippocampal neurons were starved for 24 h in medium containing 0% serum.

7.2.3 Biochemistry

7.2.3.1 Tandem affinity purification and mass spectrometry

Retroviral transduction vectors were generated by cloning open reading frames, amplified by polymerase chain reaction, into a Moloney-based vector with the Gateway site-specific recombination system to obtain C-terminal TAP fusions of Grb4 and GRIP1. Virus stocks were generated in a HEK293 Gag–Pol packaging cell

line. SK-N-BE2 cells were infected and complexes were purified by using a modified TAP protocol (Gavin et al. 2002). Cells were grown in Optimem Glutamax (Invitrogen) medium with 10% iron supplemented FBS (Sigma). Eighty 15 cm-dishes of SK-N-BE2 Grb4-CTAP or SK-N-BE2 GRIP1-CTAP cells were harvested by mechanical detachment, washed with excess PBS on ice and lysed in 10 ml lysis buffer each using a Dounce homogenizer (30 times). Afterwards, lysates were incubated spinning on a wheel for 30 min at 4°C and then centrifuged for 10 min (13,000 rpm, 4°C, SS34 rotor). The supernatant was added on 200 µl rabbit IgG agarose beads (Roche) in a 15 ml-Falcon tube and incubated for 2h at 4°C. Beads were saved by centrifugation for 1 min (1,300 rpm, 4°C, Varifuge 3.0R), transferred into a small column (0.8 ml Mobicol M1002, MoBiTec) and washed with 10 ml lysis buffer followed by a wash with 5 ml TEV cleavage buffer. Beads were resuspended in 150 µl TEV cleavage buffer and incubated upon addition of 4 µl TEV protease (recombinant, 10127-017, Invitrogen) for 3 h at 16°C in a thermoshaker (900 rpm). The TEV eluate was directly applied on calmodulin affinity resin (214303-52, Stratagene) in another column, mixed with 200 µl CBP binding buffer and incubated for 1 h at 4°C. Calmodulin beads were washed with 5 ml CBP washing buffer and the protein complexes eluted with 600 µl CBP elution buffer for 5 min at 37°C. Both the calmodulin beads after elution and the lyophilized protein samples were boiled for 5 min with 50 µl 4x sample buffer (containing 20 mM DTT) and separated by NuPAGE 4-12% Bis-Tris-PAGE (NP0321BOX, Invitrogen). Complete gel lanes were systematically cut into slices and proteins were digested in-gel with trypsin as described (Shevchenko et al. 1996). Protein identification was performed by LC-MS/MS at Cellzome AG (Heidelberg) and MS data were searched against an in-house curated version of the International Protein Index (IPI), maintained at the EBI (Hinxton, UK). Results of database searches were read into a database system for further bioinformatics analysis.

7.2.3.2 Cell lysis, immunoprecipitation, EphB2-Fc-pulldown experiments

Transiently transfected HeLa cells were washed twice with ice-cold PBS and lysed in lysis buffer on ice. After scraping off and collecting the cells from the dish, the cell lysate was centrifuged at 10,000 g for 15 min at 4°C to remove insoluble material

(nuclei, cytoskeletal components and insoluble membranes). The supernatant was placed in a fresh Eppendorf tube and directly loaded onto a SDS-Polyacrylamide gel (SDS-PAGE) or purified further (see below). Before loading on a gel, samples were boiled in 6×sample buffer for 7 min to denature the proteins.

For immunoprecipitation, 2-4 µg of the antibody against the protein of interest was prebound to protein A sepharose (for rabbit polyclonal antibodies) or protein G sepharose (for mouse monoclonal and goat polyclonal antibodies) for 30 min at RT. The total lysate was added and incubated for 2 hours on a rotating wheel at 4°C. Subsequently, the mixture was spun down at 4,000 g for 2 min at 4°C. The supernatant was discarded and the beads were washed three times with lysis buffer to remove traces of unbound proteins. 25 µl of 2×sample buffer was added to the beads and the mix was then boiled for 5 min. The entire sample was loaded on a SDS-PAGE gel under reducing conditions and further processed.

EphB2-Fc precipitation from brain tissue or immunoprecipitation of ephrinB1-HA/Grb4-YFP complexes from HeLa cells were performed following the protocol described (Cowan and Henkemeyer 2001). Briefly, 10 µg of EphB2-Fc (R&D Systems) or 4 µg of anti-HA (Roche) were coupled to protein G sepharose beads (Amersham) and incubated 2 h at 4°C with the lysates (1 mg/ml) prepared in PLC lysis buffer containing 1% NP-40. Bound proteins were then washed three times in HNTG for the EphB2-Fc pulldowns or three times in PLC lysis buffer followed by two washes in HNTG for HA-immunoprecipitations. Samples were then boiled 7 min in sample buffer, resolved by SDS-PAGE, transferred to nitrocellulose and immunoblotted with the indicated antibodies.

7.2.3.3 Immunoblotting

Protein samples derived from the procedures described above were separated by SDS-PAGE and transferred to nitrocellulose or PVDF membranes by semi-dry blotting (1 mA per cm² for 1 to 1.5 h). Membranes were blocked at least for 30 min at RT or overnight at 4°C in blocking solution and then incubated for 1 h at RT or overnight at 4°C with a primary antibody diluted in blocking solution. Subsequently, membranes were washed three times for 10 min in PBST at RT. Secondary antibodies linked to horseradish peroxidase (HRP) diluted in blocking solution were used to specifically

recognize the primary antibody. After incubation for 1 h at RT, membranes were washed three times for 10 min in PBST. To visualize signals, membranes were incubated with ECL solution for 1 min at RT and exposed to films. For reprobing, membranes were stripped with stripping buffer.

7.2.3.4 Purification of membranes and rafts from adult mice

For the analysis of detergent-insoluble complexes in flotation gradients, a membrane fraction was prepared at 4°C as follows. Two brains from adult mice were homogenized in a Dounce homogenizer in 3 ml of ice-cold homogenization buffer TNE. The extract was passed ten times through a 22G needle, ten times through 25G needle and centrifuged for 15 min (13,000 g, 4°C). The pellet was re-extracted with 1 ml of TNE buffer using a 25G or 27G needle and centrifuged again for 15 min (13,000 g, 4°C). The supernatants of both centrifugations were adjusted to 40% Optiprep and overlaid in a SW40 centrifuge tube with 7 ml of 30% and 3 ml of 5% Optiprep in TNE buffer. After centrifugation for 4 h (24,000 rpm, 4°C; SW40 rotor), the floated membranes were collected in 600 µl from the 5%/30% interface. Membranes were adjusted to 0.3% Triton X-100 following extraction for 30 min on a wheel at 4°C. The extracted membranes were adjusted to 40% of Optiprep and overlaid in a SW60 centrifuge tube with 2.5 ml 35% Optiprep and 400 µl of 5% Optiprep in TNE buffer. After centrifugation for 4 h (40,000 rpm, 4°C; SW60 rotor) seven fractions were collected from the top.

7.2.3.5 Postsynaptic density fractionation

Postsynaptic densities were prepared as described by Cho (Cho et al. 1992). In brief, hippocampi of 12 wt C57/BL-6 adult male mice were homogenized in a dounce glass Teflon homogenizer in 12 ml solution A and centrifuged at 3,000 g for 10 min at 4°C. Pellets were re-extracted with 5 ml solution A, centrifuged at 1,000 g for 10 min at 4°C, supernatants combined with the ones from the previous centrifugation and centrifuged at 10,000 g for 10 min at 4°C. Pellets were resuspended in 5 ml solution B, overlaid on a 1.2 M/1.0 M/0.85 M sucrose gradient and ultracentrifuged at 25,500

g for 2 h at 4°C. A synaptic membrane fraction was extracted at the interface of 1.2 M/1.0 M sucrose layers and a control non-synaptic fraction was extracted between the top (0.32 M) and the 0.85 M sucrose layer. The synaptosome fraction was diluted to 9 ml in solution B, 9 ml of solution C was added followed by a 15 min incubation on ice. The solution was divided into 6 samples and pelleted at 22,300 g for 20 min at 4°C. One pellet was resuspended in 100 µl solution D (PSD fraction 1), the remaining five pellets in 5 ml solution B. 2 ml of this solution were mixed with 2 ml solution C, incubated on ice for 15 min and centrifuged at 50,100 g for 60 min at 4°C. The resulting pellet was resuspended in 100 µl solution D, 0.3% SDS (PSD fraction 2). The remaining 3 ml were mixed with 3 ml sol E, incubated on ice for 15 min, centrifuged at 50,100 g for 60 min and the pellet resuspended in 100 µl solution D (PSD fraction 3). For a description of solutions used, please refer to the Materials section.

7.2.3.6 Immunocytochemistry

7.2.3.6.1 Immunostaining of cells

For normal immunocytochemistry of total protein distribution, neurons grown on coverslips were fixed with 4% PFA, 4% sucrose in PBS for 13 min at 4°C, washed once with PBS, then incubated with 50mM NH₄Cl in PBS for 10 min at 4°C and washed again before permeabilization for 5 min with ice-cold 0.1% Triton X-100 in PBS. After washing, coverslips were blocked for about 30 min at RT or overnight at 4°C with 2% bovine albumin (A-3294, Sigma) and 4% serum in PBS. After blocking, coverslips were transferred into a dark moist chamber, face up. Primary antibodies for total stainings were incubated for at least 60 min at RT in 50 µl blocking solution. After 3 washing steps with PBS for 5 min, secondary antibodies, previously diluted in 50 µl of blocking solution, were applied for 30 min at RT in the dark. After washing, samples were mounted in Gel/Mount media and dried at RT. Images were acquired using an epifluorescence microscope (Zeiss) equipped with a digital camera (SpotRT, Diagnostic Instruments) and the MetaMorph software (Visitron Systems).

7.2.3.6.2 Image analysis and quantification

Images were acquired using a digital camera (SpotRT; Diagnostic Instruments, Sterling Heights, MI) attached to an epifluorescence microscope (Zeiss, Göttingen, Germany) equipped with a 63X objective (Plan-Apochromat; Zeiss, Göttingen, Germany). All quantitative measurements were performed using MetaMorph software. Statistical analysis was performed using Microsoft Excel. Groups of protrusions were compared using t-test. Neurons expressing high levels of the constructs were chosen for quantification as follows. Approximately 100 dendrites from independent transfections were randomly selected for each construct to quantify number of protrusions in proximal 50 μm sections of dendrites. Length of protrusions was determined by measuring the distance between the tip and the base (n>500 protrusions).

7.2.4 Mouse work

Transgenic mice were crossed in a C57/Black6 (C57BL/6NCrlMpi, animal house, MPI of Neurobiology) genetic background. For experiments with adult mice, mice were separated from their parents at the age of about three weeks, males and females were housed separately. Tail biopsies were taken and mice were ear tagged using six-digit number eartag from the Nationalband & Tag company. For all experiments a heterozygous transgenic male was crossed with wild type females and the mice of the same litter were compared.

8. Bibliography

- Abe, M., M. Fukaya, T. Yagi, M. Mishina, M. Watanabe and K. Sakimura (2004). "NMDA receptor GluRepsilon/NR2 subunits are essential for postsynaptic localization and protein stability of GluRzeta1/NR1 subunit." J Neurosci **24**(33): 7292-304.
- Ackermann, M. and A. Matus (2003). "Activity-induced targeting of profilin and stabilization of dendritic spine morphology." Nat Neurosci **6**(11): 1194-200.
- Allen, K. M., J. G. Gleeson, S. Bagrodia, M. W. Partington, J. C. MacMillan, R. A. Cerione, J. C. Mulley and C. A. Walsh (1998). "PAK3 mutation in nonsyndromic X-linked mental retardation." Nat Genet **20**(1): 25-30.
- Bagrodia, S., D. Bailey, Z. Lenard, M. Hart, J. L. Guan, R. T. Premont, S. J. Taylor and R. A. Cerione (1999). "A tyrosine-phosphorylated protein that binds to an important regulatory region on the cool family of p21-activated kinase-binding proteins." J Biol Chem **274**(32): 22393-400.
- Barnes, A. P. and S. L. Milgram (2002). "Signals from the X: signal transduction and X-linked mental retardation." Int J Dev Neurosci **20**(3-5): 397-406.
- Bauer, A. and B. Kuster (2003). "Affinity purification-mass spectrometry. Powerful tools for the characterization of protein complexes." Eur J Biochem **270**(4): 570-8.
- Berardi, N., T. Pizzorusso and L. Maffei (2004). "Extracellular matrix and visual cortical plasticity: freeing the synapse." Neuron **44**(6): 905-8.
- Billuart, P., T. Bienvenu, N. Ronce, V. des Portes, M. C. Vinet, R. Zemni, A. Carrie, C. Beldjord, et al. (1998). "Oligophrenin 1 encodes a rho-GAP protein involved in X-linked mental retardation." Pathol Biol (Paris) **46**(9): 678.
- Binns, K. L., P. P. Taylor, F. Sicheri, T. Pawson and S. J. Holland (2000). "Phosphorylation of tyrosine residues in the kinase domain and juxtamembrane region regulates the biological and catalytic activities of Eph receptors." Mol Cell Biol **20**(13): 4791-805.
- Bladt, F., A. Tafuri, S. Gelkop, L. Langille and T. Pawson (2002). "Epidermolysis bullosa and embryonic lethality in mice lacking the multi-PDZ domain protein GRIP1." Proc Natl Acad Sci U S A **99**(10): 6816-21.
- Bliss, T. V. and A. R. Gardner-Medwin (1973). "Long-lasting potentiation of synaptic transmission in the dentate area of the unanaesthetized rabbit following stimulation of the perforant path." J Physiol **232**(2): 357-74.

8. Bibliography

- Bonhoeffer, T. and R. Yuste (2002). "Spine motility. Phenomenology, mechanisms, and function." Neuron **35**(6): 1019-27.
- Brantley-Sieders, D., M. Parker and J. Chen (2004). "Eph receptor tyrosine kinases in tumor and tumor microenvironment." Curr Pharm Des **10**(27): 3431-42.
- Braverman, L. E. and L. A. Quilliam (1999). "Identification of Grb4/Nckbeta, a src homology 2 and 3 domain-containing adapter protein having similar binding and biological properties to Nck." J Biol Chem **274**(9): 5542-9.
- Brouns, M. R., S. F. Matheson and J. Settleman (2001). "p190 RhoGAP is the principal Src substrate in brain and regulates axon outgrowth, guidance and fasciculation." Nat Cell Biol **3**(4): 361-7.
- Brown, D. A. and J. K. Rose (1992). "Sorting of GPI-anchored proteins to glycolipid-enriched membrane subdomains during transport to the apical cell surface." Cell **68**(3): 533-44.
- Brown, M. C., L. A. Cary, J. S. Jamieson, J. A. Cooper and C. E. Turner (2005). "Src and FAK kinases cooperate to phosphorylate paxillin kinase linker, stimulate its focal adhesion localization, and regulate cell spreading and protrusiveness." Mol Biol Cell **16**(9): 4316-28.
- Bruckner, K., J. Pablo Labrador, P. Scheiffele, A. Herb, P. H. Seeburg and R. Klein (1999). "EphrinB ligands recruit GRIP family PDZ adaptor proteins into raft membrane microdomains." Neuron **22**(3): 511-24.
- Bruckner, K., E. B. Pasquale and R. Klein (1997). "Tyrosine phosphorylation of transmembrane ligands for Eph receptors." Science **275**(5306): 1640-3.
- Carlin, R. K., D. J. Grab, R. S. Cohen and P. Siekevitz (1980). "Isolation and characterization of postsynaptic densities from various brain regions: enrichment of different types of postsynaptic densities." J Cell Biol **86**(3): 831-45.
- Carlisle, H. J. and M. B. Kennedy (2005). "Spine architecture and synaptic plasticity." Trends Neurosci **28**(4): 182-7.
- Chaudhri, M., M. Scarabel and A. Aitken (2003). "Mammalian and yeast 14-3-3 isoforms form distinct patterns of dimers in vivo." Biochem Biophys Res Commun **300**(3): 679-85.
- Chen, J., M. Wang, D. Ruan and J. She (2002). "Early chronic aluminium exposure impairs long-term potentiation and depression to the rat dentate gyrus in vivo." Neuroscience **112**(4): 879-87.

- Cho, K. O., C. A. Hunt and M. B. Kennedy (1992). "The rat brain postsynaptic density fraction contains a homolog of the *Drosophila* discs-large tumor suppressor protein." Neuron **9**(5): 929-42.
- Chong, L. D., E. K. Park, E. Latimer, R. Friesel and I. O. Daar (2000). "Fibroblast growth factor receptor-mediated rescue of x-ephrin B1-induced cell dissociation in *Xenopus* embryos." Mol Cell Biol **20**(2): 724-34.
- Clevers, H. and E. Batlle (2006). "EphB/EphrinB receptors and Wnt signaling in colorectal cancer." Cancer Res **66**(1): 2-5.
- Conover, J. C., F. Doetsch, J. M. Garcia-Verdugo, N. W. Gale, G. D. Yancopoulos and A. Alvarez-Buylla (2000). "Disruption of Eph/ephrin signaling affects migration and proliferation in the adult subventricular zone." Nat Neurosci **3**(11): 1091-7.
- Contractor, A., C. Rogers, C. Maron, M. Henkemeyer, G. T. Swanson and S. F. Heinemann (2002). "Trans-synaptic Eph receptor-ephrin signaling in hippocampal mossy fiber LTP." Science **296**(5574): 1864-9.
- Cowan, C. A. and M. Henkemeyer (2001). "The SH2/SH3 adaptor Grb4 transduces B-ephrin reverse signals." Nature **413**(6852): 174-9.
- Dailey, M. E. and S. J. Smith (1996). "The dynamics of dendritic structure in developing hippocampal slices." J Neurosci **16**(9): 2983-94.
- Dalva, M. B., M. A. Takasu, M. Z. Lin, S. M. Shamah, L. Hu, N. W. Gale and M. E. Greenberg (2000). "EphB receptors interact with NMDA receptors and regulate excitatory synapse formation." Cell **103**(6): 945-56.
- Davy, A., N. W. Gale, E. W. Murray, R. A. Klinghoffer, P. Soriano, C. Feuerstein and S. M. Robbins (1999). "Compartmentalized signaling by GPI-anchored ephrin-A5 requires the Fyn tyrosine kinase to regulate cellular adhesion." Genes Dev **13**(23): 3125-35.
- Davy, A. and S. M. Robbins (2000). "Ephrin-A5 modulates cell adhesion and morphology in an integrin-dependent manner." Embo J **19**(20): 5396-405.
- Deng, J. and A. Dunaevsky (2005). "Dynamics of dendritic spines and their afferent terminals: spines are more motile than presynaptic boutons." Dev Biol **277**(2): 366-77.
- Desmond, N. L. and W. B. Levy (1986). "Changes in the postsynaptic density with long-term potentiation in the dentate gyrus." J Comp Neurol **253**(4): 476-82.

8. Bibliography

- Dong, H., R. J. O'Brien, E. T. Fung, A. A. Lanahan, P. F. Worley and R. L. Huganir (1997). "GRIP: a synaptic PDZ domain-containing protein that interacts with AMPA receptors." Nature **386**(6622): 279-84.
- Dong, H., P. Zhang, I. Song, R. S. Petralia, D. Liao and R. L. Huganir (1999). "Characterization of the glutamate receptor-interacting proteins GRIP1 and GRIP2." J Neurosci **19**(16): 6930-41.
- Drewes, G. and T. Bouwmeester (2003). "Global approaches to protein-protein interactions." Curr Opin Cell Biol **15**(2): 199-205.
- Dunaevsky, A., R. Blazeski, R. Yuste and C. Mason (2001). "Spine motility with synaptic contact." Nat Neurosci **4**(7): 685-6.
- Dunaevsky, A. and C. A. Mason (2003). "Spine motility: a means towards an end?" Trends Neurosci **26**(3): 155-60.
- Dunaevsky, A., A. Tashiro, A. Majewska, C. Mason and R. Yuste (1999). "Developmental regulation of spine motility in the mammalian central nervous system." Proc Natl Acad Sci U S A **96**(23): 13438-43.
- Egea, J., U. V. Nissen, A. Dufour, M. Sahin, P. Greer, K. Kullander, T. D. Mrcic-Flogel, M. E. Greenberg, et al. (2005). "Regulation of EphA 4 kinase activity is required for a subset of axon guidance decisions suggesting a key role for receptor clustering in Eph function." Neuron **47**(4): 515-28.
- El-Husseini, A. E., E. Schnell, D. M. Chetkovich, R. A. Nicoll and D. S. Bredt (2000). "PSD-95 involvement in maturation of excitatory synapses." Science **290**(5495): 1364-8.
- Engert, F. and T. Bonhoeffer (1999). "Dendritic spine changes associated with hippocampal long-term synaptic plasticity." Nature **399**(6731): 66-70.
- Ethell, I. M., F. Irie, M. S. Kalo, J. R. Couchman, E. B. Pasquale and Y. Yamaguchi (2001). "EphB/syndecan-2 signaling in dendritic spine morphogenesis." Neuron **31**(6): 1001-13.
- Ethell, I. M. and Y. Yamaguchi (1999). "Cell surface heparan sulfate proteoglycan syndecan-2 induces the maturation of dendritic spines in rat hippocampal neurons." J Cell Biol **144**(3): 575-86.
- Eyre, M. D., G. Richter-Levin, A. Avital and M. G. Stewart (2003). "Morphological changes in hippocampal dentate gyrus synapses following spatial learning in rats are transient." Eur J Neurosci **17**(9): 1973-80.

- Fiala, J. C., M. Feinberg, V. Popov and K. M. Harris (1998). "Synaptogenesis via dendritic filopodia in developing hippocampal area CA1." J Neurosci **18**(21): 8900-11.
- Fiala, J. C., J. Spacek and K. M. Harris (2002). "Dendritic spine pathology: cause or consequence of neurological disorders?" Brain Res Brain Res Rev **39**(1): 29-54.
- Fifkova, E. and C. L. Anderson (1981). "Stimulation-induced changes in dimensions of stalks of dendritic spines in the dentate molecular layer." Exp Neurol **74**(2): 621-7.
- Filipenko, N. R., S. Attwell, C. Roskelley and S. Dedhar (2005). "Integrin-linked kinase activity regulates Rac- and Cdc42-mediated actin cytoskeleton reorganization via alpha-PIX." Oncogene **24**(38): 5837-49.
- Fischer, M., S. Kaech, D. Knutti and A. Matus (1998). "Rapid actin-based plasticity in dendritic spines." Neuron **20**(5): 847-54.
- Fu, H., R. R. Subramanian and S. C. Masters (2000). "14-3-3 proteins: structure, function, and regulation." Annu Rev Pharmacol Toxicol **40**: 617-47.
- Fukazawa, Y., Y. Saitoh, F. Ozawa, Y. Ohta, K. Mizuno and K. Inokuchi (2003). "Hippocampal LTP is accompanied by enhanced F-actin content within the dendritic spine that is essential for late LTP maintenance in vivo." Neuron **38**(3): 447-60.
- Furuyashiki, T., Y. Arakawa, S. Takemoto-Kimura, H. Bito and S. Narumiya (2002). "Multiple spatiotemporal modes of actin reorganization by NMDA receptors and voltage-gated Ca²⁺ channels." Proc Natl Acad Sci U S A **99**(22): 14458-63.
- Gauthier, L. R. and S. M. Robbins (2003). "Ephrin signaling: One raft to rule them all? One raft to sort them? One raft to spread their call and in signaling bind them?" Life Sci **74**(2-3): 207-16.
- Gavin, A. C., M. Bosche, R. Krause, P. Grandi, M. Marzioch, A. Bauer, J. Schultz, J. M. Rick, et al. (2002). "Functional organization of the yeast proteome by systematic analysis of protein complexes." Nature **415**(6868): 141-7.
- Goldin, M., M. Segal and E. Avignone (2001). "Functional plasticity triggers formation and pruning of dendritic spines in cultured hippocampal networks." J Neurosci **21**(1): 186-93.
- Gross, S. R. and T. G. Kinzy (2005). "Translation elongation factor 1A is essential for regulation of the actin cytoskeleton and cell morphology." Nat Struct Mol Biol **12**(9): 772-8.

8. Bibliography

- Grunwald, I. C., M. Korte, G. Adelman, A. Plueck, K. Kullander, R. H. Adams, M. Frotscher, T. Bonhoeffer, et al. (2004). "Hippocampal plasticity requires postsynaptic ephrinBs." Nat Neurosci **7**(1): 33-40.
- Grunwald, I. C., M. Korte, D. Wolfer, G. A. Wilkinson, K. Unsicker, H. P. Lipp, T. Bonhoeffer and R. Klein (2001). "Kinase-independent requirement of EphB2 receptors in hippocampal synaptic plasticity." Neuron **32**(6): 1027-40.
- Grutzendler, J., N. Kasthuri and W. B. Gan (2002). "Long-term dendritic spine stability in the adult cortex." Nature **420**(6917): 812-6.
- Haendeler, J., G. Yin, Y. Hojo, Y. Saito, M. Melaragno, C. Yan, V. K. Sharma, M. Heller, et al. (2003). "GIT1 mediates Src-dependent activation of phospholipase Cgamma by angiotensin II and epidermal growth factor." J Biol Chem **278**(50): 49936-44.
- Hall, A. and C. D. Nobes (2000). "Rho GTPases: molecular switches that control the organization and dynamics of the actin cytoskeleton." Philos Trans R Soc Lond B Biol Sci **355**(1399): 965-70.
- Harder, T., P. Scheiffele, P. Verkade and K. Simons (1998). "Lipid domain structure of the plasma membrane revealed by patching of membrane components." J Cell Biol **141**(4): 929-42.
- Harris, K. M. (1999). "Calcium from internal stores modifies dendritic spine shape." Proc Natl Acad Sci U S A **96**(22): 12213-5.
- Harris, K. M. and S. B. Kater (1994). "Dendritic spines: cellular specializations imparting both stability and flexibility to synaptic function." Annu Rev Neurosci **17**: 341-71.
- Helmchen, F. (2002). "Raising the speed limit--fast Ca(2+) handling in dendritic spines." Trends Neurosci **25**(9): 438-41; discussion 441.
- Henderson, J. T., J. Georgiou, Z. Jia, J. Robertson, S. Elowe, J. C. Roder and T. Pawson (2001). "The receptor tyrosine kinase EphB2 regulates NMDA-dependent synaptic function." Neuron **32**(6): 1041-56.
- Henkemeyer, M., O. S. Itkis, M. Ngo, P. W. Hickmott and I. M. Ethell (2003). "Multiple EphB receptor tyrosine kinases shape dendritic spines in the hippocampus." J Cell Biol **163**(6): 1313-26.
- Henkemeyer, M., D. Orioli, J. T. Henderson, T. M. Saxton, J. Roder, T. Pawson and R. Klein (1996). "Nuk controls pathfinding of commissural axons in the mammalian central nervous system." Cell **86**(1): 35-46.

- Hensch, T. K. (2004). "Critical period regulation." Annu Rev Neurosci **27**: 549-79.
- Hering, H., C. C. Lin and M. Sheng (2003). "Lipid rafts in the maintenance of synapses, dendritic spines, and surface AMPA receptor stability." J Neurosci **23**(8): 3262-71.
- Himanen, J. P., M. J. Chumley, M. Lackmann, C. Li, W. A. Barton, P. D. Jeffrey, C. Vearing, D. Geleick, et al. (2004). "Repelling class discrimination: ephrin-A5 binds to and activates EphB2 receptor signaling." Nat Neurosci **7**(5): 501-9.
- Himanen, J. P. and D. B. Nikolov (2003). "Eph signaling: a structural view." Trends Neurosci **26**(1): 46-51.
- Holmberg, J., A. Armulik, K. A. Senti, K. Edoff, K. Spalding, S. Momma, R. Cassidy, J. G. Flanagan, et al. (2005). "Ephrin-A2 reverse signaling negatively regulates neural progenitor proliferation and neurogenesis." Genes Dev **19**(4): 462-71.
- Holmberg, J., D. L. Clarke and J. Frisen (2000). "Regulation of repulsion versus adhesion by different splice forms of an Eph receptor." Nature **408**(6809): 203-6.
- Hoogenraad, C. C., A. D. Milstein, I. M. Ethell, M. Henkemeyer and M. Sheng (2005). "GRIP1 controls dendrite morphogenesis by regulating EphB receptor trafficking." Nat Neurosci **8**(7): 906-15.
- Huai, J. and U. Drescher (2001). "An ephrin-A-dependent signaling pathway controls integrin function and is linked to the tyrosine phosphorylation of a 120-kDa protein." J Biol Chem **276**(9): 6689-94.
- Hubbard, M. J. and P. Cohen (1993). "On target with a new mechanism for the regulation of protein phosphorylation." Trends Biochem Sci **18**(5): 172-7.
- Hunter, T. (2000). "Signaling--2000 and beyond." Cell **100**(1): 113-27.
- Huttenlocher, P. R. (1974). "Dendritic development in neocortex of children with mental defect and infantile spasms." Neurology **24**(3): 203-10.
- Ichimura, T., A. Wakamiya-Tsuruta, C. Itagaki, M. Taoka, T. Hayano, T. Natsume and T. Isobe (2002). "Phosphorylation-dependent interaction of kinesin light chain 2 and the 14-3-3 protein." Biochemistry **41**(17): 5566-72.
- Irie, F. and Y. Yamaguchi (2002). "EphB receptors regulate dendritic spine development via intersectin, Cdc42 and N-WASP." Nat Neurosci **5**(11): 1117-8.

8. Bibliography

- Jin, J., F. D. Smith, C. Stark, C. D. Wells, J. P. Fawcett, S. Kulkarni, P. Metalnikov, P. O'Donnell, et al. (2004). "Proteomic, functional, and domain-based analysis of in vivo 14-3-3 binding proteins involved in cytoskeletal regulation and cellular organization." Curr Biol **14**(16): 1436-50.
- Jontes, J. D. and S. J. Smith (2000). "Filopodia, spines, and the generation of synaptic diversity." Neuron **27**(1): 11-4.
- Jourdain, P., K. Fukunaga and D. Muller (2003). "Calcium/calmodulin-dependent protein kinase II contributes to activity-dependent filopodia growth and spine formation." J Neurosci **23**(33): 10645-9.
- Kalo, M. S. and E. B. Pasquale (1999). "Multiple in vivo tyrosine phosphorylation sites in EphB receptors." Biochemistry **38**(43): 14396-408.
- Kaufmann, W. E. and H. W. Moser (2000). "Dendritic anomalies in disorders associated with mental retardation." Cereb Cortex **10**(10): 981-91.
- Kim, C. H., H. J. Chung, H. K. Lee and R. L. Huganir (2001). "Interaction of the AMPA receptor subunit GluR2/3 with PDZ domains regulates hippocampal long-term depression." Proc Natl Acad Sci U S A **98**(20): 11725-30.
- Kim, C. H. and J. E. Lisman (1999). "A role of actin filament in synaptic transmission and long-term potentiation." J Neurosci **19**(11): 4314-24.
- Klann, E. and T. E. Dever (2004). "Biochemical mechanisms for translational regulation in synaptic plasticity." Nat Rev Neurosci **5**(12): 931-42.
- Knoll, B. and U. Drescher (2004). "Src family kinases are involved in EphA receptor-mediated retinal axon guidance." J Neurosci **24**(28): 6248-57.
- Knoll, B., S. Isenmann, E. Kilic, J. Walkenhorst, S. Engel, J. Wehinger, M. Bahr and U. Drescher (2001). "Graded expression patterns of ephrin-As in the superior colliculus after lesion of the adult mouse optic nerve." Mech Dev **106**(1-2): 119-27.
- Ko, J., S. Kim, J. G. Valtschanoff, H. Shin, J. R. Lee, M. Sheng, R. T. Premont, R. J. Weinberg, et al. (2003). "Interaction between liprin-alpha and GIT1 is required for AMPA receptor targeting." J Neurosci **23**(5): 1667-77.
- Krucker, T., G. R. Siggins and S. Halpain (2000). "Dynamic actin filaments are required for stable long-term potentiation (LTP) in area CA1 of the hippocampus." Proc Natl Acad Sci U S A **97**(12): 6856-61.
- Kullander, K., S. D. Croll, M. Zimmer, L. Pan, J. McClain, V. Hughes, S. Zabski, T. M. DeChiara, et al. (2001). "Ephrin-B3 is the midline barrier that prevents

- corticospinal tract axons from recrossing, allowing for unilateral motor control." Genes Dev **15**(7): 877-88.
- Kullander, K. and R. Klein (2002). "Mechanisms and functions of Eph and ephrin signalling." Nat Rev Mol Cell Biol **3**(7): 475-86.
- Kutsche, K., H. Yntema, A. Brandt, I. Jantke, H. G. Nothwang, U. Orth, M. G. Boavida, D. David, et al. (2000). "Mutations in ARHGEF6, encoding a guanine nucleotide exchange factor for Rho GTPases, in patients with X-linked mental retardation." Nat Genet **26**(2): 247-50.
- Lang, C., A. Barco, L. Zablow, E. R. Kandel, S. A. Siegelbaum and S. S. Zakharenko (2004). "Transient expansion of synaptically connected dendritic spines upon induction of hippocampal long-term potentiation." Proc Natl Acad Sci U S A **101**(47): 16665-70.
- Lee, S. H., M. Eom, S. J. Lee, S. Kim, H. J. Park and D. Park (2001). "BetaPix-enhanced p38 activation by Cdc42/Rac/PAK/MKK3/6-mediated pathway. Implication in the regulation of membrane ruffling." J Biol Chem **276**(27): 25066-72.
- Li, W., J. Fan and D. T. Woodley (2001). "Nck/Dock: an adapter between cell surface receptors and the actin cytoskeleton." Oncogene **20**(44): 6403-17.
- Lin, B., E. A. Kramar, X. Bi, F. A. Brucher, C. M. Gall and G. Lynch (2005). "Theta stimulation polymerizes actin in dendritic spines of hippocampus." J Neurosci **25**(8): 2062-9.
- Lippman, J. and A. Dunaevsky (2005). "Dendritic spine morphogenesis and plasticity." J Neurobiol **64**(1): 47-57.
- Lu, Q., E. E. Sun, R. S. Klein and J. G. Flanagan (2001). "Ephrin-B reverse signaling is mediated by a novel PDZ-RGS protein and selectively inhibits G protein-coupled chemoattraction." Cell **105**(1): 69-79.
- Lu, W. and E. B. Ziff (2005). "PICK1 interacts with ABP/GRIP to regulate AMPA receptor trafficking." Neuron **47**(3): 407-21.
- Luo, L. (2000). "Rho GTPases in neuronal morphogenesis." Nat Rev Neurosci **1**(3): 173-80.
- Mackintosh, C. (2004). "Dynamic interactions between 14-3-3 proteins and phosphoproteins regulate diverse cellular processes." Biochem J **381**(Pt 2): 329-42.

8. Bibliography

- Majewska, A., A. Tashiro and R. Yuste (2000). "Regulation of spine calcium dynamics by rapid spine motility." J Neurosci **20**(22): 8262-8.
- Maletic-Savatic, M., R. Malinow and K. Svoboda (1999). "Rapid dendritic morphogenesis in CA1 hippocampal dendrites induced by synaptic activity." Science **283**(5409): 1923-7.
- Malinow, R. and R. C. Malenka (2002). "AMPA receptor trafficking and synaptic plasticity." Annu Rev Neurosci **25**: 103-26.
- Marin-Padilla, M. (1972). "Structural abnormalities of the cerebral cortex in human chromosomal aberrations: a Golgi study." Brain Res **44**(2): 625-9.
- Marquardt, T., R. Shirasaki, S. Ghosh, S. E. Andrews, N. Carter, T. Hunter and S. L. Pfaff (2005). "Coexpressed EphA receptors and ephrin-A ligands mediate opposing actions on growth cone navigation from distinct membrane domains." Cell **121**(1): 127-39.
- Marrs, G. S., S. H. Green and M. E. Dailey (2001). "Rapid formation and remodeling of postsynaptic densities in developing dendrites." Nat Neurosci **4**(10): 1006-13.
- Marston, D. J., S. Dickinson and C. D. Nobes (2003). "Rac-dependent trans-endocytosis of ephrinBs regulates Eph-ephrin contact repulsion." Nat Cell Biol **5**(10): 879-88.
- Martin, H., J. Rostas, Y. Patel and A. Aitken (1994). "Subcellular localisation of 14-3-3 isoforms in rat brain using specific antibodies." J Neurochem **63**(6): 2259-65.
- Matsuzaki, M., G. C. Ellis-Davies, T. Nemoto, Y. Miyashita, M. Iino and H. Kasai (2001). "Dendritic spine geometry is critical for AMPA receptor expression in hippocampal CA1 pyramidal neurons." Nat Neurosci **4**(11): 1086-92.
- Matsuzaki, M., N. Honkura, G. C. Ellis-Davies and H. Kasai (2004). "Structural basis of long-term potentiation in single dendritic spines." Nature **429**(6993): 761-6.
- Matus, A., H. Brinkhaus and U. Wagner (2000). "Actin dynamics in dendritic spines: a form of regulated plasticity at excitatory synapses." Hippocampus **10**(5): 555-60.
- Meek, S. E., W. S. Lane and H. Piwnicka-Worms (2004). "Comprehensive proteomic analysis of interphase and mitotic 14-3-3-binding proteins." J Biol Chem **279**(31): 32046-54.

- Miller, M. and A. Peters (1981). "Maturation of rat visual cortex. II. A combined Golgi-electron microscope study of pyramidal neurons." J Comp Neurol **203**(4): 555-73.
- Moeller, M. L., Y. Shi, L. F. Reichardt and I. M. Ethell (2006). "EphB receptors regulate dendritic spine morphogenesis through the recruitment/phosphorylation of focal adhesion kinase and RhoA activation." J Biol Chem **281**(3): 1587-98.
- Muller, J., S. Ory, T. Copeland, H. Piwnica-Worms and D. K. Morrison (2001). "C-TAK1 regulates Ras signaling by phosphorylating the MAPK scaffold, KSR1." Mol Cell **8**(5): 983-93.
- Mundel, P., H. W. Heid, T. M. Mundel, M. Kruger, J. Reiser and W. Kriz (1997). "Synaptopodin: an actin-associated protein in telencephalic dendrites and renal podocytes." J Cell Biol **139**(1): 193-204.
- Murai, K. K., L. N. Nguyen, F. Irie, Y. Yamaguchi and E. B. Pasquale (2003). "Control of hippocampal dendritic spine morphology through ephrin-A3/EphA4 signaling." Nat Neurosci **6**(2): 153-60.
- Murai, K. K. and E. B. Pasquale (2003). "Eph'ective signaling: forward, reverse and crosstalk." J Cell Sci **116**(Pt 14): 2823-32.
- Murphy, D. D., N. B. Cole, V. Greenberger and M. Segal (1998). "Estradiol increases dendritic spine density by reducing GABA neurotransmission in hippocampal neurons." J Neurosci **18**(7): 2550-9.
- Muslin, A. J., J. W. Tanner, P. M. Allen and A. S. Shaw (1996). "Interaction of 14-3-3 with signaling proteins is mediated by the recognition of phosphoserine." Cell **84**(6): 889-97.
- Nagerl, U. V., N. Eberhorn, S. B. Cambridge and T. Bonhoeffer (2004). "Bidirectional activity-dependent morphological plasticity in hippocampal neurons." Neuron **44**(5): 759-67.
- Noren, N. K. and E. B. Pasquale (2004). "Eph receptor-ephrin bidirectional signals that target Ras and Rho proteins." Cell Signal **16**(6): 655-66.
- Obermeier, A., S. Ahmed, E. Manser, S. C. Yen, C. Hall and L. Lim (1998). "PAK promotes morphological changes by acting upstream of Rac." Embo J **17**(15): 4328-39.
- Obsil, T., R. Ghirlando, D. C. Klein, S. Ganguly and F. Dyda (2001). "Crystal structure of the 14-3-3zeta:serotonin N-acetyltransferase complex. a role for scaffolding in enzyme regulation." Cell **105**(2): 257-67.

8. Bibliography

- Ogg, S., B. Gabrielli and H. Piwnica-Worms (1994). "Purification of a serine kinase that associates with and phosphorylates human Cdc25C on serine 216." J Biol Chem **269**(48): 30461-9.
- Okabe, S., A. Miwa and H. Okado (2001). "Spine formation and correlated assembly of presynaptic and postsynaptic molecules." J Neurosci **21**(16): 6105-14.
- Okamoto, K., T. Nagai, A. Miyawaki and Y. Hayashi (2004). "Rapid and persistent modulation of actin dynamics regulates postsynaptic reorganization underlying bidirectional plasticity." Nat Neurosci **7**(10): 1104-12.
- O'Malley, A., C. O'Connell, K. J. Murphy and C. M. Regan (2000). "Transient spine density increases in the mid-molecular layer of hippocampal dentate gyrus accompany consolidation of a spatial learning task in the rodent." Neuroscience **99**(2): 229-32.
- Otmakhov, N., J. H. Tao-Cheng, S. Carpenter, B. Asrican, A. Dosemeci, T. S. Reese and J. Lisman (2004). "Persistent accumulation of calcium/calmodulin-dependent protein kinase II in dendritic spines after induction of NMDA receptor-dependent chemical long-term potentiation." J Neurosci **24**(42): 9324-31.
- Palmer, A. and R. Klein (2003). "Multiple roles of ephrins in morphogenesis, neuronal networking, and brain function." Genes Dev **17**(12): 1429-50.
- Palmer, A., M. Zimmer, K. S. Erdmann, V. Eulenburg, A. Porthin, R. Heumann, U. Deutsch and R. Klein (2002). "EphrinB phosphorylation and reverse signaling: regulation by Src kinases and PTP-BL phosphatase." Mol Cell **9**(4): 725-37.
- Pasquale, E. B. (2004). "Eph-ephrin promiscuity is now crystal clear." Nat Neurosci **7**(5): 417-8.
- Pasquale, E. B. (2005). "Eph receptor signalling casts a wide net on cell behaviour." Nat Rev Mol Cell Biol **6**(6): 462-75.
- Pawson, T. and P. Nash (2003). "Assembly of cell regulatory systems through protein interaction domains." Science **300**(5618): 445-52.
- Pawson, T. and J. D. Scott (1997). "Signaling through scaffold, anchoring, and adaptor proteins." Science **278**(5346): 2075-80.
- Peng, C. Y., P. R. Graves, S. Ogg, R. S. Thoma, M. J. Byrnes, 3rd, Z. Wu, M. T. Stephenson and H. Piwnica-Worms (1998). "C-TAK1 protein kinase phosphorylates human Cdc25C on serine 216 and promotes 14-3-3 protein binding." Cell Growth Differ **9**(3): 197-208.

- Penzes, P., A. Beeser, J. Chernoff, M. R. Schiller, B. A. Eipper, R. E. Mains and R. L. Huganir (2003). "Rapid induction of dendritic spine morphogenesis by trans-synaptic ephrinB-EphB receptor activation of the Rho-GEF kalirin." Neuron **37**(2): 263-74.
- Pilpel, Y. and M. Segal (2004). "Activation of PKC induces rapid morphological plasticity in dendrites of hippocampal neurons via Rac and Rho-dependent mechanisms." Eur J Neurosci **19**(12): 3151-64.
- Portera-Cailliau, C., D. T. Pan and R. Yuste (2003). "Activity-regulated dynamic behavior of early dendritic protrusions: evidence for different types of dendritic filopodia." J Neurosci **23**(18): 7129-42.
- Pozuelo Rubio, M., K. M. Geraghty, B. H. Wong, N. T. Wood, D. G. Campbell, N. Morrice and C. Mackintosh (2004). "14-3-3-affinity purification of over 200 human phosphoproteins reveals new links to regulation of cellular metabolism, proliferation and trafficking." Biochem J **379**(Pt 2): 395-408.
- Premont, R. T., A. Claing, N. Vitale, J. L. Freeman, J. A. Pitcher, W. A. Patton, J. Moss, M. Vaughan, et al. (1998). "beta2-Adrenergic receptor regulation by GIT1, a G protein-coupled receptor kinase-associated ADP ribosylation factor GTPase-activating protein." Proc Natl Acad Sci U S A **95**(24): 14082-7.
- Prevost, N., D. Woulfe, M. Tognolini and L. F. Brass (2003). "Contact-dependent signaling during the late events of platelet activation." J Thromb Haemost **1**(7): 1613-27.
- Purpura, D. P. (1974). "Dendritic spine "dysgenesis" and mental retardation." Science **186**(4169): 1126-8.
- Rabenstein, R. L., N. A. Addy, B. J. Caldarone, Y. Asaka, L. M. Gruenbaum, L. L. Peters, D. M. Gilligan, R. M. Fitzsimonds, et al. (2005). "Impaired synaptic plasticity and learning in mice lacking beta-adducin, an actin-regulating protein." J Neurosci **25**(8): 2138-45.
- Ramakers, G. J. (2002). "Rho proteins, mental retardation and the cellular basis of cognition." Trends Neurosci **25**(4): 191-9.
- Rao, A., E. Kim, M. Sheng and A. M. Craig (1998). "Heterogeneity in the molecular composition of excitatory postsynaptic sites during development of hippocampal neurons in culture." J Neurosci **18**(4): 1217-29.
- Richards, D. A., V. De Paola, P. Caroni, B. H. Gahwiler and R. A. McKinney (2004). "AMPA-receptor activation regulates the diffusion of a membrane marker in parallel with dendritic spine motility in the mouse hippocampus." J Physiol **558**(Pt 2): 503-12.

8. Bibliography

- Rigaut, G., A. Shevchenko, B. Rutz, M. Wilm, M. Mann and B. Seraphin (1999). "A generic protein purification method for protein complex characterization and proteome exploration." Nat Biotechnol **17**(10): 1030-2.
- Roelandse, M., A. Welman, U. Wagner, J. Hagmann and A. Matus (2003). "Focal motility determines the geometry of dendritic spines." Neuroscience **121**(1): 39-49.
- Sambrook, J., E. Fritsch and T. Maniatis (1989). Molecular Cloning: A Laboratory Manual. New York, Cold Spring Harbor Laboratory Press.
- Schorpp, M., R. Jager, K. Schellander, J. Schenkel, E. F. Wagner, H. Weiher and P. Angel (1996). "The human ubiquitin C promoter directs high ubiquitous expression of transgenes in mice." Nucleic Acids Res **24**(9): 1787-8.
- Segal, M. and P. Andersen (2000). "Dendritic spines shaped by synaptic activity." Curr Opin Neurobiol **10**(5): 582-6.
- Sekerkova, G., P. A. Loomis, B. Changyaleket, L. Zheng, R. Eytan, B. Chen, E. Mugnaini and J. R. Bartles (2003). "Novel espin actin-bundling proteins are localized to Purkinje cell dendritic spines and bind the Src homology 3 adapter protein insulin receptor substrate p53." J Neurosci **23**(4): 1310-9.
- Setou, M., D. H. Seog, Y. Tanaka, Y. Kanai, Y. Takei, M. Kawagishi and N. Hirokawa (2002). "Glutamate-receptor-interacting protein GRIP1 directly steers kinesin to dendrites." Nature **417**(6884): 83-7.
- Shevchenko, A., O. N. Jensen, A. V. Podtelejnikov, F. Sagliocco, M. Wilm, O. Vorm, P. Mortensen, H. Boucherie, et al. (1996). "Linking genome and proteome by mass spectrometry: large-scale identification of yeast proteins from two dimensional gels." Proc Natl Acad Sci U S A **93**(25): 14440-5.
- Simons, K. and D. Toomre (2000). "Lipid rafts and signal transduction." Nat Rev Mol Cell Biol **1**(1): 31-9.
- Smith, F. M., C. Vearing, M. Lackmann, H. Treutlein, J. Himanen, K. Chen, A. Saul, D. Nikolov, et al. (2004). "Dissecting the EphA3/Ephrin-A5 interactions using a novel functional mutagenesis screen." J Biol Chem **279**(10): 9522-31.
- Songyang, Z., S. E. Shoelson, M. Chaudhuri, G. Gish, T. Pawson, W. G. Haser, F. King, T. Roberts, et al. (1993). "SH2 domains recognize specific phosphopeptide sequences." Cell **72**(5): 767-78.
- Sotelo, C., R. M. Alvarado-Mallart, R. Gardette and F. Crepel (1990). "Fate of grafted embryonic Purkinje cells in the cerebellum of the adult "Purkinje cell degeneration" mutant mouse. I. Development of reciprocal graft-host interactions." J Comp Neurol **295**(2): 165-87.

- Star, E. N., D. J. Kwiatkowski and V. N. Murthy (2002). "Rapid turnover of actin in dendritic spines and its regulation by activity." *Nat Neurosci* **5**(3): 239-46.
- Stein, E., A. A. Lane, D. P. Cerretti, H. O. Schoecklmann, A. D. Schroff, R. L. Van Etten and T. O. Daniel (1998). "Eph receptors discriminate specific ligand oligomers to determine alternative signaling complexes, attachment, and assembly responses." *Genes Dev* **12**(5): 667-78.
- Steiner, P., S. Alberi, K. Kulangara, A. Yersin, J. C. Sarria, E. Regulier, S. Kasas, G. Dietler, et al. (2005). "Interactions between NEEP21, GRIP1 and GluR2 regulate sorting and recycling of the glutamate receptor subunit GluR2." *Embo J* **24**(16): 2873-84.
- Steward, O. and E. M. Schuman (2003). "Compartmentalized synthesis and degradation of proteins in neurons." *Neuron* **40**(2): 347-59.
- Takacs, J., G. Gombos, T. Gorcs, T. Becker, J. de Barry and J. Hamori (1997). "Distribution of metabotropic glutamate receptor type 1a in Purkinje cell dendritic spines is independent of the presence of presynaptic parallel fibers." *J Neurosci Res* **50**(3): 433-42.
- Takamiya, K., V. Kostourou, S. Adams, S. Jadeja, G. Chalepakis, P. J. Scambler, R. L. Haganir and R. H. Adams (2004). "A direct functional link between the multi-PDZ domain protein GRIP1 and the Fraser syndrome protein Fras1." *Nat Genet* **36**(2): 172-7.
- Takasu, M. A., M. B. Dalva, R. E. Zigmond and M. E. Greenberg (2002). "Modulation of NMDA receptor-dependent calcium influx and gene expression through EphB receptors." *Science* **295**(5554): 491-5.
- Tanaka, M., T. Kamo, S. Ota and H. Sugimura (2003). "Association of Dishevelled with Eph tyrosine kinase receptor and ephrin mediates cell repulsion." *Embo J* **22**(4): 847-58.
- Tanaka, M., R. Ohashi, R. Nakamura, K. Shinmura, T. Kamo, R. Sakai and H. Sugimura (2004). "Tiam1 mediates neurite outgrowth induced by ephrin-B1 and EphA2." *Embo J* **23**(5): 1075-88.
- Tolias, K. F., J. B. Bikoff, A. Burette, S. Paradis, D. Harrar, S. Tavazoie, R. J. Weinberg and M. E. Greenberg (2005). "The Rac1-GEF Tiam1 couples the NMDA receptor to the activity-dependent development of dendritic arbors and spines." *Neuron* **45**(4): 525-38.
- Torres, R., B. L. Firestein, H. Dong, J. Staudinger, E. N. Olson, R. L. Haganir, D. S. Bredt, N. W. Gale, et al. (1998). "PDZ proteins bind, cluster, and synaptically colocalize with Eph receptors and their ephrin ligands." *Neuron* **21**(6): 1453-63.

8. Bibliography

- Trachtenberg, J. T., B. E. Chen, G. W. Knott, G. Feng, J. R. Sanes, E. Welker and K. Svoboda (2002). "Long-term in vivo imaging of experience-dependent synaptic plasticity in adult cortex." Nature **420**(6917): 788-94.
- Tsukada, M., A. Prokscha, E. Ungewickell and G. Eichele (2005). "Doublecortin association with actin filaments is regulated by neurabin II." J Biol Chem **280**(12): 11361-8.
- van Hemert, M. J., H. Y. Steensma and G. P. van Heusden (2001). "14-3-3 proteins: key regulators of cell division, signalling and apoptosis." Bioessays **23**(10): 936-46.
- van Nieuw Amerongen, G. P., K. Natarajan, G. Yin, R. J. Hoefen, M. Osawa, J. Haendeler, A. J. Ridley, K. Fujiwara, et al. (2004). "GIT1 mediates thrombin signaling in endothelial cells: role in turnover of RhoA-type focal adhesions." Circ Res **94**(8): 1041-9.
- Volpicelli-Daley, L. A., Y. Li, C. J. Zhang and R. A. Kahn (2005). "Isoform-selective effects of the depletion of ADP-ribosylation factors 1-5 on membrane traffic." Mol Biol Cell **16**(10): 4495-508.
- Wang, Z. Z., L. He, J. Chen, B. Dinger, L. Stensaas and S. Fidone (1999). "Protein phosphorylation signaling mechanisms in carotid body chemoreception." Biol Signals Recept **8**(6): 366-74.
- Wimmer-Kleikamp, S. H., P. W. Janes, A. Squire, P. I. Bastiaens and M. Lackmann (2004). "Recruitment of Eph receptors into signaling clusters does not require ephrin contact." J Cell Biol **164**(5): 661-6.
- Wohlfahrt, J. G., C. Karagiannidis, S. Kunzmann, M. M. Epstein, W. Kempf, K. Blaser and C. B. Schmidt-Weber (2004). "Ephrin-A1 suppresses Th2 cell activation and provides a regulatory link to lung epithelial cells." J Immunol **172**(2): 843-50.
- Woolley, C. S. and B. S. McEwen (1993). "Roles of estradiol and progesterone in regulation of hippocampal dendritic spine density during the estrous cycle in the rat." J Comp Neurol **336**(2): 293-306.
- Wu, C., S. Butz, Y. Ying and R. G. Anderson (1997). "Tyrosine kinase receptors concentrated in caveolae-like domains from neuronal plasma membrane." J Biol Chem **272**(6): 3554-9.
- Wyszynski, M., E. Kim, A. W. Dunah, M. Passafaro, J. G. Valtschanoff, C. Serra-Pages, M. Streuli, R. J. Weinberg, et al. (2002). "Interaction between GRIP and liprin-alpha/SYD2 is required for AMPA receptor targeting." Neuron **34**(1): 39-52.

- Yaffe, M. B. (2002). "How do 14-3-3 proteins work?-- Gatekeeper phosphorylation and the molecular anvil hypothesis." FEBS Lett **513**(1): 53-7.
- Yaffe, M. B., K. Rittinger, S. Volinia, P. R. Caron, A. Aitken, H. Leffers, S. J. Gamblin, S. J. Smerdon, et al. (1997). "The structural basis for 14-3-3:phosphopeptide binding specificity." Cell **91**(7): 961-71.
- Ye, B., D. Liao, X. Zhang, P. Zhang, H. Dong and R. L. Huganir (2000). "GRASP-1: a neuronal RasGEF associated with the AMPA receptor/GRIP complex." Neuron **26**(3): 603-17.
- Yuste, R. and T. Bonhoeffer (2001). "Morphological changes in dendritic spines associated with long-term synaptic plasticity." Annu Rev Neurosci **24**: 1071-89.
- Yuste, R. and T. Bonhoeffer (2004). "Genesis of dendritic spines: insights from ultrastructural and imaging studies." Nat Rev Neurosci **5**(1): 24-34.
- Zajchowski, L. D. and S. M. Robbins (2002). "Lipid rafts and little caves. Compartmentalized signalling in membrane microdomains." Eur J Biochem **269**(3): 737-52.
- Zhang, H., D. J. Webb, H. Asmussen and A. F. Horwitz (2003). "Synapse formation is regulated by the signaling adaptor GIT1." J Cell Biol **161**(1): 131-42.
- Zhang, H., D. J. Webb, H. Asmussen, S. Niu and A. F. Horwitz (2005). "A GIT1/PIX/Rac/PAK signaling module regulates spine morphogenesis and synapse formation through MLC." J Neurosci **25**(13): 3379-88.
- Zhang, S. H., R. Kobayashi, P. R. Graves, H. Piwnica-Worms and N. K. Tonks (1997). "Serine phosphorylation-dependent association of the band 4.1-related protein-tyrosine phosphatase PTPH1 with 14-3-3beta protein." J Biol Chem **272**(43): 27281-7.
- Zhao, Z. S., E. Manser and L. Lim (2000a). "Interaction between PAK and nck: a template for Nck targets and role of PAK autophosphorylation." Mol Cell Biol **20**(11): 3906-17.
- Zhao, Z. S., E. Manser, T. H. Loo and L. Lim (2000b). "Coupling of PAK-interacting exchange factor PIX to GIT1 promotes focal complex disassembly." Mol Cell Biol **20**(17): 6354-63.
- Zhou, Q., K. J. Homma and M. M. Poo (2004). "Shrinkage of dendritic spines associated with long-term depression of hippocampal synapses." Neuron **44**(5): 749-57.

8. Bibliography

- Zimmer, M., A. Palmer, J. Kohler and R. Klein (2003). "EphB-ephrinB bi-directional endocytosis terminates adhesion allowing contact mediated repulsion." Nat Cell Biol **5**(10): 869-78.
- Zisch, A. H., C. Pazzagli, A. L. Freeman, M. Schneller, M. Hadman, J. W. Smith, E. Ruoslahti and E. B. Pasquale (2000). "Replacing two conserved tyrosines of the EphB2 receptor with glutamic acid prevents binding of SH2 domains without abrogating kinase activity and biological responses." Oncogene **19**(2): 177-87.
- Ziv, N. E. and S. J. Smith (1996). "Evidence for a role of dendritic filopodia in synaptogenesis and spine formation." Neuron **17**(1): 91-102.
- Zou, J. X., B. Wang, M. S. Kalo, A. H. Zisch, E. B. Pasquale and E. Ruoslahti (1999). "An Eph receptor regulates integrin activity through R-Ras." Proc Natl Acad Sci U S A **96**(24): 13813-8.

9. Curriculum vitae

Personal data

Name	Stefan Weinges
Date of Birth	June 11, 1975
Place of Birth	Mannheim, Germany
Nationality	German

Education

since Dec 2001	Doctoral thesis, Max Planck Institute of Neurobiology, Martinsried, Department of Molecular Neurobiology, laboratory of Dr. Amparo Acker-Palmer
Feb - Sept 2001	Diploma thesis, final degree "sehr gut", German Cancer Research Centre (DKFZ), Heidelberg, Department of Molecular Biology of the Cell I, laboratory of Prof. Günther Schütz, Topic: „Profiling of Gene Expression in CREB/CREM mutants by <i>in situ</i> hybridization”
Oct 1996 - Sept 2001	Diploma in Biology, final degree "sehr gut", Ruprecht-Karls-University, Heidelberg, and Flinders University, Adelaide, Australia, major in Molecular Biology, minors in Biochemistry and Cell Biology
Aug 1995 - Sept 1996	Civil Service German Cancer Research Centre (DKFZ), Heidelberg, laboratory of PD Hanswalter Zentgraf